DETERMINATION OF THE RESONANT FREQUENCIES OF LOADED TIRES ROLLING ON A FLAT ROADWAY

by

JACK LEE WINGER, B.S.

A THESIS

IN

MECHANICAL ENGINEERING

Submitted to the Graduate Faculty
of Texas Tech University in
Partial Fulfillment of
the Requirements for
the Degree of

MASTER OF SCIENCE
IN
MECHANICAL ENGINEERING

Approved

Accepted

August, 1976

AC
805
T3
1976
No.95
cop.2

ACKNOWLEDGEMENTS

I would like to thank Dr. Clarence A. Bell for his patience in directing this work, and the other member of my committee, Dr. Donald J. Helmers, for his cooperation. I would also like to express my appreciation to Mr. L. Jack Powers for his technical advice during preliminary testing sequences.

A special thanks and indebtedness goes to Mr. Wilson and Technical Sergeant Schaffer from Reese Air Force Base Field Maintenance Electric Shop for providing parts and technical information on the direct current (D.C.) equipment.

TABLE OF CONTENTS

		Page
ACKNOWLEDGMENTS		ii
LIST OF TABLES		iv
LIST OF ILLUSTRATIONS		vi
I.	INTRODUCTION	1
	Purpose	3
II.	TRAILER IMPROVEMENTS	4
III.	ANALYSIS OF DISK SEPARATION	14
IV.	LOADING OF THE TRAILER	25
	Trailer Stabilization	33
V.	COLLECTING OF BASELINE DATA	36
VI.	COLLECTING OF ROADWAY DATA	48
	Data Analysis	53
VII.	CONCLUSIONS AND RECOMMENDATIONS	62
LIST OF REFERENCES		67
APPENDIX A		69
APPENDIX B		82
APPENDIX C		93
APPENDIX D		122

LIST OF TABLES

Table — Page

I. Geometric "Broken" Model # 1..... 20

II. Geometric "Broken" Model # 2..... 20

III. Initial Baseline Trailer Data Without and With A Test Tire..... 47

IVa. Summary of Resonant Frequencies From Roadway Tests (Hewlett-Packard Sanborn Oscillographic Recorder)..... 62

IVb. Summary of Resonant Frequencies From Roadway Tests (Fast Fourier Frequency Analysis)..... 63

V. Penetration Constants For THOR Computer Program..... 82

VI. Computer Output From THOR Program For .125 Inch Mild Steel Plate..... 88

VII. Computer Output From THOR Program For .250 Inch Mild Steel Plate..... 88

VIII. Computer Output From THOR Program For .375 Inch Mild Steel Plate..... 89

IX. Computer Output From Beam Matrix Method For Fixed-Fixed Beam Response..... 102

X. Computer Output From Beam Matrix Method For Fixed-Pinned Beam Response..... 104

XI. Computer Output From Beam Matrix Method For Fixed-Free Beam Response..... 106

Table Page

XII. Computer Output From Beam Matrix Method For Pinned-Pinned Beam Response..... 108

XIII. Computer Output From Beam Matrix Method For Pinned-Fixed Beam Response..... 110

XIV. Computer Output From Beam Matrix Method For Pinned-Free Beam Response..... 112

XV. Computer Output From Beam Matrix Method For Free-Free Beam Response..... 114

XVI. Computer Output From Beam Matrix Method For Free-Fixed Beam Response..... 116

XVII. Computer Output From Beam Matrix Method For Free-Pinned Beam Response..... 118

XVIII. Section Parameters of Lumped Element Model..... 120

LIST OF FIGURES

Figure		Page
2-1.	Scale Drawing of Respective Sizes of the Old Control Panel to the New Control Box	5
2-2.	Redesigned Control Box	7
2-3.	Wiring Diagram - D.C. Motor Control	11
2-4.	Wiring Diagram - Trailer to Control Box	12
2-5.	Dust Cover to Protect Spur Gears	13
3-1.	Individual Counter-rotating Disk	15
3-2.	Rotating "Broken" Disk Model # 1	17
3-3.	Rotating "Broken" Disk Model # 2	18
3-4.	Installation of Vertical Safety Shields	24
4-1.	Ballast Container	26
4-2.	Installation of Ballast Container	27
4-3.	Upper Subframe Loading	29
4-4.	Lower Subframe Loading	30
4-5.	Stabilization Trailer Loading	31
4-6.	Relative Positioning of Upper and Lower Subframe	32
4-7.	Installation of Stabilization Torsion Rod and Horizontal Flat Plate	35
5-1.	Upper Idler Pulley	42
5-2.	Lower Idler Pulley	43
5-3.	Installation of Idler Pulleys	44
5-4.	New Positioning of Accelerometer	46

Figure Page

6-1. Selected Roadway Test Site..... 51

6-2. Tire Resonant Frequencies Plotted as a Function of Roadway Speed (Hewlett-Packard Sanborn Oscillographic Recorder)..... 55

6-3. Tire Resonant Frequencies Plotted as a Function of Tire Pressure (Hewlett-Packard Sanborn Oscillographic Recorder)..... 56

6-4. Compiled Tire Resonant Frequency Data From Mathew (4)..... 58

6-5. Tire Resonant Frequencies Plotted as a Function of Roadway Speed (Fourier Analysis)..... 60

6-6. Tire Resonant Frequencies Plotted as a Function of Tire Pressure (Fourier Analysis)..... 61

A-1. Typical Unsymmetrical Trailer Response Before Modifications Were Incorporated..... 72

A-2. Typical Trailer Response Under Laboratory Conditions..... 73

A-3. Typical Trailer Response From Roadway Testing... 74

A-4. Fourier Analysis - Static Laboratory Conditions. 75

A-5. Fourier Analysis - Roadway Speeds For 18 PSIG... 76

A-6. Fourier Analysis - Roadway Speeds For 23 PSIG... 78

A-7. Fourier Analysis - Roadway Speeds For 28 PSIG... 80

B-1. Computer Plot of a 1293 Grain Mild Steel Fragment Penetrating .125 Inch Mild Steel Plate. 90

Figure Page

B-2. Computer Plot of a 900 Grain Mild Steel Fragment Penetrating .125 Inch Mild Steel Plate. 91

B-3. Computer Plot of a 650 Grain Mild Steel Fragment Penetrating .125 Inch Mild Steel Plate. 92

C-1. Computer Plot of a Fixed-Fixed Beam Response... 103

C-2. Computer Plot of a Fixed-Pinned Beam Response.. 105

C-3. Computer Plot of a Fixed-Free Beam Response.... 107

C-4. Computer Plot of a Pinned-Pinned Beam Response. 109

C-5. Computer Plot of a Pinned-Fixed Beam Response.. 111

C-6. Computer Plot of a Pinned-Free Beam Response... 113

C-7. Computer Plot of a Free-Free Beam Response..... 115

C-8. Computer Plot of a Free-Fixed Beam Response.... 117

C-9. Computer Plot of a Free-Pinned Beam Response... 119

CHAPTER I

INTRODUCTION

This report is a continuation of a complex project being conducted by the Mechanical Engineering Department of the Texas Tech University to determine the resonant frequencies of automobile tires rolling on a flat roadway. Normally, these frequencies are experimentally determined by automotive tire companies rolling loaded tires against large steel drums. More recently, tire companies have developed more sophisticated testing equipment for simulating roadways thru using large steel hoops rolling on large drums with a loaded tire placed against the hoop. Of the above mentioned tire testing methods, only an actual road test will provide accurate data of tire structural performance. Therefore, following this line of reasoning Texas Tech University, through efforts of a Research Graduate Advisor along with many graduate and undergraduate students, have designed and constructed an instrumented trailer for collecting actual road test data. This report will present data collected using Texas Tech's specially instrumented trailer and a Firestone Steel Radial 500 GR70-15 tire that has been furnished by the Firestone Tire and Rubber Company, Arkon, Ohio. During the test series, tire pressures were varied from 18 to 28 psig with highway

speeds increased from 15 to 55 miles per hour. Before actual road testing was started, a series of baseline static tests (tire vibrating, but no rolling motion) were performed in the Mechanical Engineering Laboratory to be used for comparative analysis with the roadway tests plus they would be used to separate out the tire frequencies from those produced by the trailer.

This analysis can be performed due to previous efforts of Campbell (1), Tavakoli (2) and Pirtle (3). They have performed the majority of the work which has produced a usable instrumentated trailer. Campbell (1) presents the development and construction of the vibrational test trailer that will be used to collect static and roadway data. Tavakoli (2) develops and defines the initial electrical system that was used to produce vibratory excitation through the counter-rotating disks. Pirtle (3) discusses initial refinement of the trailer's instrumentation and presents a preliminary static test of a GR70-15 steel-belted radial tire, plus a vibrational test of the trailer without a test tire. This established initial resonant frequencies along with a step-by-step operational procedure for conducting individual tests.

Purpose

The purpose of this thesis is to describe significant changes and modifications that were incorporated to insure accurate and responsive trailer operations and to conduct resonance frequency tests on a GR70-15 steel-belted radial tire. These changes also allowed the trailer to be more versatile and could be applicable to a wider range of road test operations. The primary section of this thesis is a presentation of static baseline and roadway data for the sample GR70-15 steel-belted radial tire at three pressures and five roadway speeds.

CHAPTER II

TRAILER IMPROVEMENTS

Reviewing the method of trailer operations from Pirtle (3), it was decided that a more simplified method of overall operation was needed. The old method called for the operator to carry around a 1.5 ft x 2.5 ft plywood board that contained an ampere meter, a large variable ohm resistor, a tachometer, two 60 ampere knife switches and a 500 milliohm shunt, Figure 2-1. The operator had to simultaneously operate all the components of the board, monitor a Tanberg tape recorder, observe the D.C. motor tachometer (to prevent motor over revving) and to receive road speeds from the towing vehicle operator. This appeared to be too much instrumentation for one person to handle, plus did not permit accurate control over the variable speed D.C. motor. Therefore, an improved system was developed that would reduce the manipulation the operator would have to perform, provide better control over the variable speed D.C. motor, and enable less cabling between the trailer and the control panel. To start with, the old cabling consisted of three 5/8 inch welding cables, two 1/8 inch diameter bell wires, and two 14 gauge multistranded wires laced with a cotton cord, forming a 2 1/2 inch diameter single wire bundle from the towing vehicle to the trailer. This bundle was

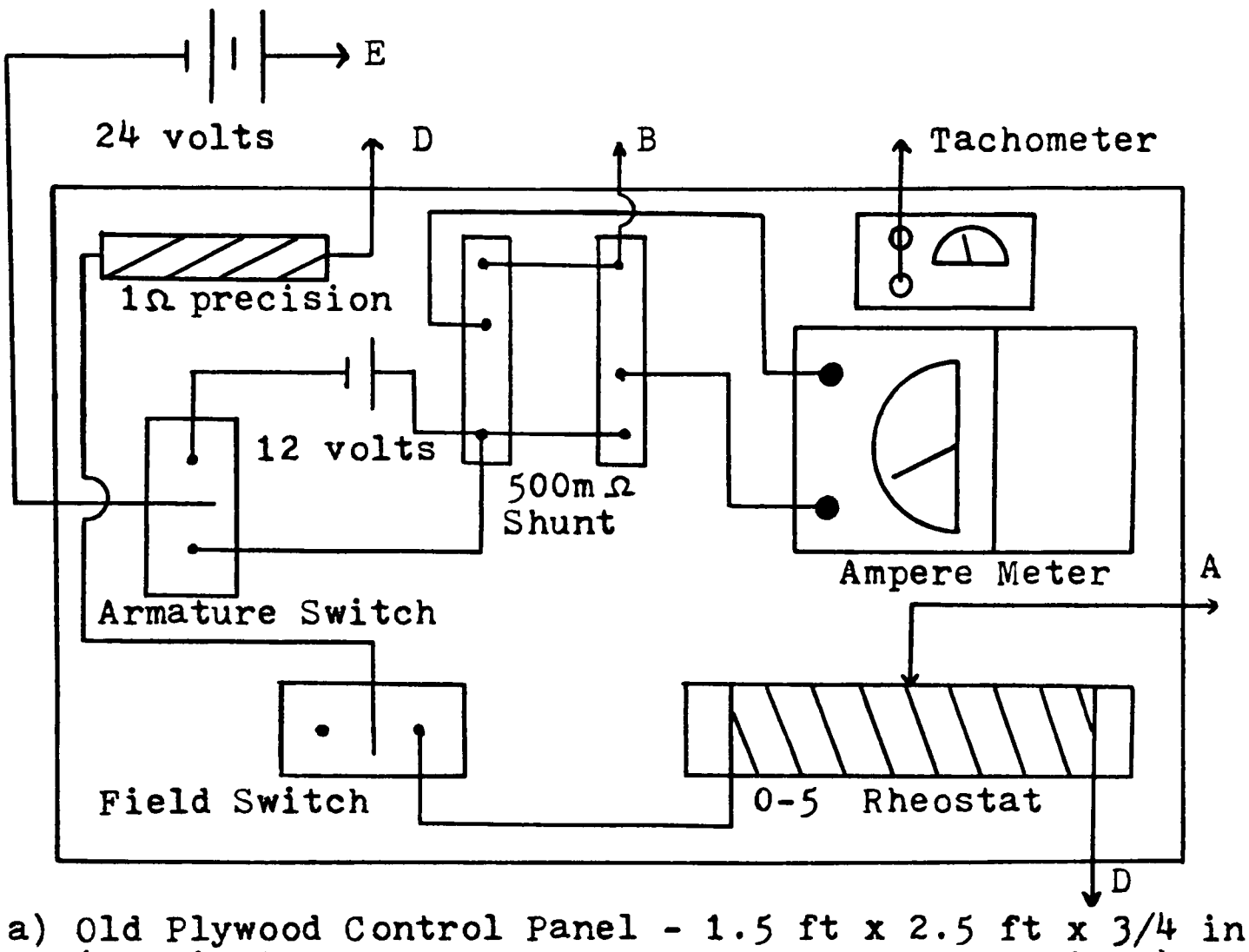

a) Old Plywood Control Panel - 1.5 ft x 2.5 ft x 3/4 in
(Terminals A,B,D and E Are D.C.Motor Connections)

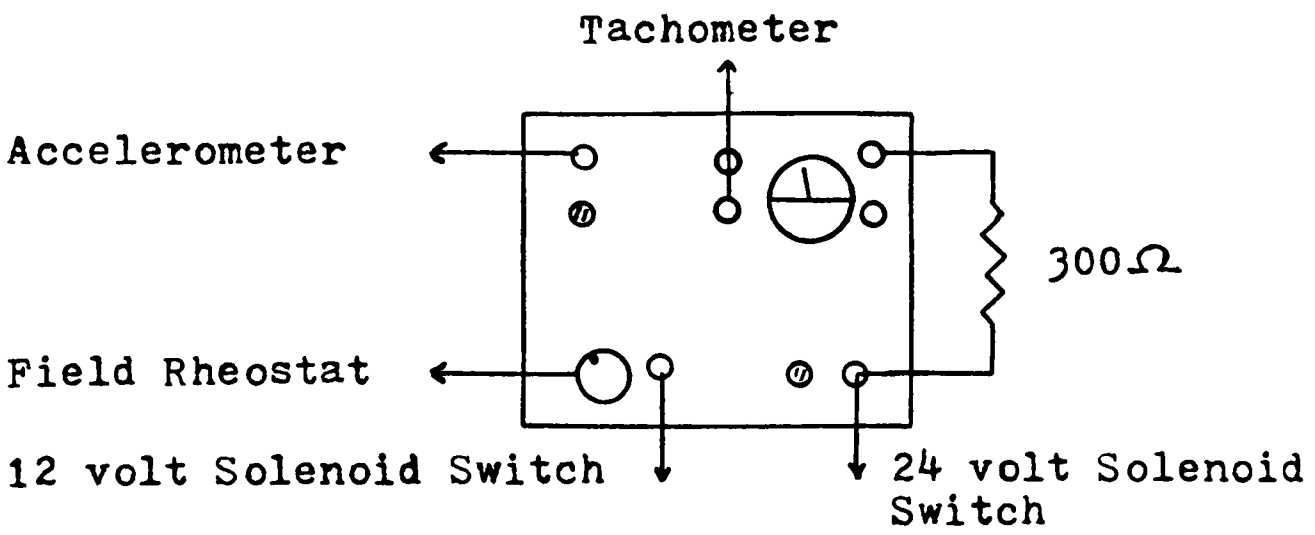

b) New Control Box - 7 in x 9 in x 4 in

Figure 2-1. Scale Drawing Of Respective Sizes Of The Old Control Panel To The New Control Box

replaced with a surplus nine stranded, 1 inch diameter, U.S. Air Force aircraft wiring harness which had its own protective plastic shielding. This reduced the size of the cabling plus improved the packaging of the wiring bundle. Along with the new cabling, a new control box, Figure 2-2, was designed to include switches for the accelerometers, the main control solenoids, a D.C. motor field rheostat control, and the D.C. motor monitoring tachometer. This box was constructed from .0625 inch 2024T3 aluminum and required only a space of 7 inches by 9 inches by 4 inches to house all the components. Upon assemblying the control box, several weak links in the overall control system were noted. One weakness was the method used to control the speed of the D.C. motor. It employed a 2 ohm resistor, a 12 volt battery, and a 0-5 ohm variable resistor, which was used to force reverse current through the field windings thus "controlling" the speed. These components were replaced with a 25 ohm, 10 watt variable control rheostat and five 125 ohm resistors connected in parallel. The rheostat and the parallel connected resistors were then connected in parallel between the D.C. motor terminals B and D, Figure 2-3. This connection served to prevent motor over revving and allowed for greater motor control through the rheostat. Motor over revving causes a dangerous situation where the motor and the counter-rotating disks could fail in tension, sending metal everywhere. This condition

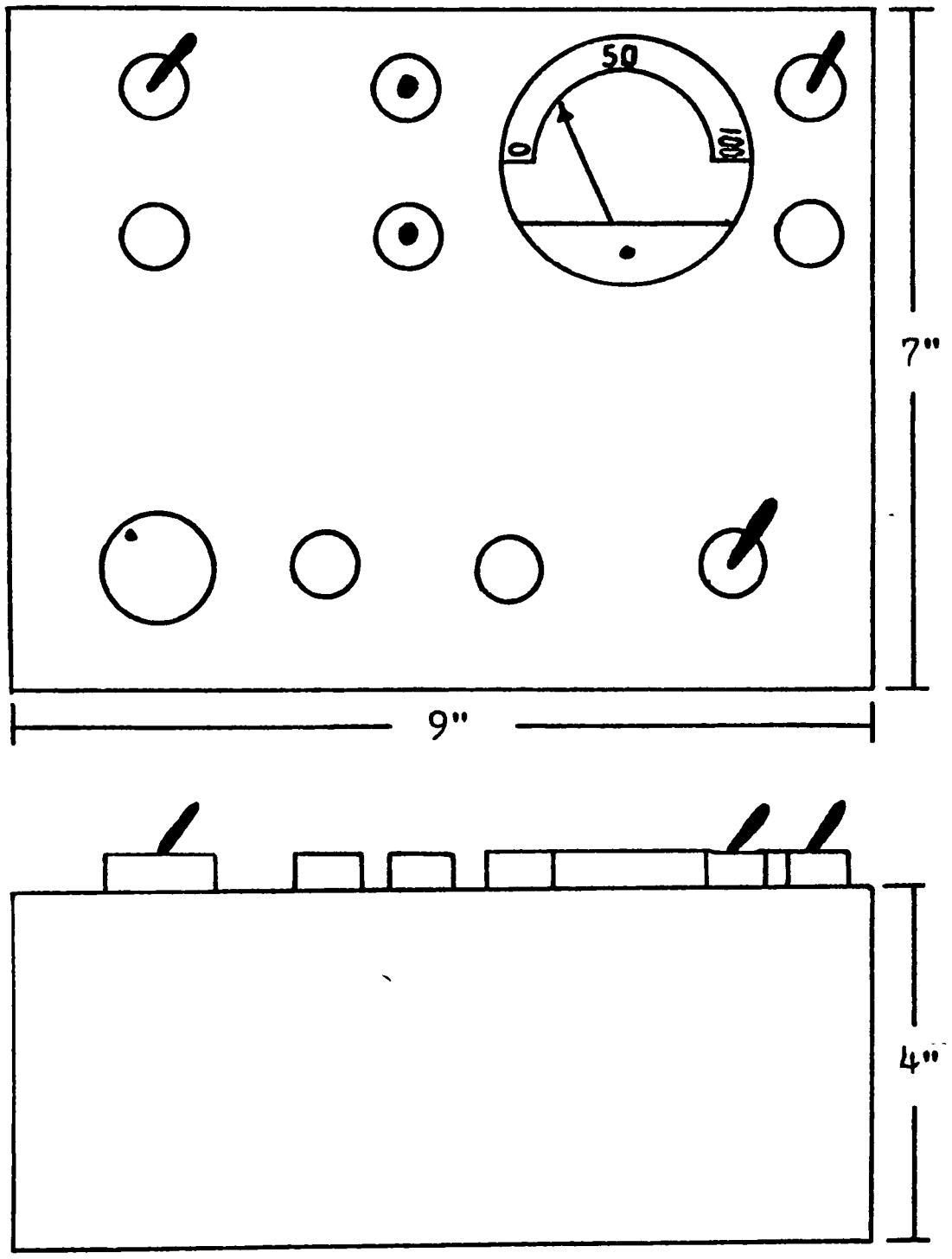

Figure 2-2. Redesigned Control Box

was not adequately considered during the original design due to lack of knowledge of the particularly obtained D.C. motor which is labeled a D.C. starter-generator. Complete information concerning the proper operation of this generator, used as a motor, was obtained by the author through personal contact with the U.S. Air Force's Reese Air Force Base Field Maintenance Electric Shop. They provided a complete wiring diagram with usable salvaged parts so that this generator could be operated safely as a motor.

Another weak link in the original trailer operation was the use of a 60 ampere knife switch to change the D.C. motor from an input of 24 volts to 36 volts, thus obtaining operating speeds of approximately 3300 rev/min. Upon initial testing of the circuitry, this switch failed after four operating sequences. Again, using information obtained from Reese Air Force Base personnel, it was discovered that this switch was handling approximately 125-150 ampere load. The knife switch was replaced using parts obtained through the Reese Air Force Base Property Disposal Office and the Electrical Shop. The parts consisted of two 200 ampere, 28 volt solenoid switches and three 300 ampere, 28 volt Reverse Current Relays (one used at a time). To accommodate these parts, the electric circuit controlling the D.C. motor was rewired. The two 200 ampere, 28 volt solenoids were connected in parallel and permitted only 24 volts to reach the motor. The Reverse Current Relay was

used to deliver 12 volts to the motor (useful for low system frequency responses). All switches were mounted directly to the main frame behind the eight 12 volt batteries that are used for all trailer operations. The 12 and 24 volt solenoids are each controlled by a 3 ampere toggle switch mounted in the new control box. Again using information supplied by Reese Air Force Base personnel, it should be noted that the system does not require 36 volts, as mentioned in Tavakoli (2), to obtain an overall motor maximum speed of 3300 rev/min. In fact, using a voltage potential of only 28 volts and allowing the motor to perform as it is designed, using no controlling resistors, the motor could possibly obtain speeds of over 8000 rev/min, which creates a very dangerous situation, because the motor is rated between 4500 to 6000 rev/min.

Another change incorporated was to move the accelerometer toggle switch from the trailer frame mount into the control box.

In order to integrate the new control box containing the accelerometer and motor control switches into the trailer control circuitry, the entire trailer had to be completely rewired. As noted later, due to excess electrical noise, this rewiring was accomplished using shielded wire. All new connections that were required by this rewiring were handled through an existing electrical buss bar mounted on the right front side of the stabilization

trailer. A complete wiring diagram is given in Figures 2-3 and 2-4. With the installation of this new control box, the trailer operation was significantly simplified and the modes of operation were enhanced greatly.

Another less important trailer improvement that was developed, for maintenance purposes, was a protective dust shield around the counter-rotating disk gear drive. A 4.5 inch x 7 inch x 9 inch, 1/16 inch thick galvanized steel box was constructed, Figure 2-5. This box was split in half to permit easy removal for regreasing of the spur gears after a series of road tests have been performed. Previously no protective dust shield existed. This dust shield will permit longer trailer operations, with a reasonable amount of protection, in the dusty climate found around Texas Tech University.

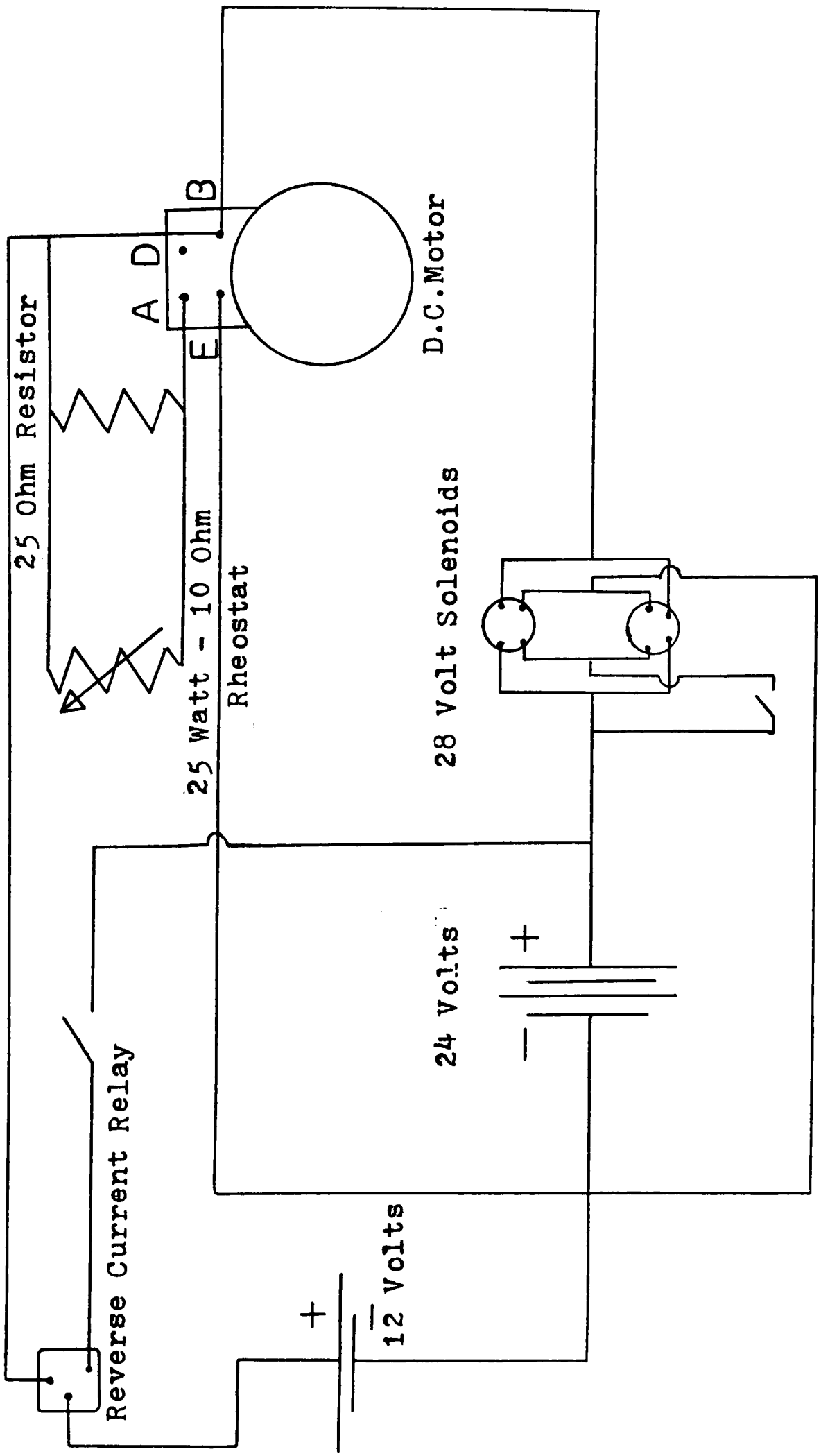

Figure 2-3. Wiring Diagram - D.C.Control Motor

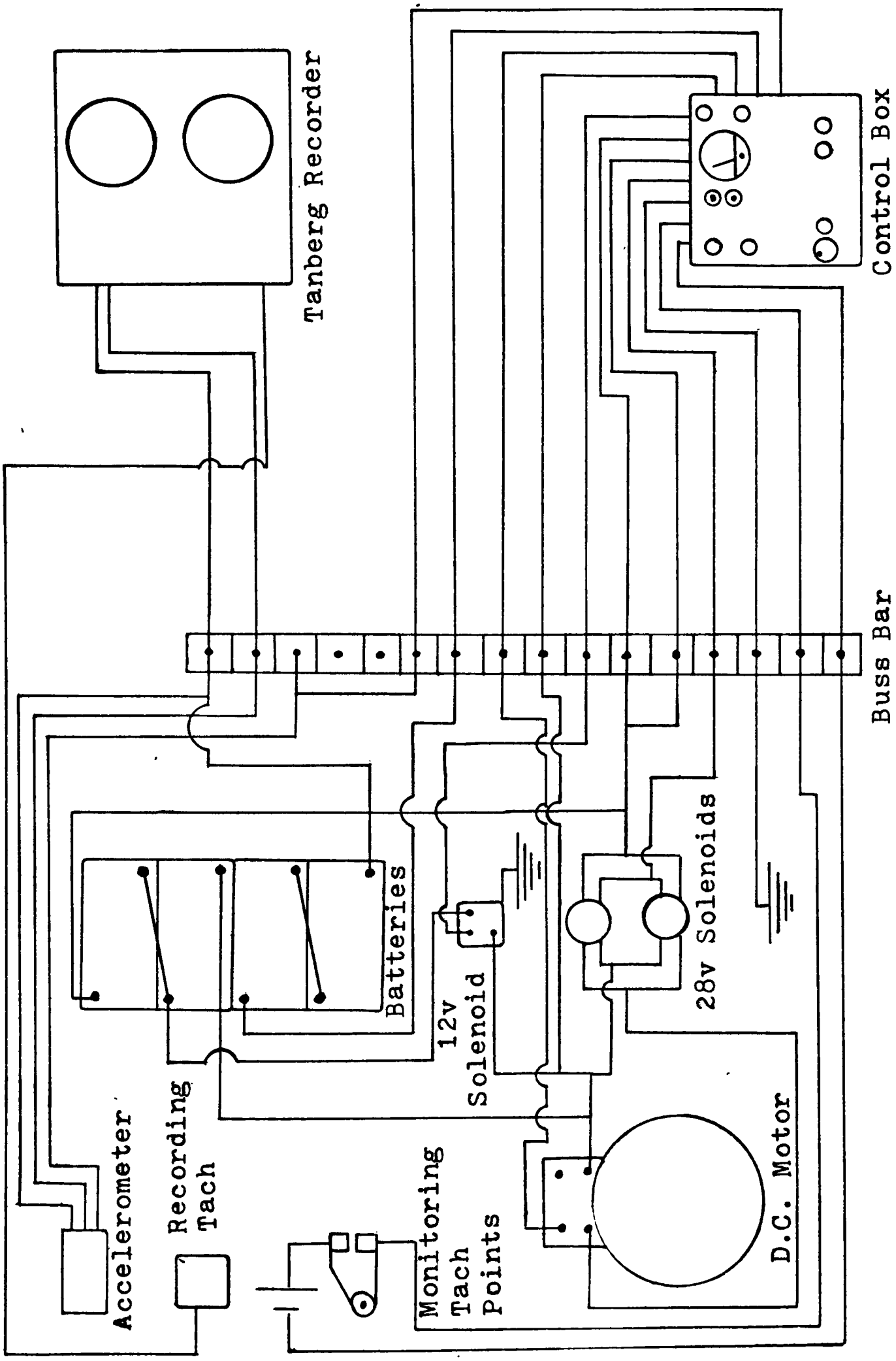

Figure 2-4. Wiring Diagram - Trailer To Control Box and Recorder

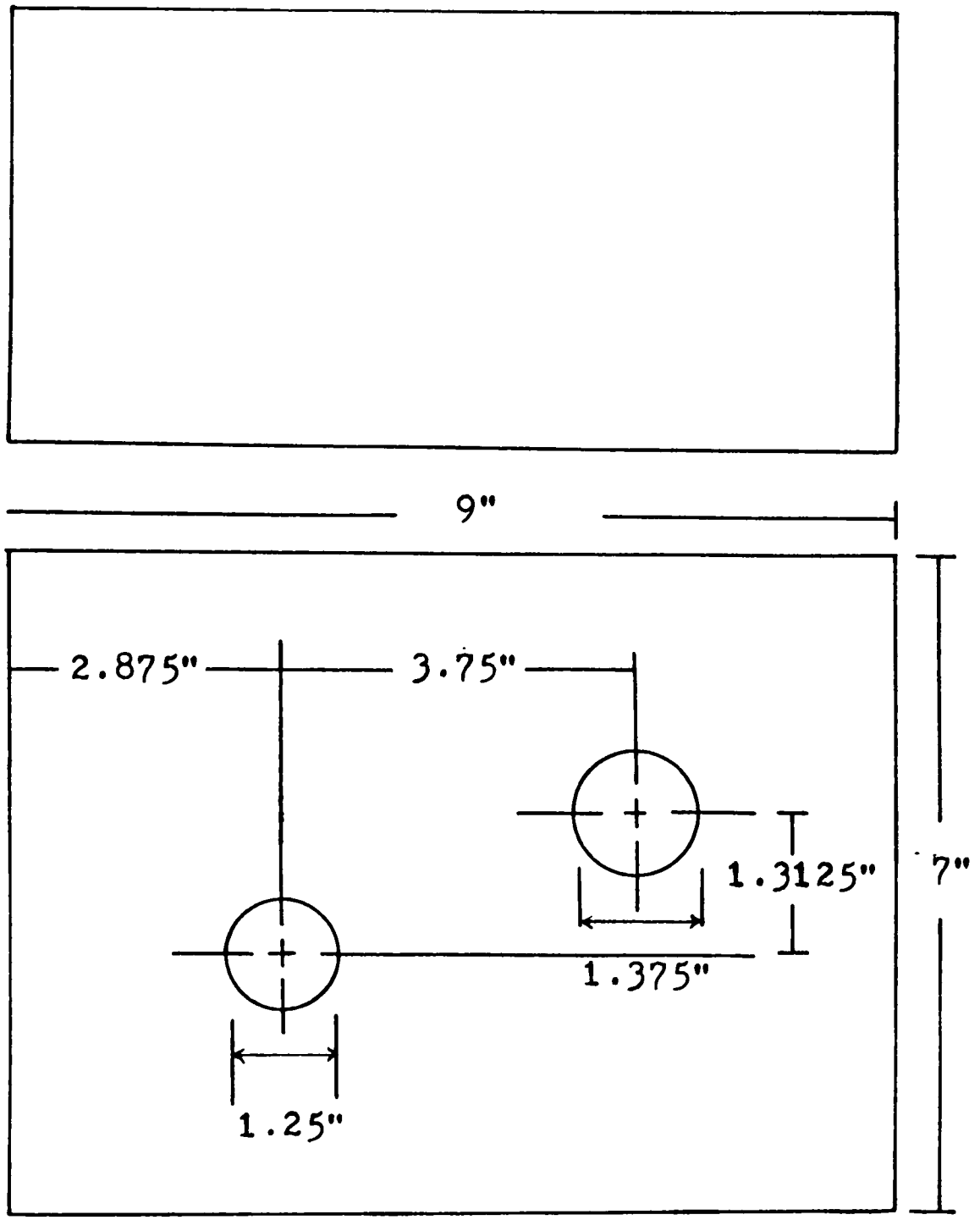

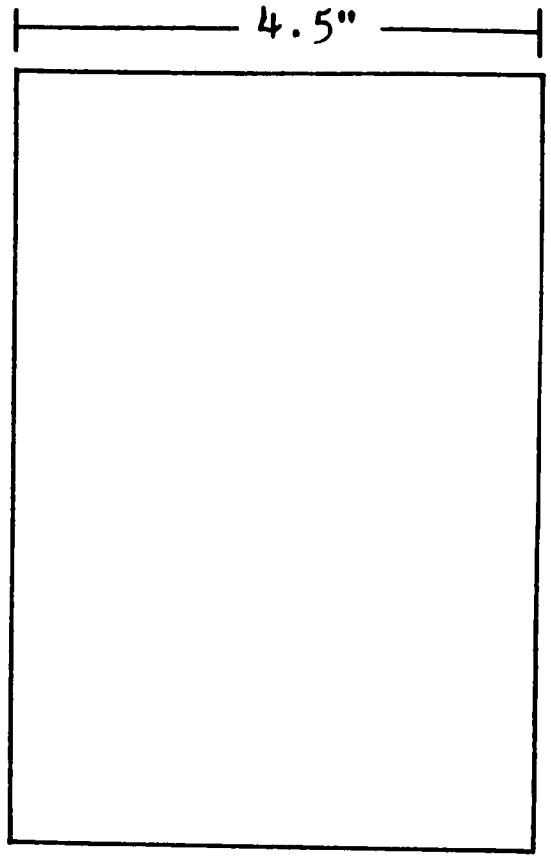

Figure 2-5. Dust Cover To Protect Spur Gears

CHAPTER III

ANALYSIS OF DISK SEPARATION

The design and fabrication of the counter-rotating disks with a safety design factor of 4.0 are presented in Campbell (1). Pirtle (3) describes two 3/16 inch safety shields that were recommended, constructed and installed on the instrumentation trailer over the counter-rotating disks, but unfortunately no design parameters were presented. Upon a discussion of these safety shields and eccentric weight loading of the disks with the Research Graduate Advisor, it was decided that a more complete study of the shields was needed. The first parameter to be researched was the individual counter-rotating disk separation. Using Figure 3-1 as the overall construction of an individual disk, a breakup or separation pattern was developed. Since there is no exact mathematical model to predict material separation constructed in circular form, two geometric models were hypothesized and an analysis was conducted for each model type. The reason that no mathematical model exists for material separation is because of differences in machining techniques, individual material composition and individual stresses occurring in each disk due to the stresses caused by the bolts, washers and nuts being placed into the disks (so as to produce forced

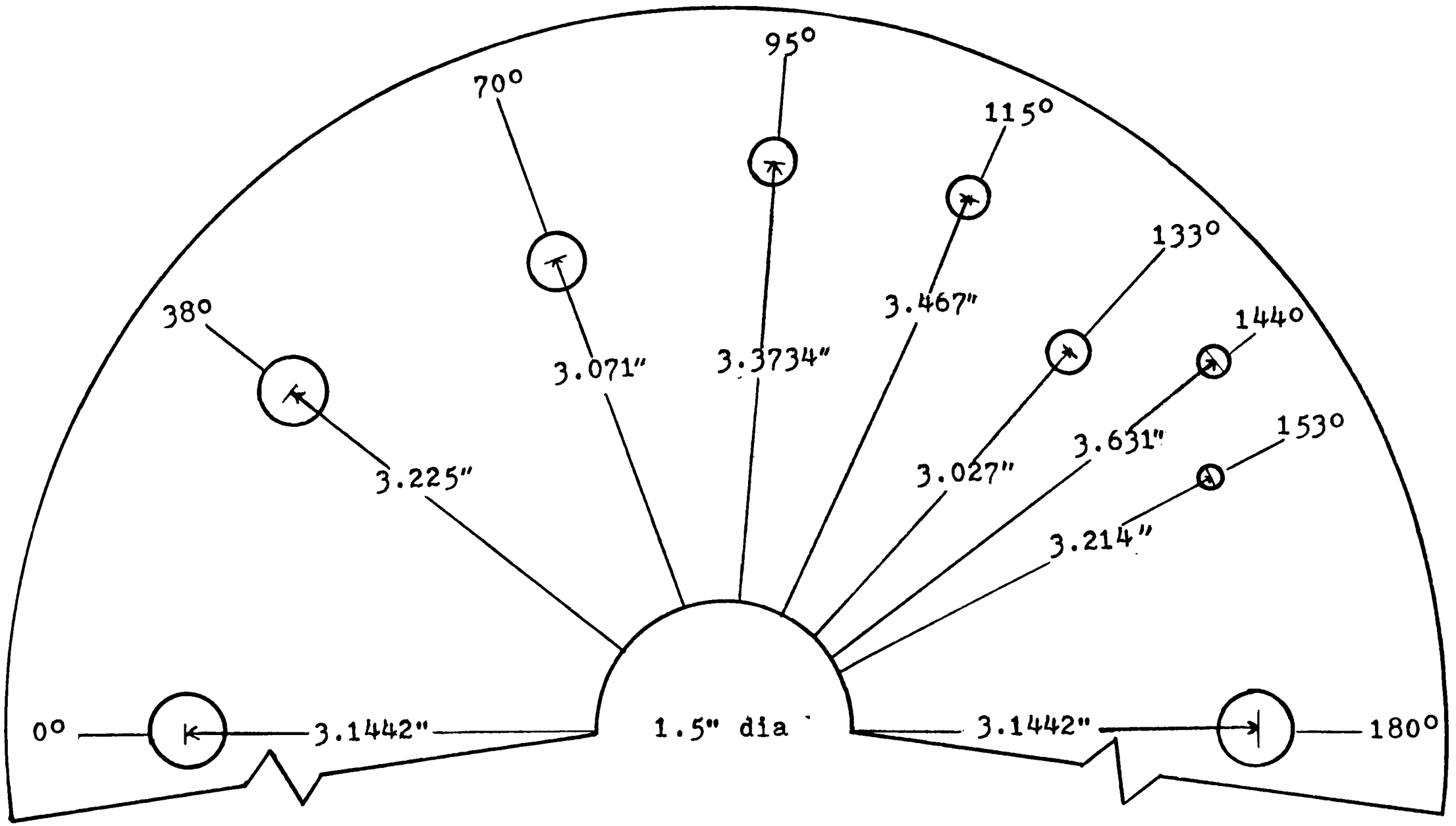

Figure 3-1. Individual Counter-Rotating Disk

vertical vibration) and then tightened Campbell (1). Therefore, two geometric models, Figures 3-2 and 3-3, were developed using two basic assumptions:

1. Principle direction of a principle stress occurs in a straight line (not necessarily true, due to material composition and/or machining techniques).

2. Principle stresses occur parallel to the rotating axis (chord of a circle) or radially outward from the point of main stress.

These models were then mathematically separated and each "broken piece" was then weighed using grain measurement (7000 grains equal one pound). The results of this mathematical separation and weighing are tabulated in Tables I and II. This data could now be used as input to an empirical formula useful for determining fragment penetration through flat plate material, i.e., the "broken" pieces penetrating through the 3/16 inch safety shields.

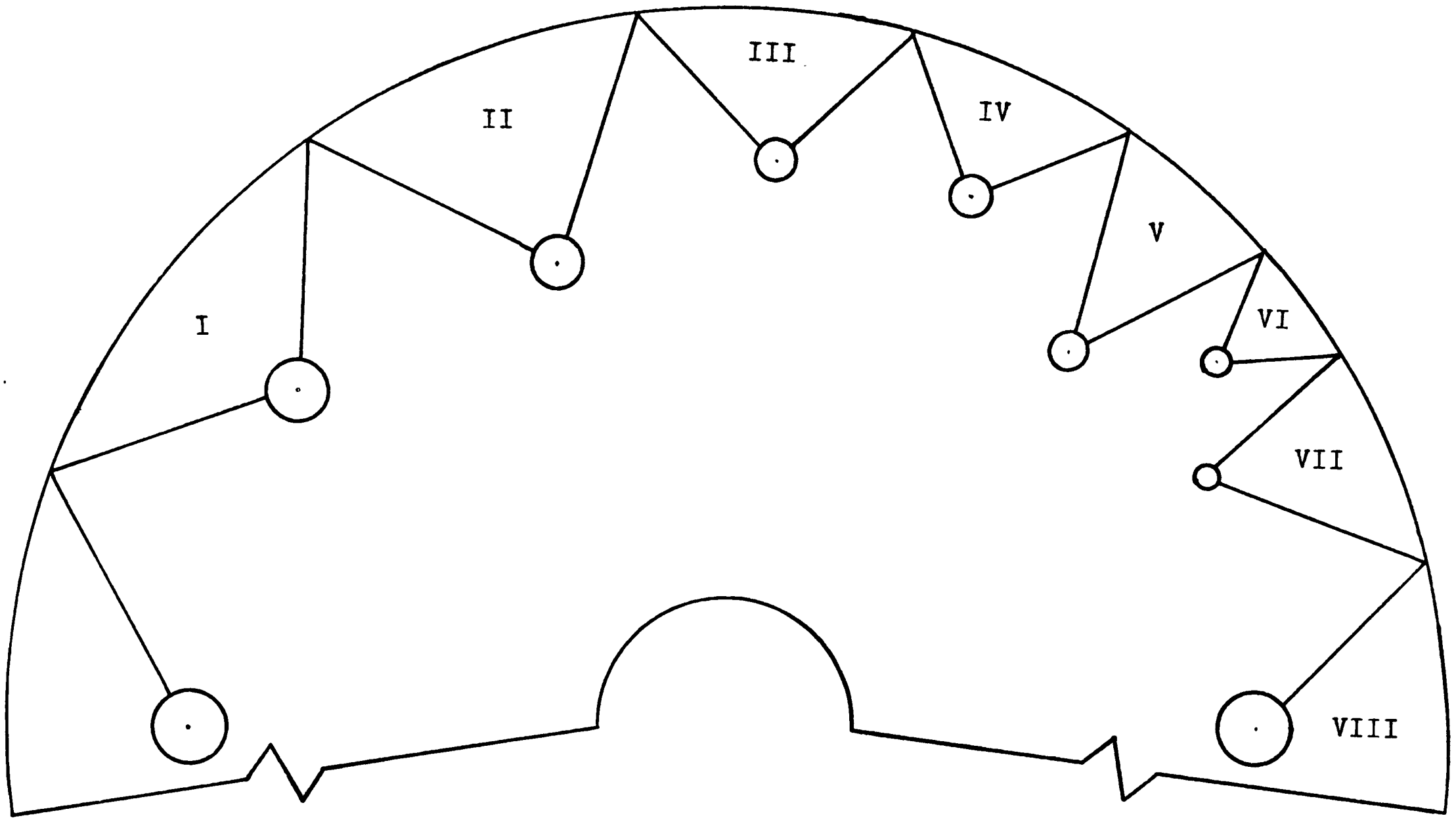

Figure 3-2. Rotating "Broken" Disk Model # 1

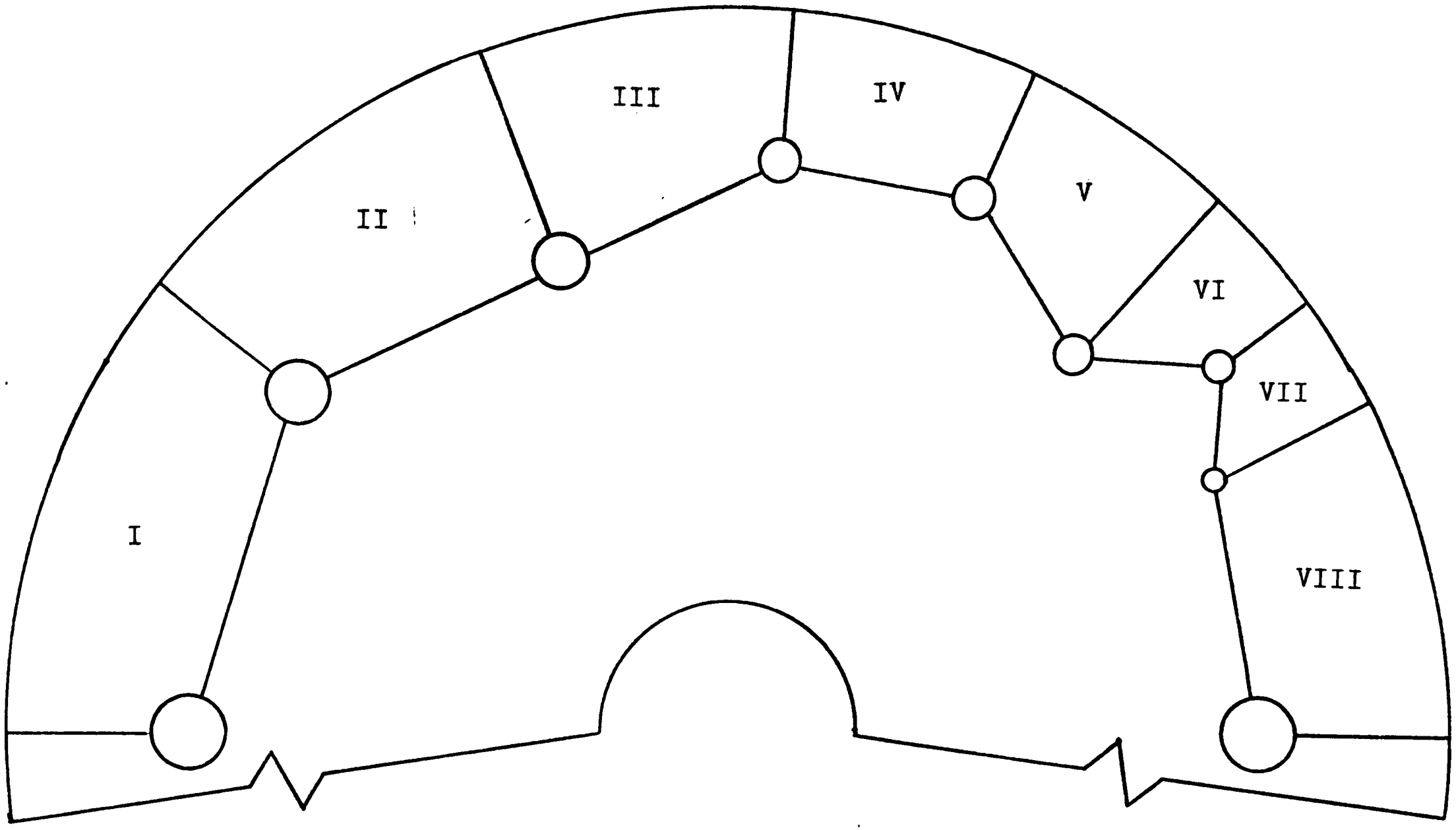

Figure 3-3. Rotating "Broken" Disk Model # 2

Project THOR (6) presents a variety of empirical penetration formulas and complicated data into graphic form for nine different material types and ten individual mild steel fragment weights. These data analyses were conducted through a U.S. Army program, Project THOR, in the early sixties. Through this project six differently shaped mild steel fragments were singularly fired at four different obliquity angles against the various material types. An obliquity angle is the angle measured from a line constructed perpendicular from the face of the test firing plate to the line of sight path of the impacting fragment. For example, if a fragment strikes the test plate perpendicular to the face of the test plate, the obliquity angle is 0°. Likewise, if a fragment does not strike the face of the test plate, but flies in a path parallel to the face of the plate, the obliquity angle is 90°. For the analysis, the obliquity angle was assumed to be 0°. This is the most detrimental obliquity angle due to the minimum line of sight distance through the impacted plate.

Other input parameters for this analysis were the mild steel pieces separated from the rotating disk, selected from either Table I or II and a mild steel plate, the 3/16 inch safety shield. These were combined into a penetration formula which would predict the residual velocity of the metal fragment after it had penetrated the struck plate. The penetration equation applicable to this case is as

TABLE I GEOMETRIC "BROKEN" MODEL # 1

Piece Number	Average Arc Length (Inches)	Total Area (Inches^3)	Weight (Grains)
I	1.31	.328	650.05
II	1.23	.308	612.02
III	.727	.182	360.69
IV	.549	.137	272.65
V	.656	.164	325.57
VI	.229	.057	113.84
VII	.689	.172	341.71
VIII	1.276	.319	633.04

TABLE II GEOMETRIC "BROKEN" MODEL # 2

Piece Number	Average Arc Length (Inches)	Total Area (Inches^3)	Weight (Grains)
I	1.065 x 2.45	.652	1293.34
II	1.102 x 2.06	.566	1123.50
III	1.028 x 1.63	.418	828.90
IV	.829 x 1.34	.277	550.06
V	1.003 x 1.18	.295	585.25
VI	.921 x .727	.167	332.36
VII	.828 x .602	.125	247.34
VIII	1.071 x 1.743	.466	926.23

follows:

$$V_R = V_S - 10^C (eA)^{\alpha} M_S^{\beta} (\sec\theta)^{\gamma} V_S^{\lambda}$$

where: V_R = residual velocity - ft/sec

V_S = impact velocity of fragment - ft/sec

e = target plate thickness - inches

A = average impact area of fragment - inches ^{2}

M_S = weight of impacting fragment - grains

θ = obliquity angle of impacting fragment - degrees

$C, \alpha, \beta, \gamma, \lambda$ - penetration constants determined separately for each material type penetrated under

Penetration Constants for Mild Steel Plates:

C	α	β	γ	λ
6.399	.889	-.945	1.262	.019

Now, all penetration parameters were known for the formula except the striking velocity, V_S. This could be computed from the rotational speeds of the counter-rotating disks.

Velocity = R.P.M. x π x D

where: R.P.M. = rotational speed of the disks

D = diameter of an individual disk

Appendix B contains a complete computer program, containing three other sets of data constants applicable

for hard steel, cast iron and aluminum materials. This program will predict penetration residual velocity and mass given an impact velocity, mass and expected obliquity angle.

Knowing that the safety shields would provide protection for all speeds, the maximum disk speed anticipated was 6600 revolutions per minute (rev/min) which yielded an average fly-off velocity for a piece separated from the disk of 245 feet per second (ft/sec). But, if the motor gets out of control, this velocity could increase to approximately 300 ft/sec. Therefore, instead of computing all the fragment sizes which can be accomplished using the computer program in Appendix B, only the largest "broken piece" was considered. Substituting all these parameters into the formula, a residual velocity of -282.49 ft/sec was computed. The minus sign means the "broken piece" would not have penetrated, but this only allowed a safety factor of 1.15. Pursuing this analysis further, and analyzing an out of control speed of 8000 rev/min, the safety factor was reduced to .80. Noting a significant drop in the safety factor and trying to maintain an overall safety factor between 3.0 and 4.0, comparable with the rest of the trailer, it was decided to investigate replacing the safety shields with 3/8 inch mild steel plates. Recomputing the individual safety factors for the two speeds yielded a 3.00 for the slower and 2.30 for the faster speed. Because

of the improvement of the safety factor and noting the normal speed safety factor was within the constraints of the test, the 3/8 inch mild steel plates were cut to size and installed. Also to further increase the safety of the trailer operation which places the operator directly in front of the trailer, riding in the towing vehicle, additional safety shields were welded to the trailer frame directly in front of the counter-rotating disk drive pulleys, Figure 3-4. Now tire vibrational road testing could be conducted with a reasonable assurance of safety.

TEXAS TECH LIBRARY

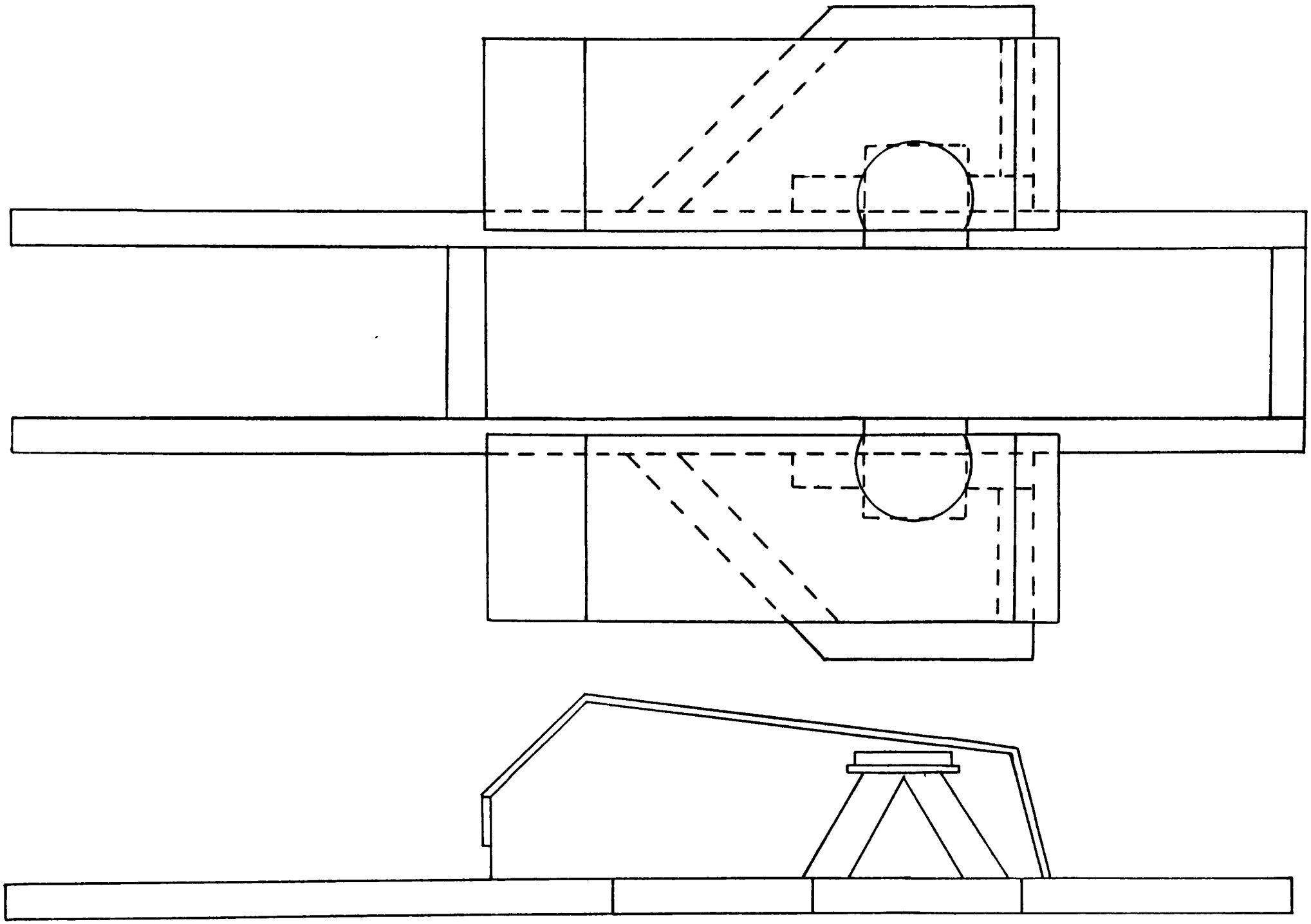

Figure 3-4. Installation Of Vertical Safety Shields

TEXAS TECH LIBRARY

CHAPTER IV

LOADING OF THE TRAILER

As pointed out in Pirtle (3), individual test tire loading is an important parameter that must be considered for tire vibrational analysis. In a conversation with the Research Graduate Advisor, it was decided to load the tire's axle with approximately one-fourth of an average car's weight, 1000 pounds. This weight was to be a composite of the trailer's structural weight, all components attached to the trailer frame, plus additional added ballast that could be positioned on the upper subframe. Trailer frame component weights are included as part of Campbell (1), Appendix A, and as part of Figure 4-6. Therefore, the only task needed to be accomplished was to add the additional ballast to the upper subframe. Due to the availability of scrap lead plates and steel shafts from the Mechanical Engineering Laboratory, a container was designed and installed on the upper subframe. A convenient and inexpensive container was constructed from a fifteen and a thirty gallon steel drum, Figure 4-1. These drums were split in half, welded together and mounted on the upper subframe by two 2 inch x 1/8 inch steel strips attached through four 5/16 inch bolts, Figure 4-2. This arrangement permits the addition or subtraction of

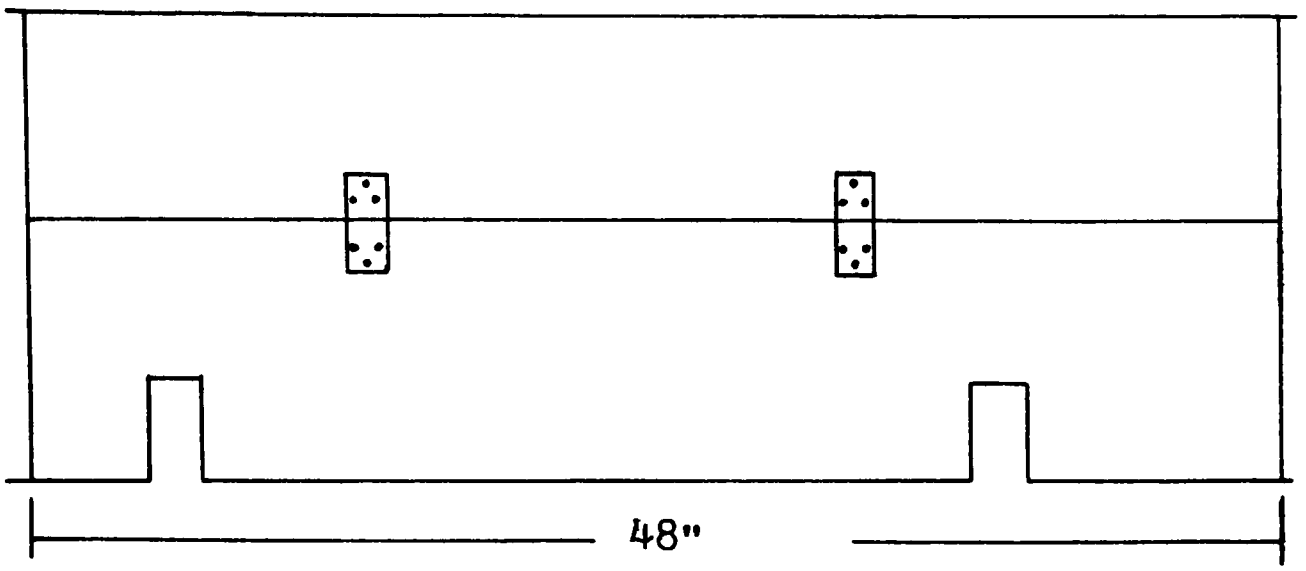

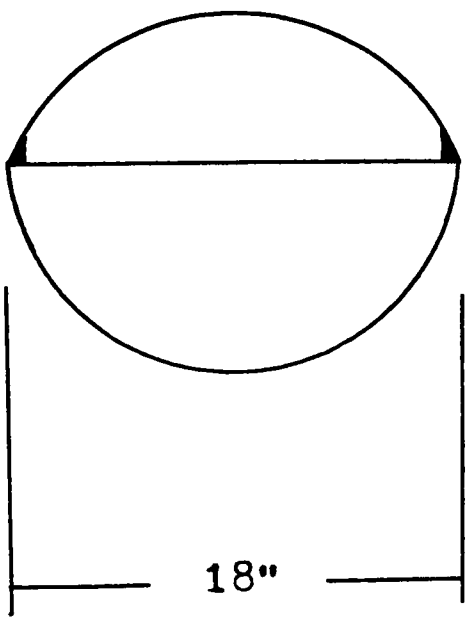

Figure 4-1. Ballast Container

TEXAS TECH LIBRARY

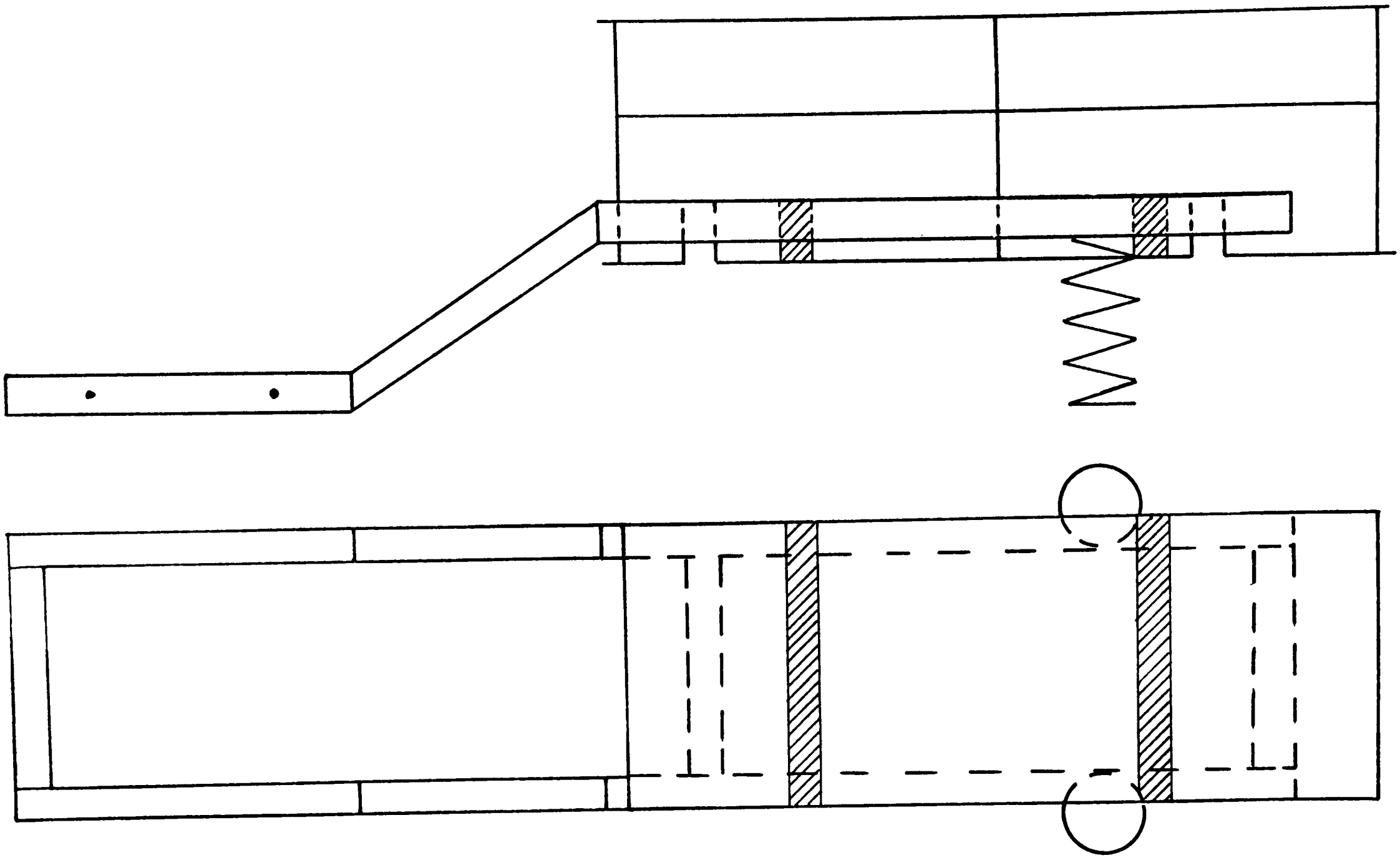

Figure 4-2. Installation Of Ballast Container

ballast, as individual testing sequences requires, to increase or decrease the axle tire loading. Using this arrangement and calculations of the trailer loading, 700 pounds of ballast were added to produce the axle tire loading of 1000 pounds, Figures 4-3, 4-4, 4-5 and 4-6. This loading of the upper subframe will produce an approximate trailer tongue load of 365 pounds which permits safe towing of the trailer by the towing vehicle. After the additional weight had been added to the upper subframe, it was evident that the original coil springs were not sufficiently adequate to support the 700 pound load. A helical spring formula from Stamper (12) was used to determine the total spring displacement which could be expected when the 3/8 inch rod diameter coil springs were fully loaded with the 700 pounds.

$$K = \frac{Gd^4}{64\ N\ R^3}$$

where: K = spring stiffness

G = modulus of elasticity, assuming the springs will be made of mild steel, $G = 12 \times 10^6$

d = diameter of spring rod (.5 in)

N = number of coil turns (7.5 turns)

R = radius of overall coil (2.375 in)

Using this formula, it was determined that the 3/8 inch rod diameter springs would have a total of 9.48 inch

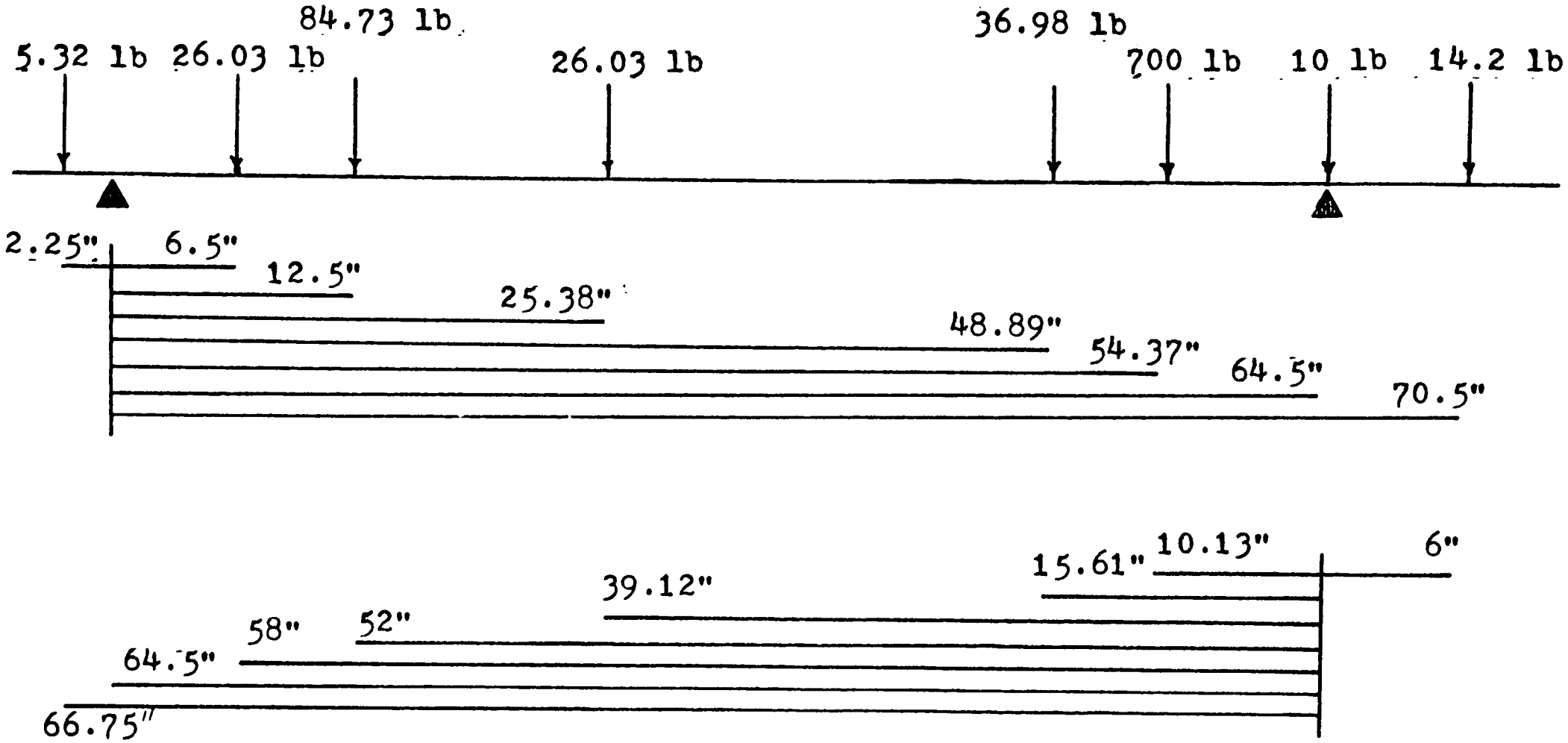

Figure 4-3. Upper Subframe Loading

TEXAS TECH LIBRARY

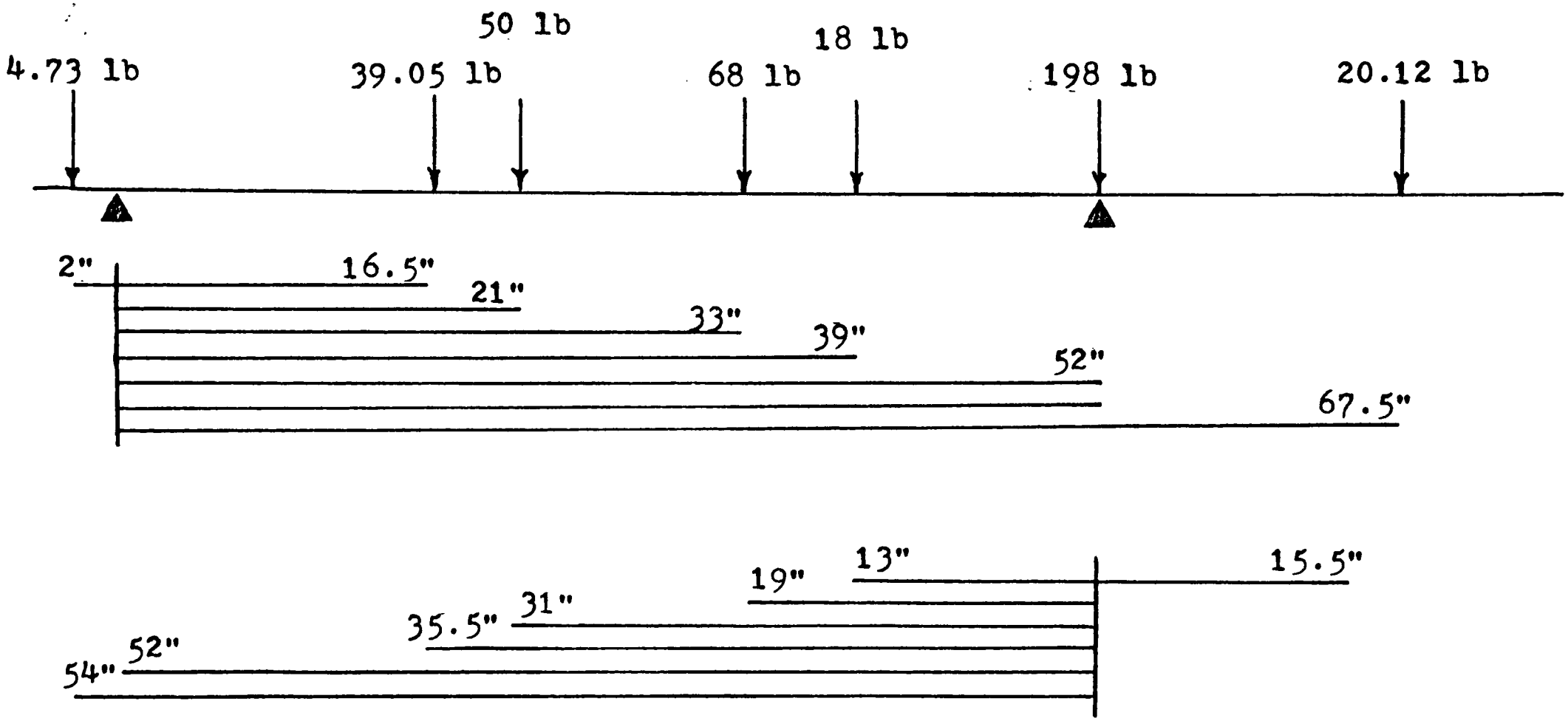

Figure 4-4. Lower Subframe Loading

TEXAS TECH LIBRARY

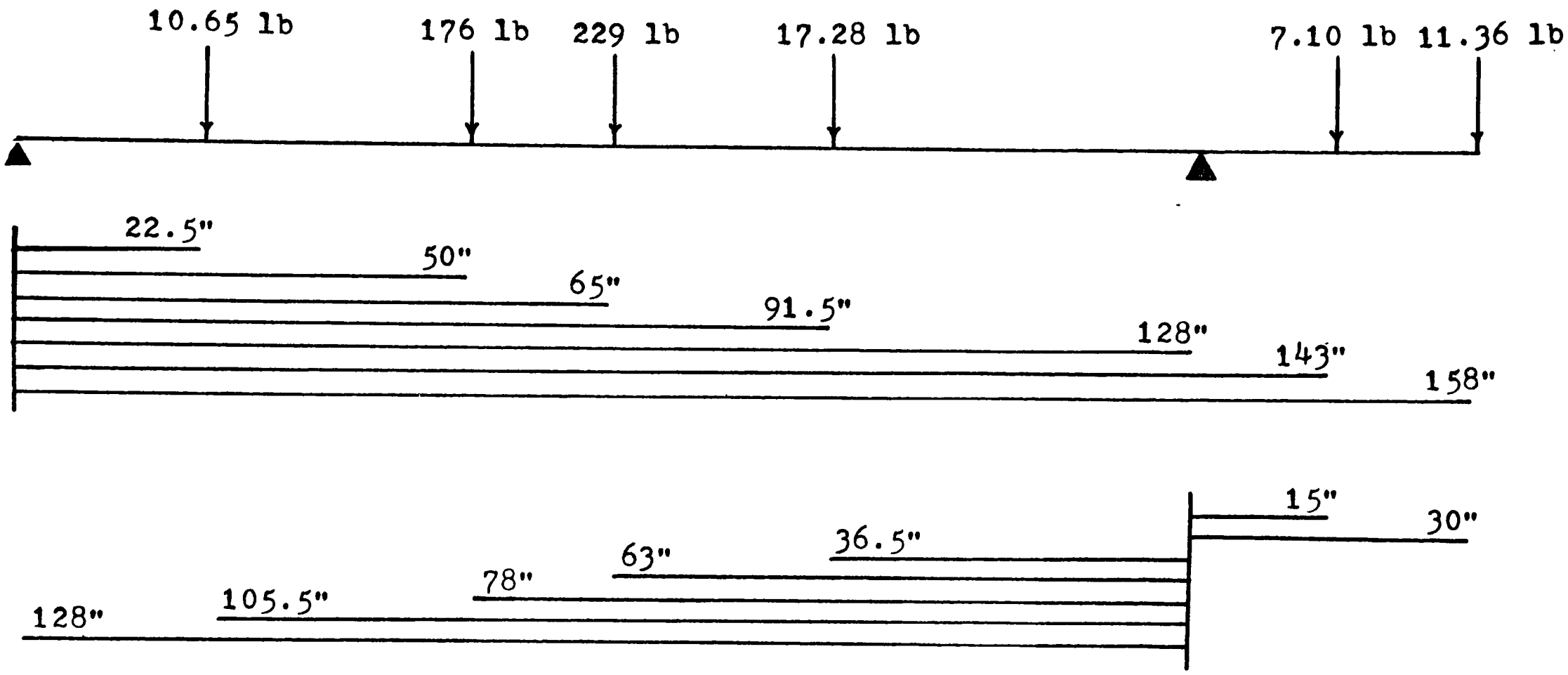

Figure 4-5. Stabilization Trailer Loading

TEXAS TECH LIBRARY

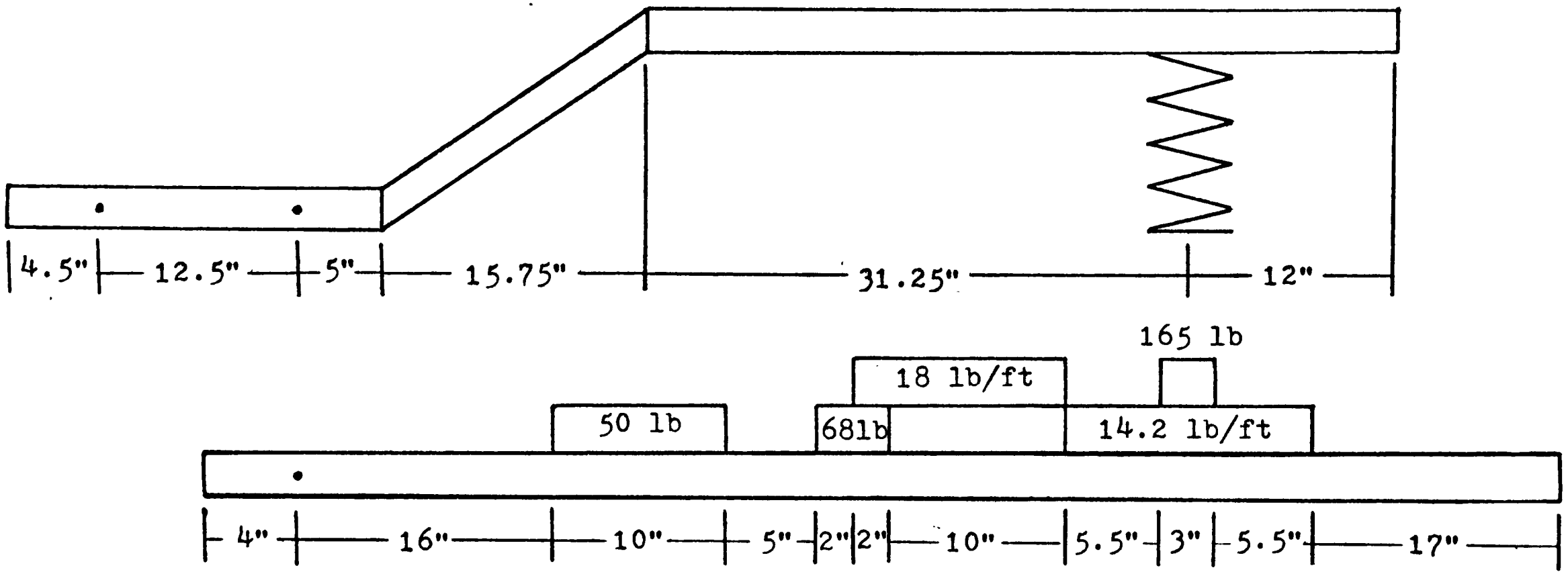

Figure 4-6. Relative Positioning Of Upper and Lower Subframe

TEXAS TECH LIBRARY

deflection. This presented a serious problem when transporting the trailer to any test site, i.e., this amount of free travel, would cause the trailer to "bottom out" if the trailer encountered a sharp bump in the road, thus damaging the mounted test equipment along with possible deformation to the structure of the trailer. It was decided to change the 3/8 inch rod springs in favor of new coil springs which would limit free deflection. Again using the helical spring formula, and knowing the amount of spring deflection allowed, a new spring design could be computed. Assuming that 1/2 inch diameter rod springs could be easily obtained from a local salvage dealer, a total deflection of 3 inches was computed. This deflection was within the design constraints of the overall trailer, so the new springs were ordered. Reviewing available coil springs at a local salvage dealer, it was decided to use 1973 Chevy Vega front end coil springs. This significantly increased the load capacity and provided for safer trailer operations. Also, adding these coil springs would permit any loading combination that should be required for future testing with the trailer.

Trailer Stabilization

After the additional weight was added to the upper subframe, an instability phenomenon was noted. This instability would present serious problems when the trailer

was transported from the Mechanical Engineering Laboratory to a test site. To correct this problem, a two-way stabilization system was designed and constructed to permit safe transportation from place to place. To restrict the up and down motion and the side sway of the ballast, a torsion bar was placed between the upper subframe right hand side and the lower subframe left hand side, Figure 4-7. This will reduce the instability caused by the trailer hitting a chuck hole or the stabilization trailer's wheel falling off the berm of the road. To further restrict the vertical movement of the lower subframe, two 10 inch square, 1/4 inch thick mild steel plates were attached to the rear of the lower subframe and the rear of the stabilization trailer, Figure 4-7. The two plates are clamped together onto the frames by six 1/2 inch x 4 inch bolts. Both pieces of stability equipment have been designed to permit easy attachment and removal in the field.

TECH LIBRARY

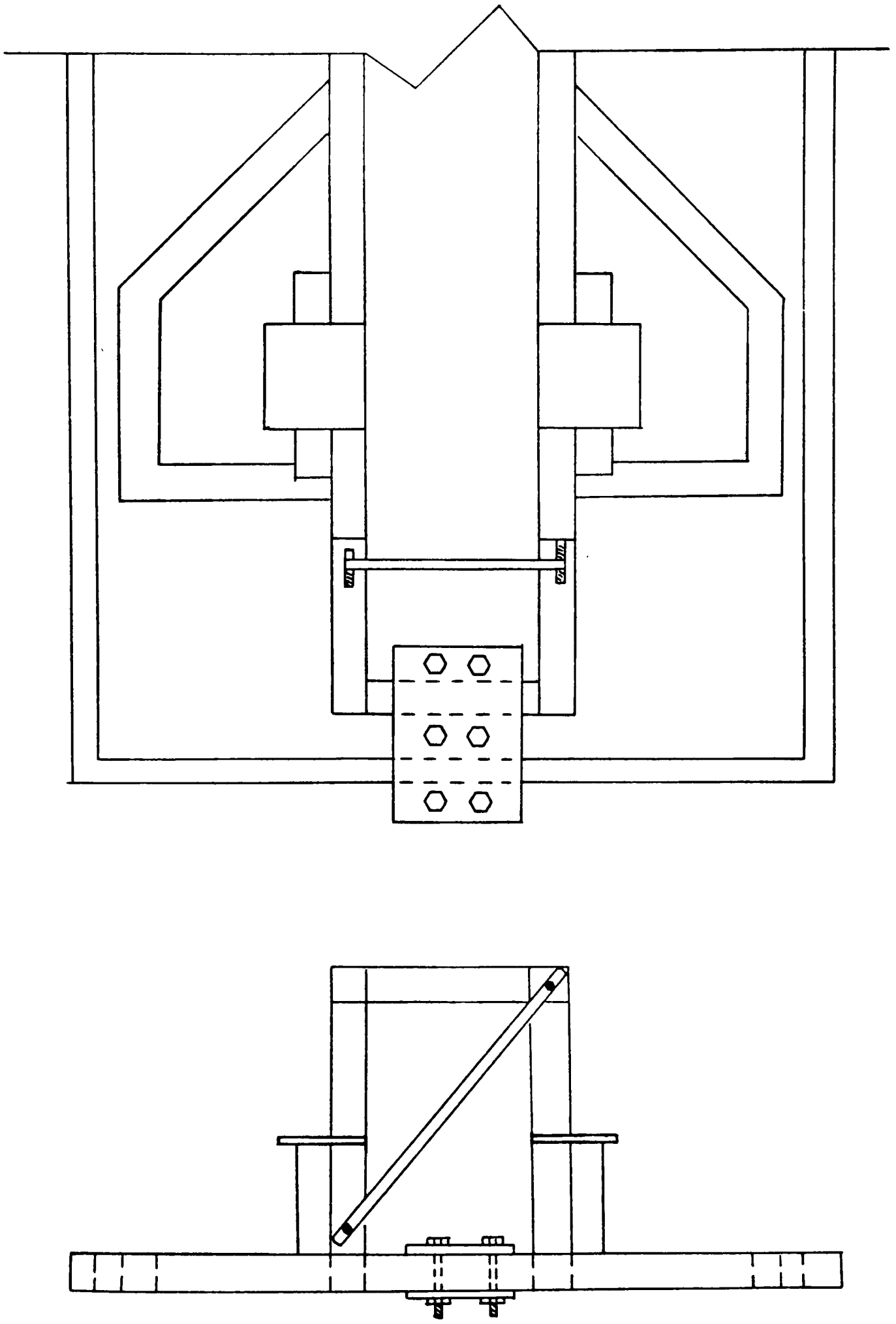

Figure 4-7. Installation Of Stabilization Torsion Rod And Horizontal Flat Plate

TEXAS TECH LIBRARY

CHAPTER V

COLLECTING OF BASELINE DATA

The installation of the new control box required that a new set of instructions had to be developed before any results could be collected for establishing baseline data. The baseline data would be used in comparison with previously collected data for the test tire, Mathew (4). The new instructions used to test a sample tire are as follows:

1. First select the amount of frequency excitation desired in the rotating disks from installation of bolts, washers and nuts. Both Campbell (1) and Pirtle (3) include tables useful for making the proper selection.

2. Check all belts, pulleys, bearings, guards, etc, for mechanical looseness and connect the battery cables to the appropriate terminals, Figure 2-4.

3. Plug the black and brown cables (accelerometer and magnetic pickup tachometer) from the trailer into the inputs of channels 1 and 3 of the Tanberg data recorder, Figure 2-4. Channels 1 and 3 of the recorder have an input range of 5 and 2 volts respectively. Channel 4 was used for voice instructions.

4. With the accelerometer switch turned on at the control box, use the input offset knobs on the Tanberg recorder to zero the incoming signal (position tracking

TEXAS LIBRARY

beam on the center line of the monitoring window of the Tanberg recorder).

5. With the accelerometer current on, record a few feet of tape to record the D.C. signal offset.

6. On the trailer, turn on the switch that supplies voltage to the breaker circuit for the tachometer in the control box. Make sure the tachometer cabling is plugged into the proper receptacles in the control box (red to red, black to black).

7. Before turning on the motor switch on the control box, make sure the field rheostat control is turned completely clockwise (low speed). All other switches, except the accelerometer switch which is on from step 4, should be in the off position.

8. The system is now ready to record test data. Press the Record Button, and move the tape drive lever up to the forward (→) position. Recording now begins. After recording a few feet of data (D.C. offset), turn the motor switch on. There is a choice of motor switches. The one near the field rheostat is used for 12 volt operations (slow speeds) and the motor switch on the right (24 volts) is used for all other operations. This will produce frequencies up to approximately 110 Hz, depending upon the condition of the batteries used to drive the motor. Normally, the 24 volts system is used for all trailer operations. After the motor switch is turned on, the

TEXAS TECH LIBRARY

field rheostat is turned slowly counterclockwise as far as it will go. During this operation the motor will speed up quickly. After reaching maximum counterclockwise position with the rheostat, slowly turn the field rheostat in a clockwise direction (motor slowing down) to its lowest setting, then turn off the motor switch.

9. After the motor and system have stopped moving, turn the accelerometer switch off along with the recorder's forward switch.

This entire procedure was repeated for other tests, i.e., different road speeds and tire pressures.

The recorded data is then previewed using a dual scope oscilliscope which will relate the recorder output from the accelerometer and tachometer channels. If the recorded data is acceptable, rewind the data, plug the output channels into the Hewlett-Packard Sanborn oscillographic recorder and replay the data at a speed that is desirable for analysis purposes.

After a series of testing with one tire and a set of bolts:

1. Turn off the recorder.
2. Turn off the breaker points switch on the trailer.
3. Turn off the oscilliscope.
4. Disconnect the battery connections.
5. Check the trailer for loose equipment and parts.
6. Examine all bearings for heat, oil leakage and

TEXAS TECH LIBRARY

other possible failures.

7. Check the timing belts for possible excess slack.

After establishing the above procedures, baseline test data could be acquired for the GR70-15 steel belted radial tire, plus an analysis of the trailer without a test tire attached (trailer resonant frequencies). After one tire pressure and the bare trailer were tested, serious problems were noted when trying to analyze the recorded data. The initial tests were conducted using previously installed instrumentation. This instrumentation consisted of three Genisco, Model GM02063, $\pm$ 50 g's accelerometers. They had been installed at three locations on the trailer to monitor, as closely as possible, the tire vibrations generated by the counter-rotating disks. These accelerometers could not be directly mounted to the trailer axle, which is the desired location, due to having a live axle (an axle which turns). Therefore, the accelerometers were positioned on the axle mounting housing, one on the right side, the other on the left side. The other accelerometer had been mounted on the upper subframe to monitor the vibration effects on the ballast. Unfortunately no discernable resonant frequencies could be read, and unsymmetrical traces appeared after the data was recorded on the Hewlett-Packard oscillographic recorder. Sample oscillographic charts are presented in Appendix A. It was decided to replace all the accelerometers for more

TEXAS TECH LIBRARY

sensitive ones. New accelerometers, manufactured by CONRAC Corporation, Model 24158, having a sensitivity of ± 5 g's were installed in the same location as the old Genisco accelerometers. After the installation was completed, tests were conducted and analyzed. The output from the new accelerometer was more desirable, but random noise spikes were generated which prohibited reading the exact points where maximum frequencies occurred. A constructive program was developed and followed to determine and eliminate the cause of this noise. First, the entire trailer was rewired using shielded cable. Then each accelerometer was mounted on a piece of 1/8 inch rubber sheeting. Still the noise spikes persisted. The D.C. motor was covered with a piece of aluminum foil. Still the spikes persisted. The accelerometers were removed, and mounted on a shaker table to determine if any accelerometer was defective, over stressed, or if the noise was coming from elsewhere within the trailer. The shaker table results concluded that the noise spikes were coming from within the trailer. Upon analyzing the trailer, it was noted when the original trailer was developed, the designer was cautious to eliminate all the up and down vibration within the trailer, except the vibrational forces caused by running the timing belts, which drive the counter-rotating disks. At high revolution per minute, these belts developed "belt slap" which was being transmitted through the trailer into the

TEXAS TECH LIBRARY

accelerometers. To eliminate this "belt slap", idler tension pulleys were constructed and installed on the lower subframe, Figures 5-1, 5-2, and 5-3. Another test run was performed and the results analyzed. The noise level was significantly reduced, but not eliminated completely. Also the same unsymmetrical results between the left side and right side lower subframe axle mountings were still present. Again using the shaker table, respective outputs were compared. It was established that under the same type of vibrational driving potential, these accelerometers would produce almost the same results. After a discussion with the Research Advisor, it was decided to install more sensitive piezoelectric accelerometers on the lower subframe axle mountings. The use of these piezoelectric accelerometers required the use of a Brüel and Kjaer charge amplifier which had an input sensitivity from 1-10 pC/g. Again the shaker table was used to determine if the individual output levels were equal. After setting the charge amplifiers, to produce similar outputs, another trailer test run was conducted again with the same unsymmetrical results. It was then thought that the accelerometers were either overdriven or underdriven through the use of the 1/4 inch eccentric bolts. Therefore, both smaller and larger bolts, nuts, and washers were installed and the testing procedure was repeated. Again the same unsymmetrical results. The author then hypothesized that

TEXAS TECH LIBRARY

TEXAS TECH LIBRARY

Figure 5-1. Upper Idler Pulley

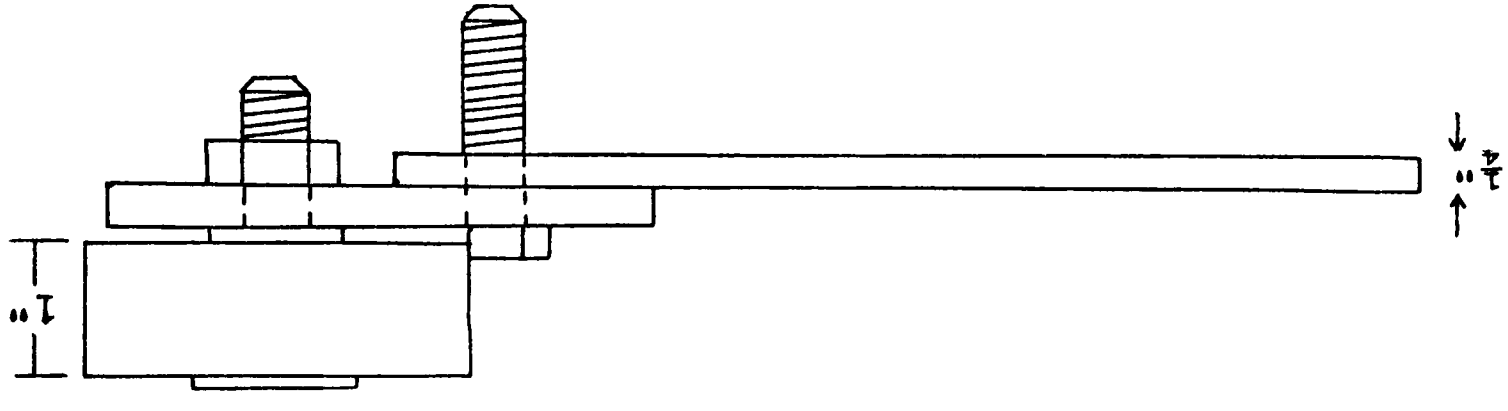

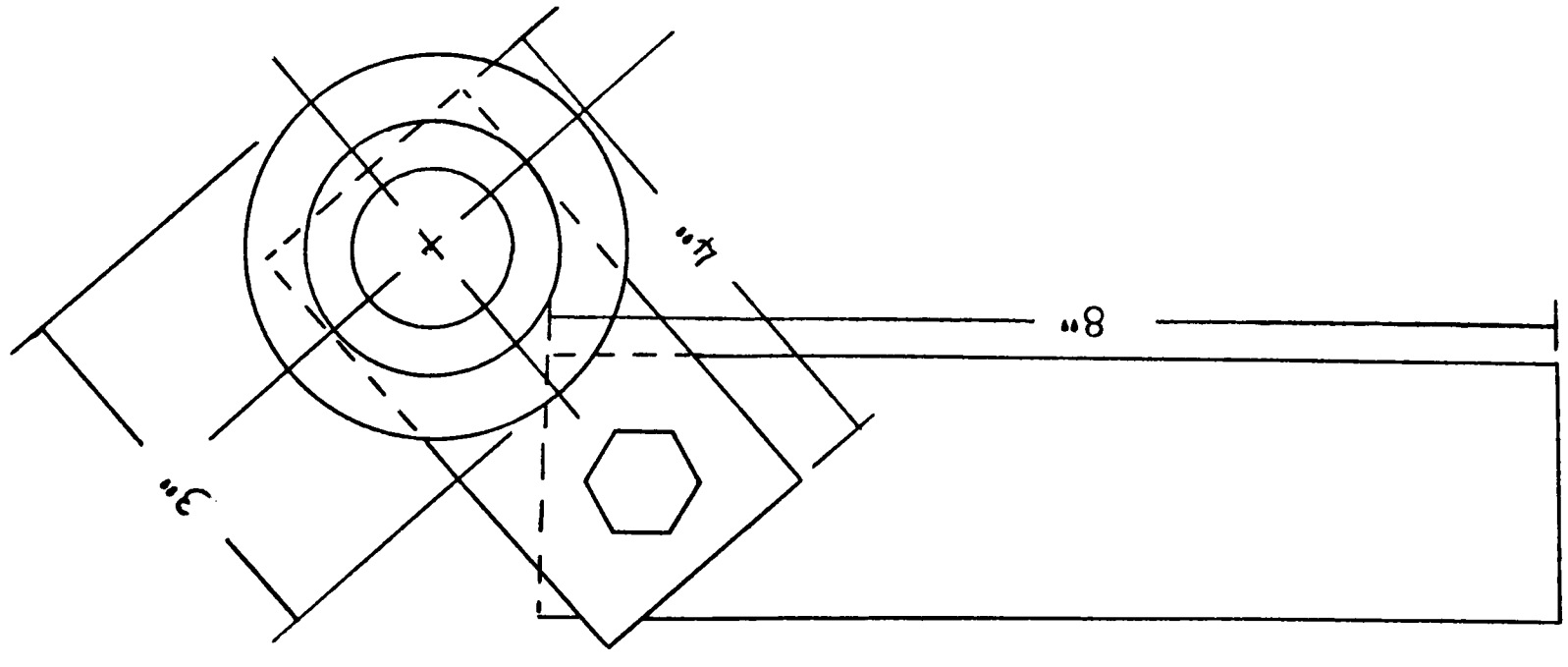

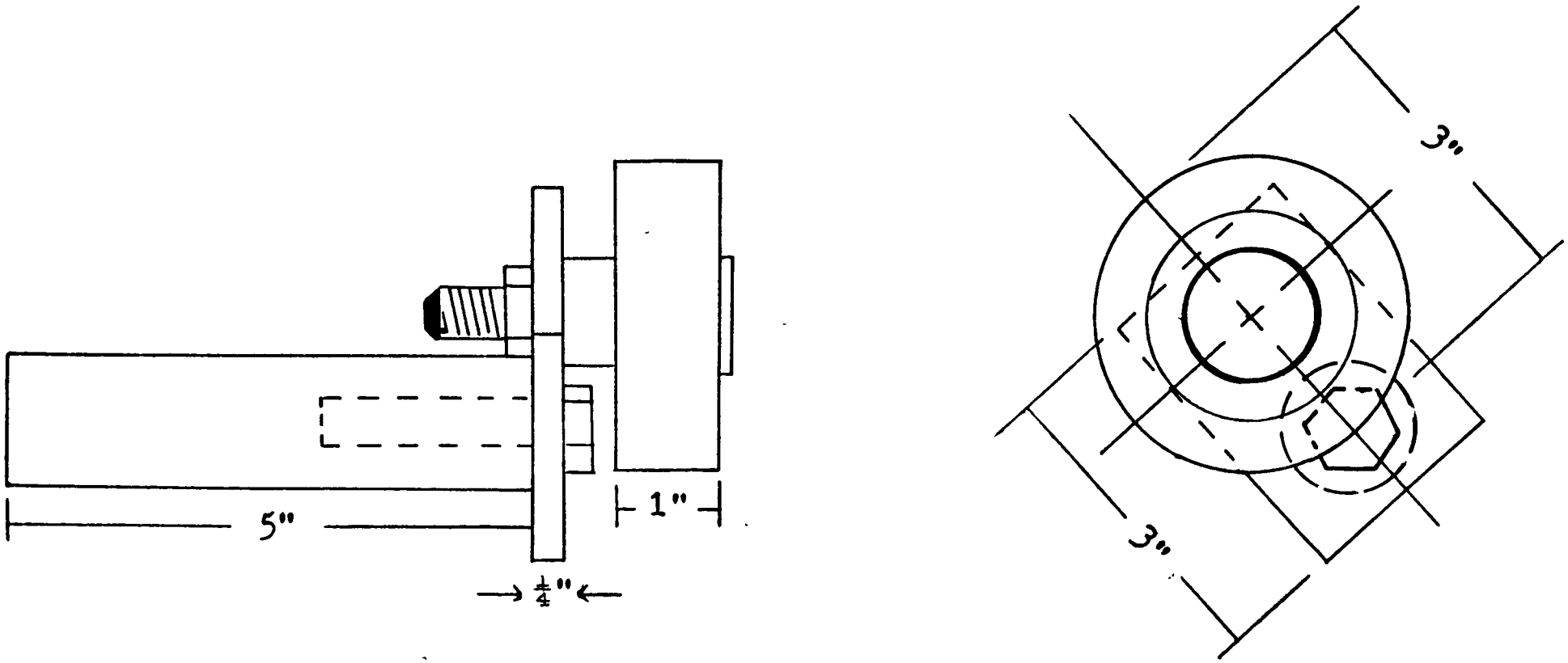

Figure 5-2. Lower Idler Pulley

TEXAS TECH LIBRARY

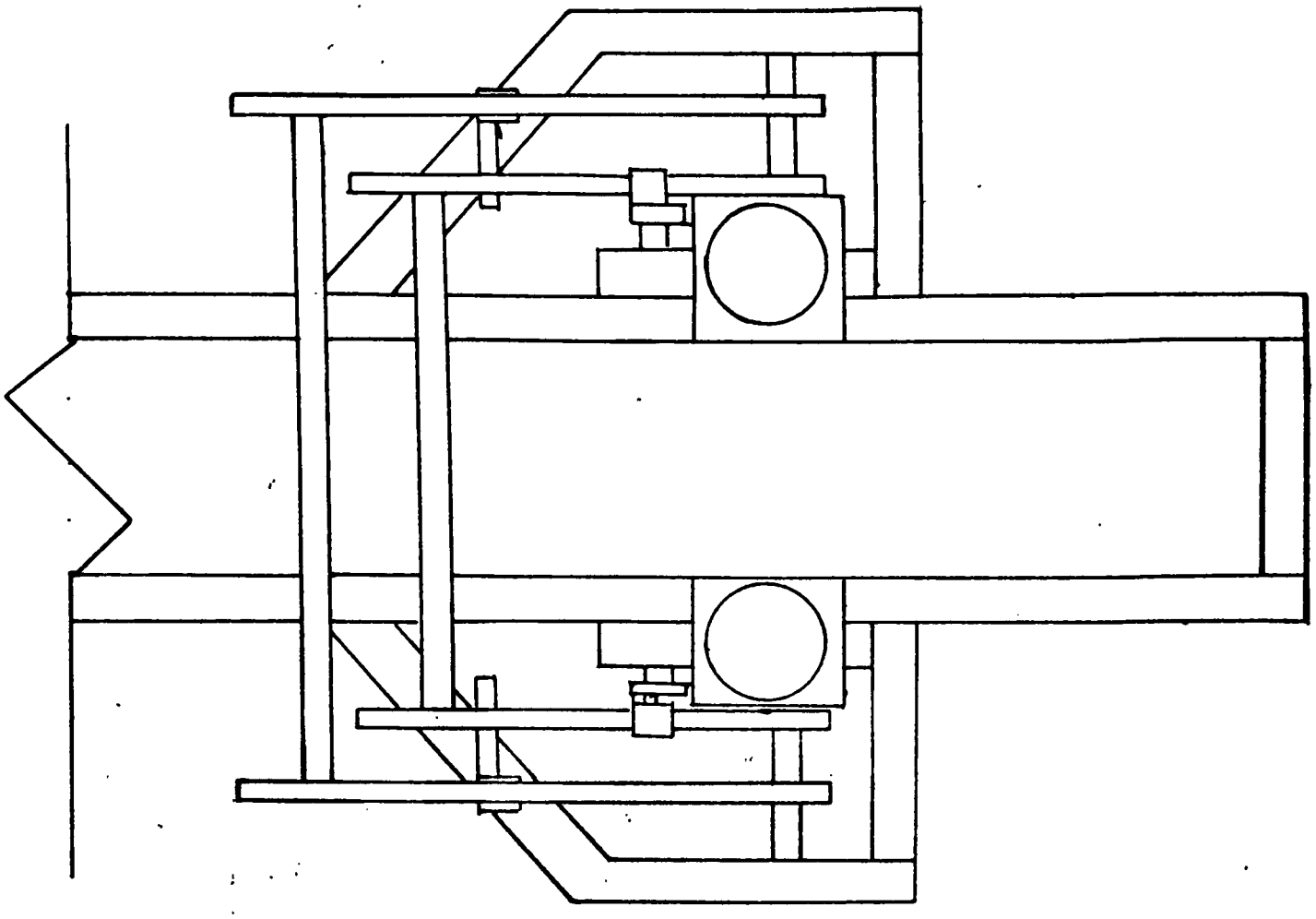

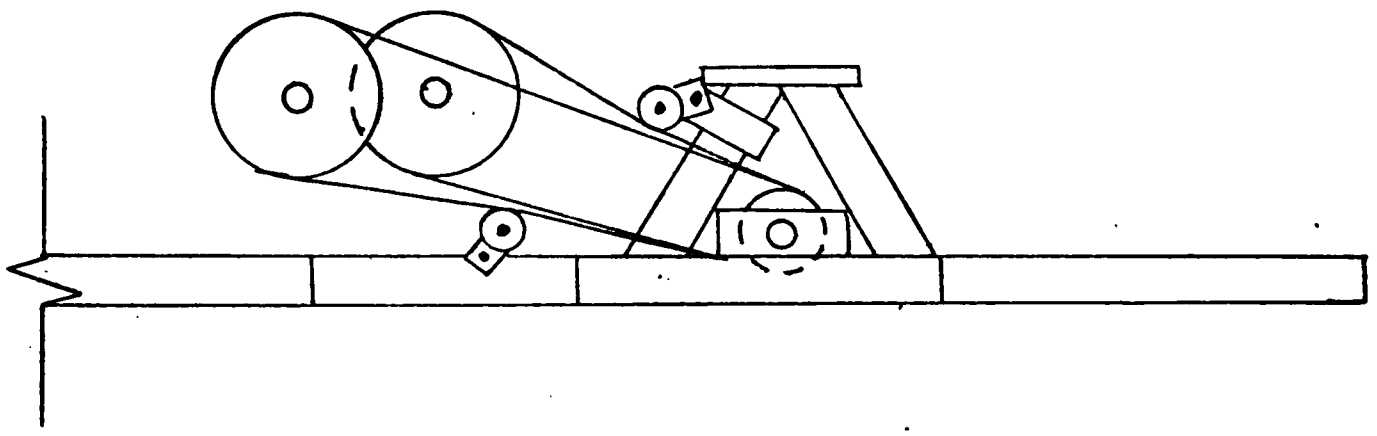

Figure 5-3. Installation Of Idler Pulleys

TEXAS LIBRARY

due to the human factor that went into the construction of the trailer and the manufacturing of the counter-rotating disks, that regardless of what types of accelerometer used, the accelerometers could never have the same readings. Although this unsymmetrical situation could possibly be corrected if (a) the trailer was reconstructed with a different axle arrangement and (b) if the accelerometers could be mounted directly on the axle. The Research Advisor did not consider that this project deserved such an extensive and costly redesign. As an alternative, it was decided to replace the two accelerometer mountings on the axle housing for one central mounted accelerometer placed directly above the test tire and located halfway between each side frame member, Figure 5-4. The initial test was rerun and the results produced data that could now be analyzed. The initial tests were completed for the trailer without the test tire and for the individual sample of the GR70-15 Firestone steel-belted radial tire, accomplishing each test five times to assure consistency. The results of the initial testing are presented in Table III. [47]

This table will be used to subtract out the bare trailer frequencies away from those recorded of each tire test, at a given tire pressure, and road speed. The remaining test data was used to compare resonant frequencies with those recorded for the individual tire in Mathew (4). After the baseline testing was completed,

TEXAS TECH LIBRARY

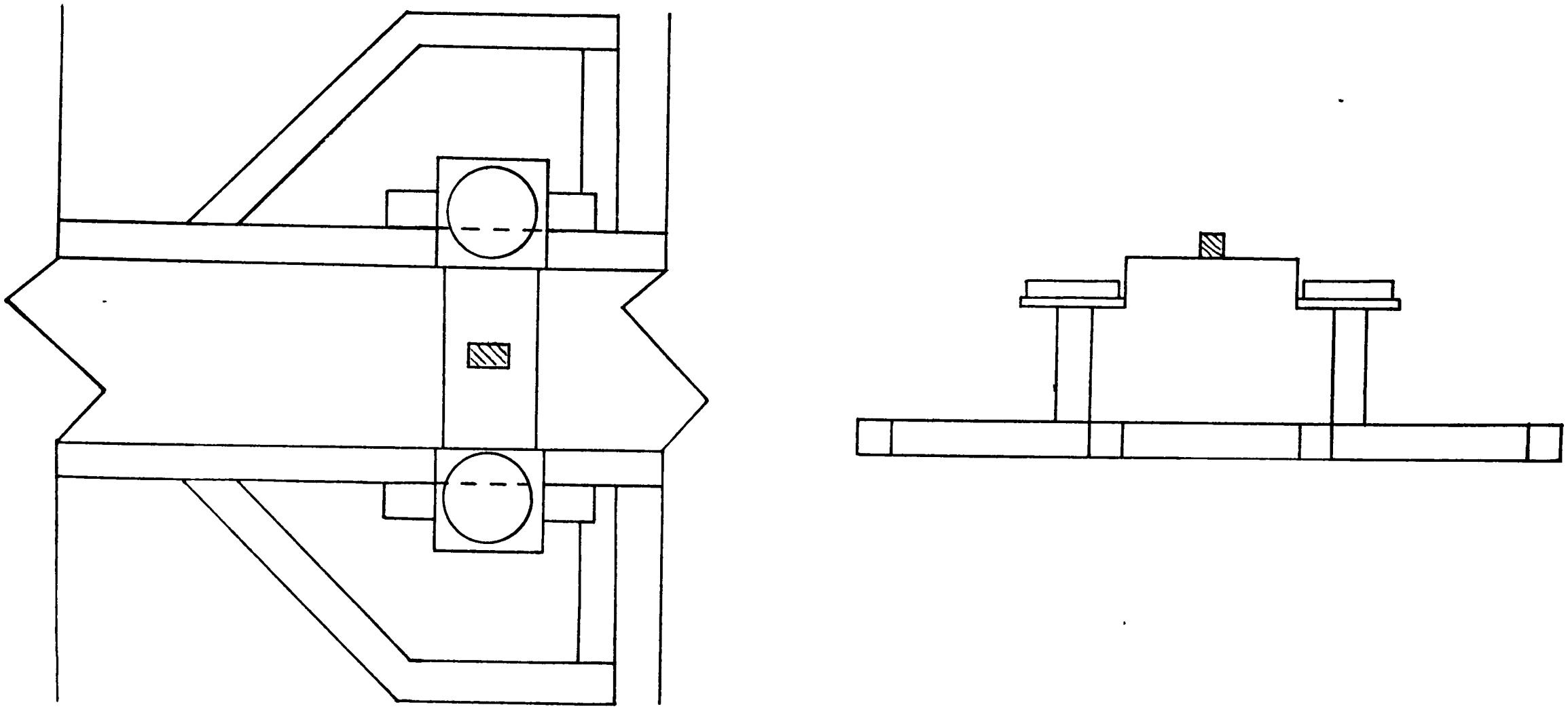

Figure 5-4. New Positioning Of Accelerometer

TEXAS TECH LIBRARY

the trailer was transported outside to conduct the road testing analysis.

TABLE III

INITIAL BASELINE TRAILER DATA WITHOUT AND WITH A TEST TIRE

	No Tire	GR70-15 Steel Belted 28 PSIG	23 PSIG	Radial 18 PSIG
Recorded Frequencies	95	93.01	91.30	92.10
	82	80.55	80.63	80.10
	78	68.91	69.43	67.10
		47.60	51.00	47.40
	28	28.00	28.00	28.00

TECH LIBRARY

CHAPTER VI

COLLECTION OF ROADWAY DATA

The instrumented trailer, having been significantly modified and refined during laboratory testing, was transported outside for the series of roadway tests. In selecting a testing site for conducting all roadway tests, a section of road had to be located which would permit repetitious testing and produce consistent results. It was also desirable to locate a section of roadway which was free of all local traffic. Scouring the local countryside for a desirable test site, two compatible locations were discovered. One site was the Lubbock Drag Raceway and the other was a 1600 foot section of Reese Air Force Base taxiway. Due to the availability of resources and the author being a government employee, it was decided to attempt to use the 1600 foot level concrete taxiway of Reese Air Force Base.

The first person contacted was the Reese Air Force Base Operations Officer, Major Genereaux, who could not grant the required permission to use the taxiway. Major Genereaux informed the author that permission to use the taxiway was secured through the Deputy of Operations, Colonel Crooke, and the Base Wing Commander, Colonel Mendel. Therefore, the author requested permission to use the selected taxiway through Colonel Crooke. The

TECH LIBRARY

permission was obtained predicated on the fact that a standard release form, required by base regulations to release the Air Force from liability, could be obtained from Texas Tech University. This standard release form was obtained through the Reese Air Force Base Legal Office and transmitted to the Texas Tech University Legal Office for approval. Upon reviewing the standard release form, the University Legal Council, Mr. C. B. Dodson, informed the author that he could not recommend to the University that they sign the release form. The wording of the release form was not compatible with Texas state laws governing university procedures. The release form was returned to the Reese Air Force Base Legal Office for a revision writing which would conform with Texas state university laws. After the Air Force Legal Council, Captain P. Cox, reviewed the changes requested by Mr. Dodson, Captain Cox rewrote the release form and the author transported the form back to the University Legal Office. After reviewing the revised release form, Mr. Dodson still refused to recommend to the University that they sign the form. At this point, Mr. Dodson recommended that the author take the release form to the University Contract Maintenance Office to obtain the proper wording that was required by the Texas state laws. Again the release form was rewritten, and it was transported back to Captain Cox for his approval. When Captain Cox read the revised release form, he agreed that the form was

TEXAS TECH LIBRARY

acceptable to the Air Force. Next, the revised form was returned to the University Legal Council for a signature. Mr. Dodson reviewed the revised release form, rewritten by University personnel, and after all these tedious negotiations, he refused to recommend to the University that they could sign the release form. He also recommended that the University should not accept the responsibility since the activity (tire vibrational tests) was not under the direction, supervision, control and a part of the educational and research activities of the University personnel per se. Therefore, this official status recommendation to the University President, Vice President, and the Graduate School Dean, along with the failure to obtain the required University signature, meant that all roadway tests would have to be conducted elsewhere.

As mentioned previously, the Lubbock Drag Raceway had been selected as a compatible test site. Further investigations of this possible test site revealed that there would be scheduling problems. Also, because of the increased distance of the test site from the University (testing necessitated that the batteries be frequently recharged to continue testing), it was decided to search for an alternate test site.

Again combing the local area around Lubbock, an alternate test site was selected. This site was on West Fourth Street, outside the city limits of Lubbock, Figure 6-1.

TECH LIBRARY

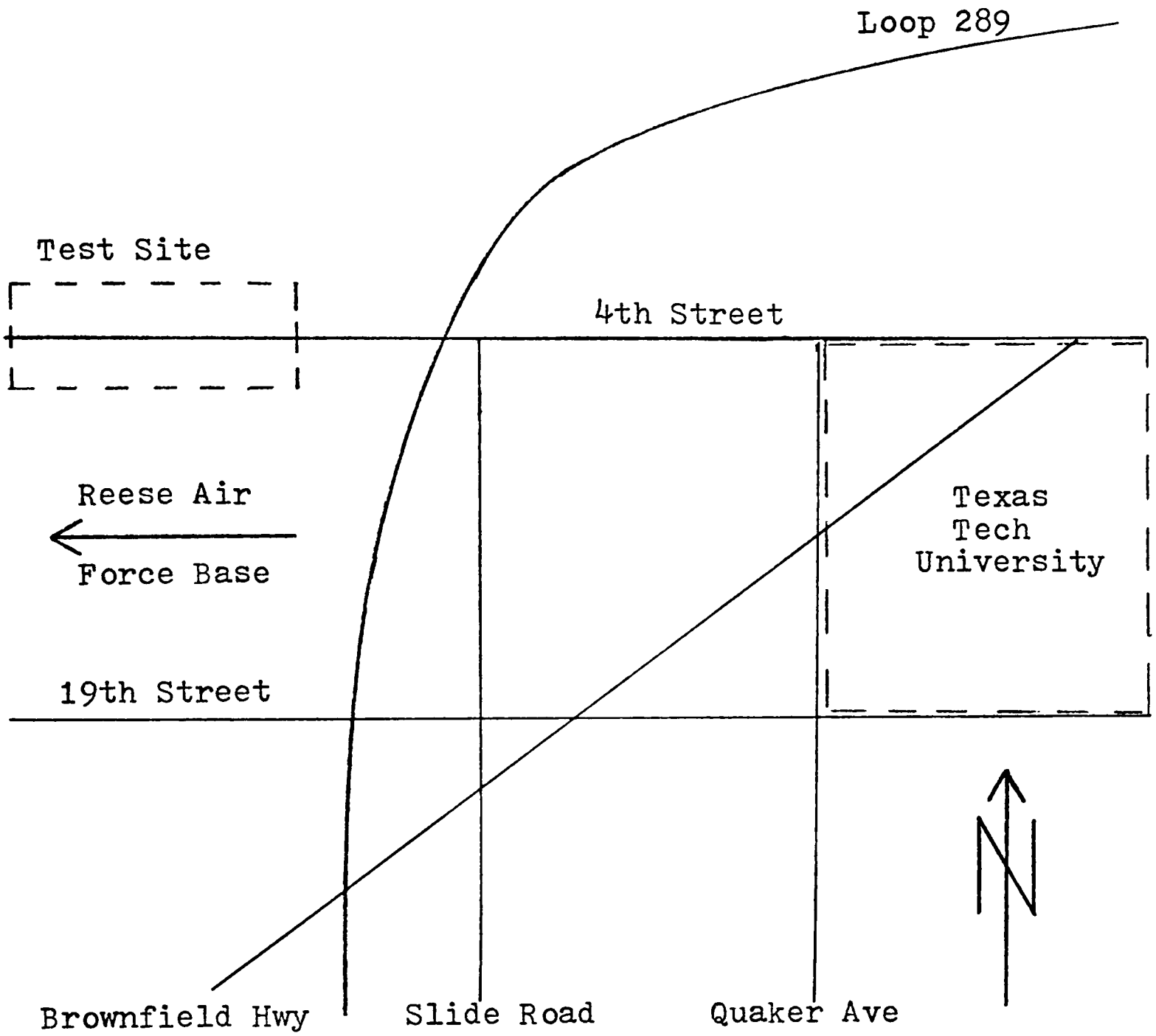

Figure 6-1. Selected Roadway Test Site

This test site was less desirable than the Reese Air Force Base taxiway or the Lubbock Drag Raceway due to the non-level surfaces, pot holes and other imperfections normally found in any asphalt road. It should also be noted that most testing was accomplished after 10:00 pm to

TEXAS TECH LIBRARY

eliminate the safety hazard caused by the local vehicular traffic. Using the outstanding driving assistance of Mr. Donald E. Gonder, a Mechanical Engineering graduate student, all tire tests were conducted on this stretch of road. It was discovered that if the trailer was towed in the center portion of this four lane highway, a nominal six hertz towing frequency was encountered. Assuming this frequency would not affect the data reduction, specific roadway tests were begun. Initial testing started at 55 mph with a tire pressure of 28 pounds per square inch gauge (psig). Also for each test series, the tire temperature was recorded by placing a thermometer against the tire sidewall for 5 minutes. During all tests this temperature did not vary significantly with an average temperature of 70° F. All tests were performed a minimum of three times for each road speed and tire pressure. After the first tire pressure was run, the trailer speed was reduced 10 mph and the next test was performed. Having completed six test runs (three at 55 mph - 28 psig and 45 mph - 28 psig), the trailer was stopped and the tire pressure was reduced to 23 psig. The roadway tests then continued with 55 mph - 23 psig and 45 mph - 23 psig. After two roadway speeds were finished using the three different tire pressures (18 tests), the trailer was brought back to the author's house and the batteries were recharged. During the battery recharging phase, the

TECH LIBRARY

analog taped roadway data was previewed using a dual beam oscilloscope. This previewing gave an indication of which tests would have to be reaccomplished. Having noted which tests were to be rerun and the batteries recharged, the next series of roadway tests could begin.

At this point the general method of collecting roadway data will be explained. First the trailer was attached to the towing vehicle, the author's 1973 Dodge Van. The cables from the accelerometer and the monitoring tachometer, black and brown respectively, were connected to channels 1 and 3 on the Tanberg recorder. A 110 volt power supply inverter was provided by the Mechanical Engineering Department to run the Tanberg recorder. The trailer control box was placed in the van beside the recorder. Now all trailer operations could be controlled, monitored (using the recorder's viewing window) and recorded from the interior of the van. This basic setup was used to perform all roadway testing.

Data Analysis

After all roadway data tests were conducted, the Tanberg recorder was transported back to the Mechanical Engineering Laboratory where it was connected to the Hewlett-Packard Sanborn oscillographic recorder. This oscillographic recorder allowed all taped roadway data to be converted into strip chart graphs which displayed the

accelerometer response and the D.C. motor speed (monitoring tachometer) simultaneously.

These strip chart graphs were reduced using a magnifying glass and counting the number of sinusoidal curves that occurred when a resonant frequency was reached, a point when the accelerometer output graph reached a maximum amplitude. Appendix A presents typical strip chart graphs that were read for all laboratory and roadway tests. Note these data are analyzed by locating a peak point on the accelerometer graph, then reading the frequency from the monitoring tachometer graph (the number of counted curves from the tachometer trace must be doubled to read the actual number of sinusoidal curves - motor speed x 2 = disk speed). After reducing all the strip chart graphs, resonant frequency plots were constructed by averaging similar frequency values of a minimum of three runs made for each specific tire pressure and road speed. These resonant frequencies were plotted as a function of road speed, Figure 6-2, and as a function of tire pressure, Figure 6-3. Notice that the top curve in Figure 6-2 has a slightly negative slope when compared with the other curves in the graph. This negative slope can be explained as follows. When each strip chart was processed, a relative maximum deflection in the accelerometer graph was present at the maximum D.C. motor speed (around 3300 rpm). But when this deflection was compared with the other deflection

TEXAS TECH LIBRARY

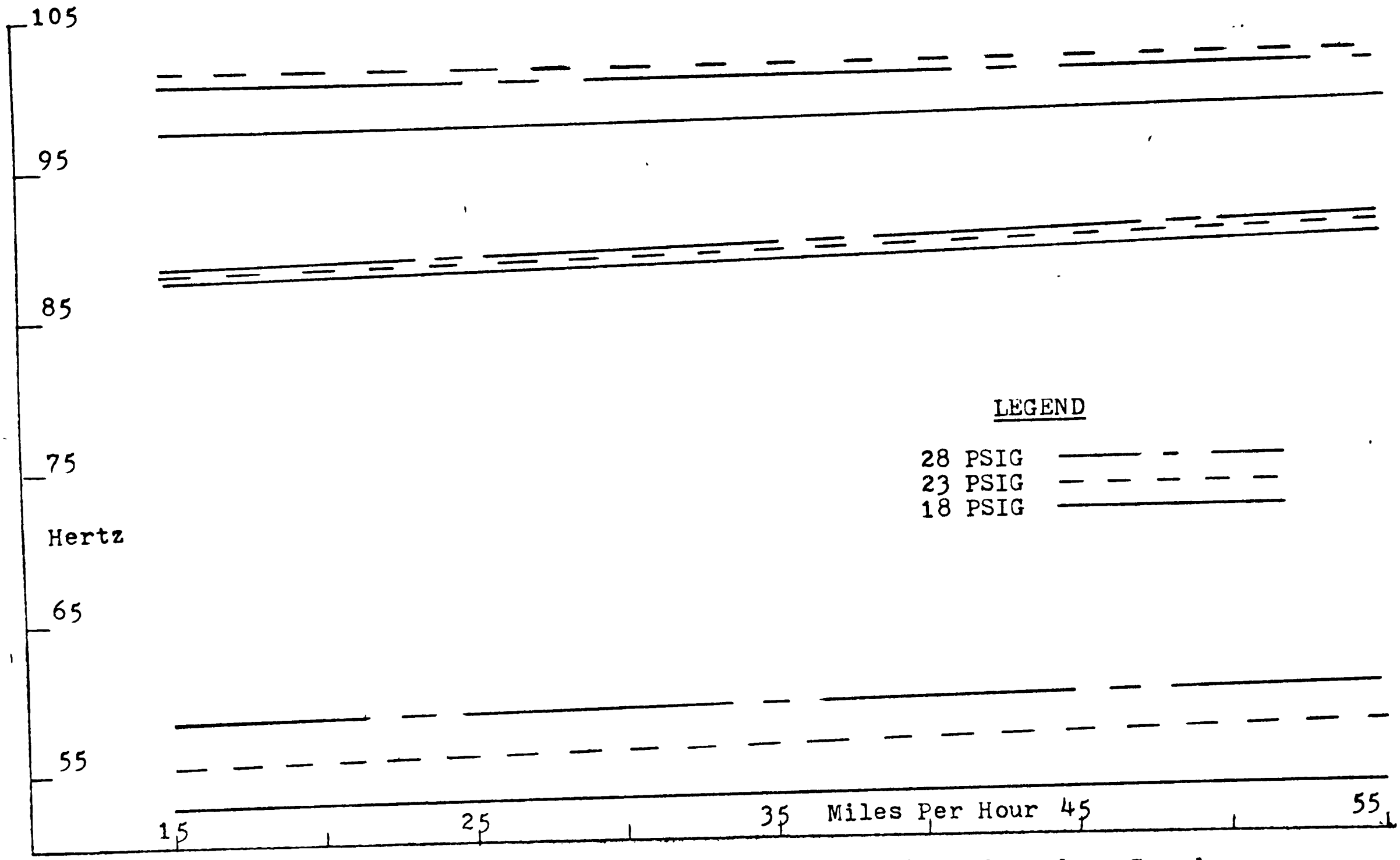

Figure 6-2. Tire Resonant Frequencies Plotted As A Function Of Roadway Speed (Hewlett-Packard Sanborn Oscillographic Recorder)

VETERS FIELD LIBRARY

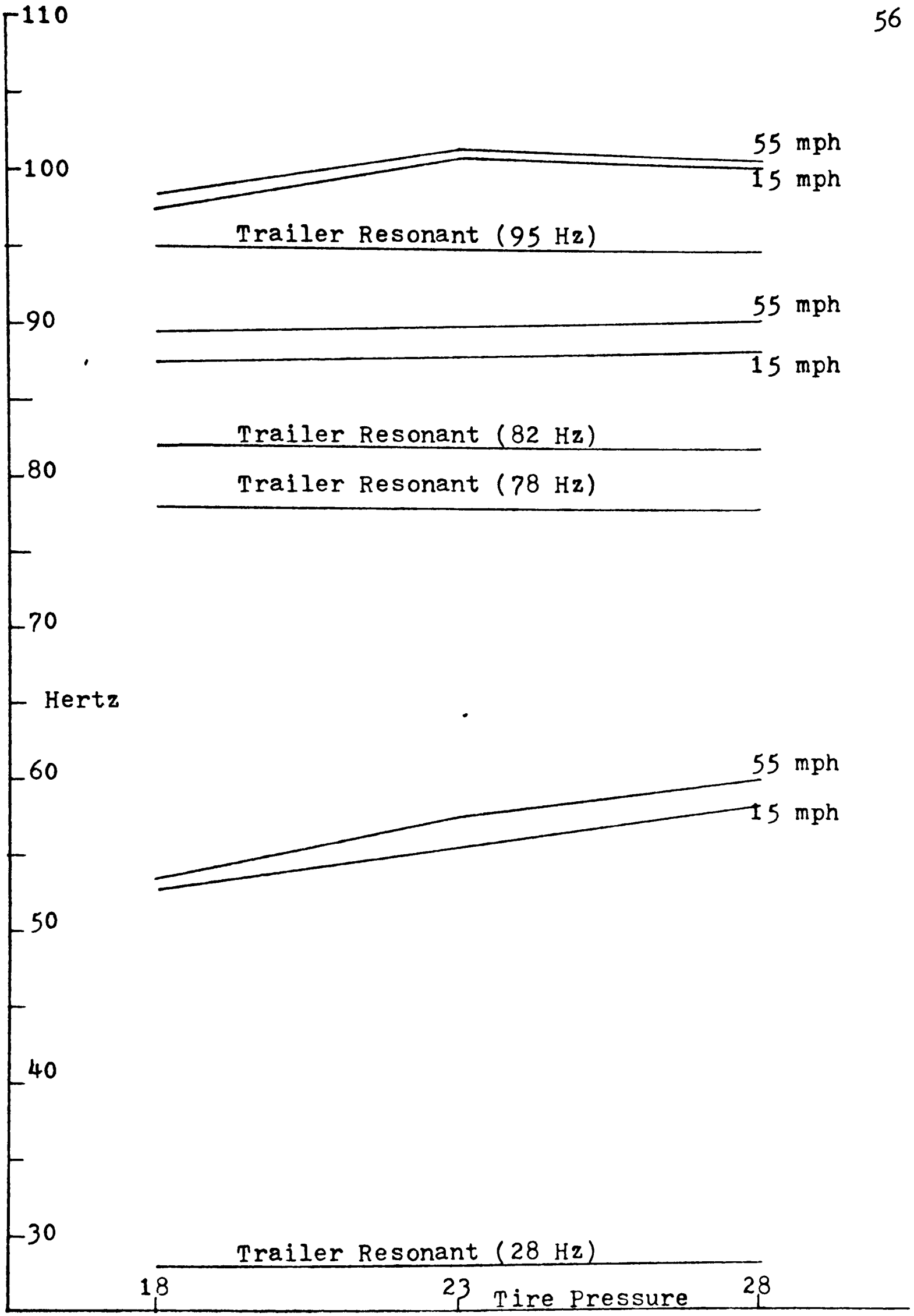

Figure 6-3. Tire Frequencies Plotted As A Function Of Tire Pressure (Hewlett-Packard Oscillographic Recorder)

points, it was not accurately defined, but approached a resonant frequency. Therefore, it was included as a data point. If a higher disk speed could have been obtained, this high resonant frequency point would have been clearly defined (motor speeds over 4000 rpm). Using this edification, the upper curve in Figure 6-2 could have a positive slope if the higher disks speeds could have been obtained.

Figure 6-3 can be compared directly with the reduced data presented in Mathew (4). Figure 6-4 is a reproduced copy of this reduced data and can be compared directly with Figure 6-3. Also included in Figure 6-3, are the trailer resonant frequencies to show that they did not vary from test to test (neither tire pressure or roadway speed related). Figure 6-3 only represents the low tire resonant frequencies because to obtain the higher frequencies as defined in Figure 6-4, the motor speed would have to have been over 5000 rpm or disk speeds of more than 10000 rpm. These speeds can not be obtained with the present trailer setup. Besides the overall trailer construction had not been designed for these high speeds. Attempts to obtain these higher speeds, using the present setup, could result in possible catastrophic results (disk separation, ruined bearings, shattered safety shields, etc).

The Hewlett-Packard Sanborn frequency oscillographic recorder produced preliminary data analysis that was very subjective to human reading error. Therefore, a more

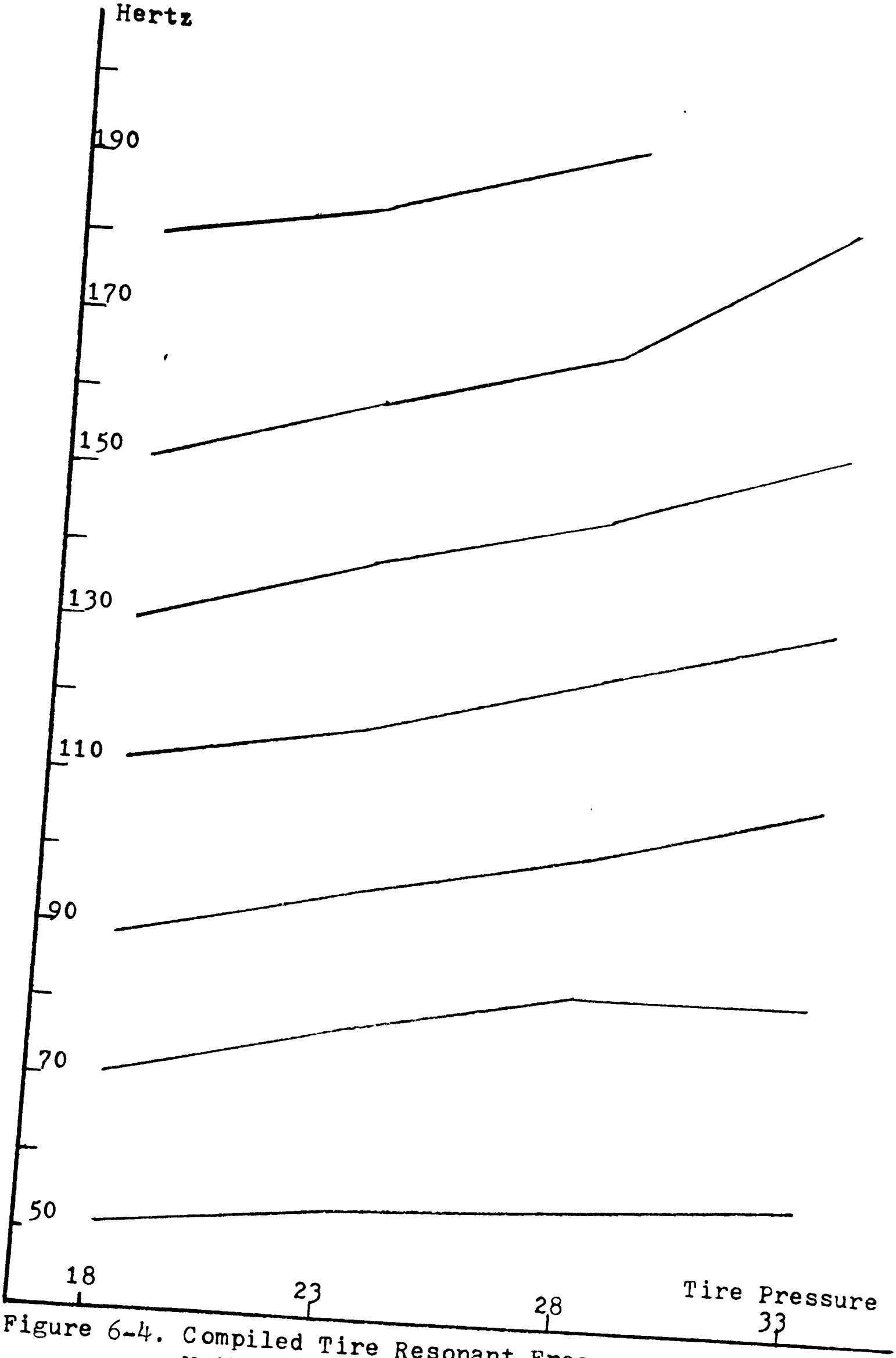

Figure 6-4. Compiled Tire Resonant Frequency Data From Mathew (4). (Tire Temperature Is 80^{o}_{F})

sophisticated method of reducing the analog tape data was employed. This method used an analog to digital electronic converter and a digital computer, coupled to an X - Y plotter. Using this equipment, a Fourier Frequency Analysis was computed for each individual group of roadway speed and tire pressure. This sophisticated analysis was performed by the Firestone Rubber and Tire Company, Research Division, Arkon, Ohio, through arrangements made with the Research Graduate Advisor, Dr. C.A. Bell. The Fourier analysis scans the analog data, taking sample data points at a preselected time interval, and plots the data as signal intensity versus frequency. After the Fourier analysis was received and reduced, frequency graphs similar to those produced using the Hewlett-Packard Sanborn oscillographic recorder were generated--frequency versus roadway speed and individual tire pressure, Figures 6-5 and 6-6. Figure 6-6 can also be compared directly with the reduced data presented in Figure 6-4. These graphs also do not include frequencies above 110 hertz due to the trailer's design limitations. As stated before, any attempts to obtain the higher frequency excitation could result in possible catastrophic results.

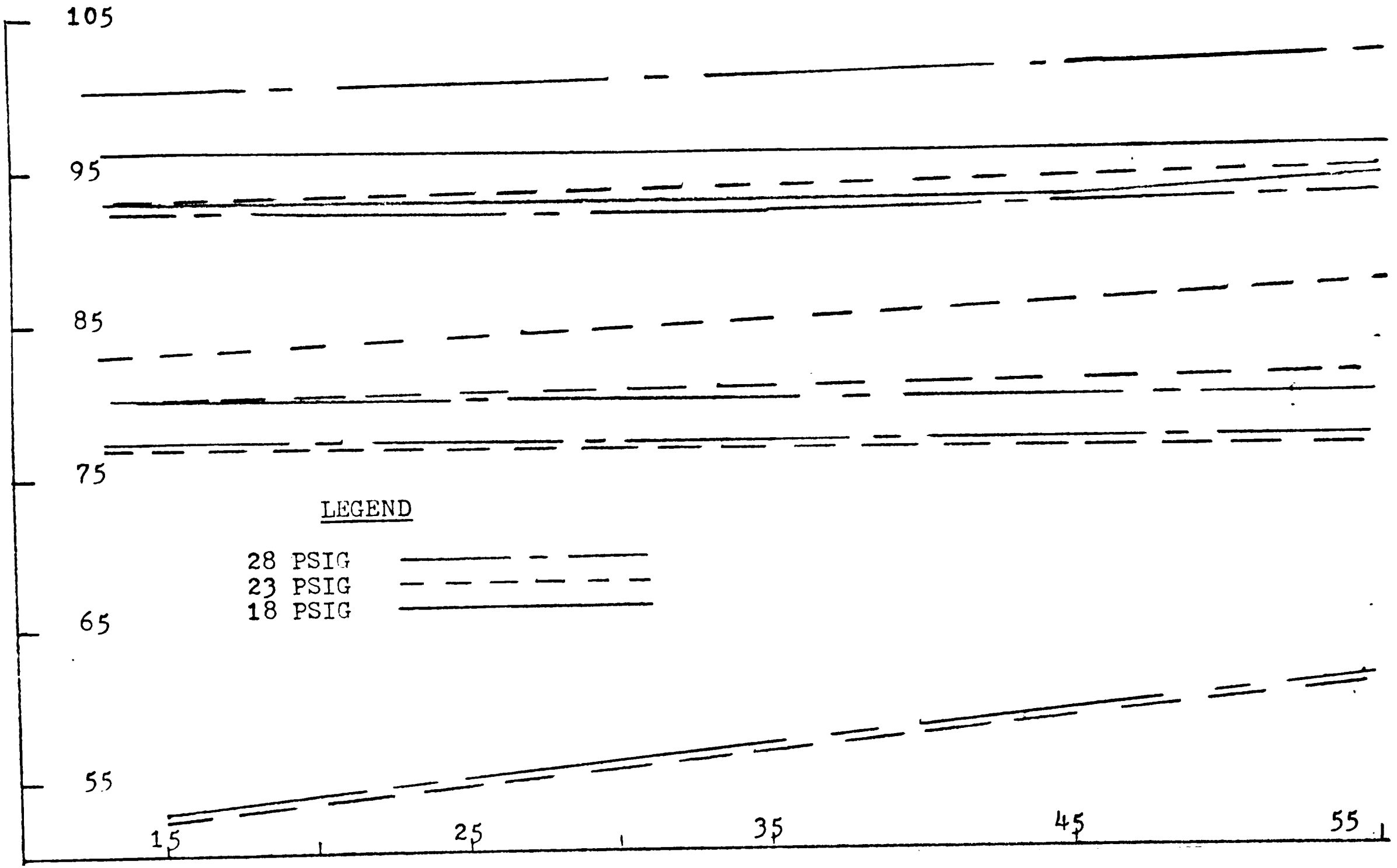

Figure 6-5. Tire Resonant Frequencies Plotted As A Function Of Roadway Speed (Fouries Analysis)

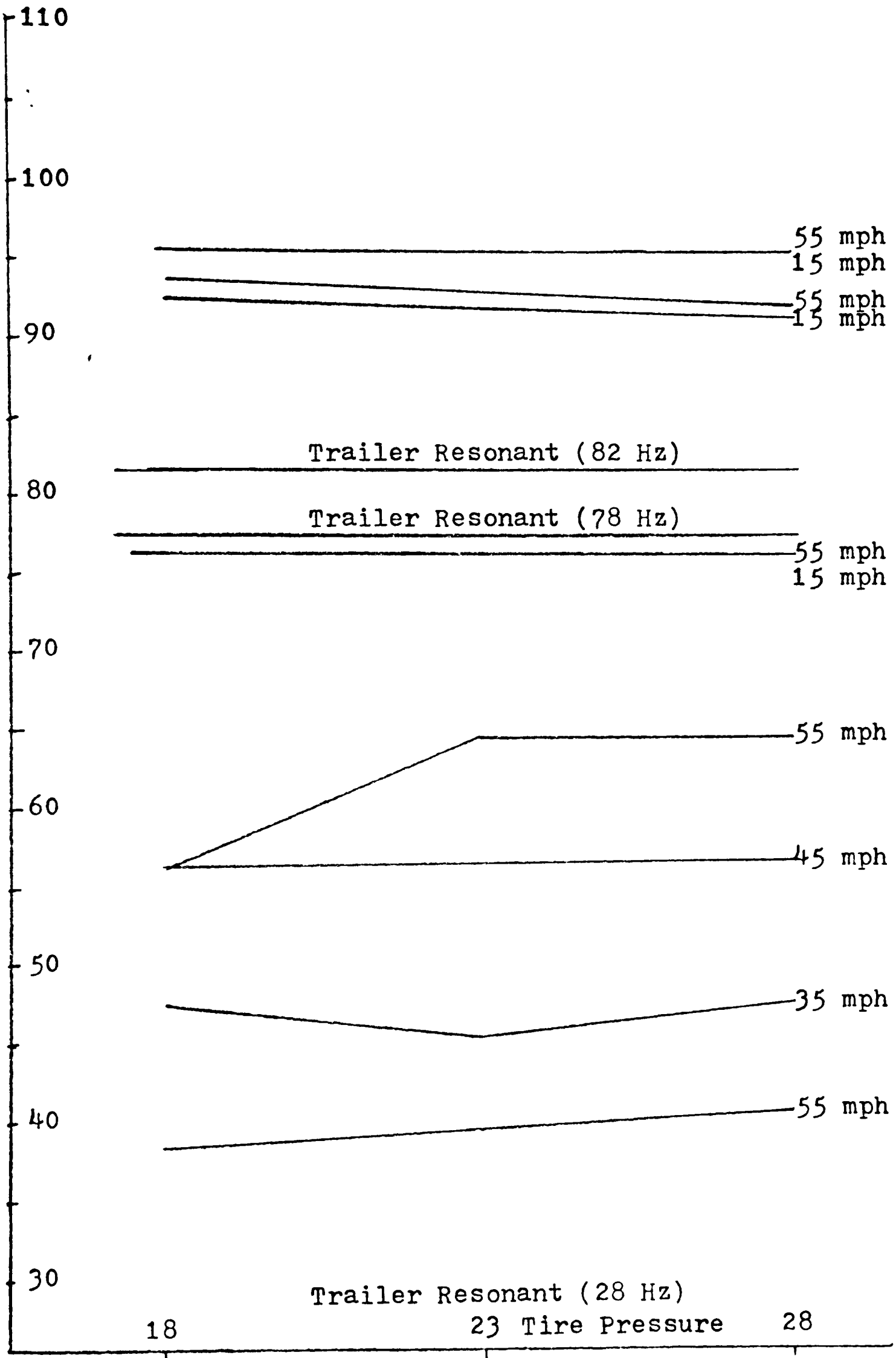

Figure 6-6. Tire Resonant Frequencies Plotted As A Function Of Tire Pressure (Fouries Analysis)

CHAPTER VII

CONCLUSIONS AND RECOMMENDATIONS

Individual tire resonant frequencies discovered during this thesis are presented in Table IVa and Table IVb. Resonant frequencies above 110 hertz could not be obtained due to the initial trailer design and construction.

TABLE IVa

SUMMARY OF RESONANT FREQUENCIES FROM ROADWAY TESTS
(Hewlett-Packard Sanborn Oscillographic Recorder)

Tire Pressure PSIG	Roadway Speeds - MPH 15	25	35	45	55
	100.5	100.6	100.8	100.9	101.0
28	88.5	89.3	90.0	90.8	91.5
	58.3	58.7	59.2	59.6	60.0
	101.0	101.1	101.3	101.4	101.5
23	88.0	88.6	89.3	89.9	90.5
	55.3	55.8	56.3	56.8	57.3
	97.3	97.6	97.8	98.1	98.3
18	87.5	88.0	88.6	89.2	89.7
	52.5	52.7	52.9	53.1	53.3

Note: Maximum frequencies may not be accurate, see Chapter VI.

TABLE IVb

SUMMARY OF RESONANT FREQUENCIES FROM ROADWAY DATA
(Fast Fourier Frequency Analysis)

Tire Pressure PSIG	Roadway Speeds - MPH				
	15	25	35	45	55
28	100.0	100.5	101.0	101.5	102.0
	92.0	92.0	92.0	92.0	92.0
	53.0	55.0	57.0	59.0	61.0
	45.0	46.0	47.0	48.0	49.0
23	93.0	93.5	94.0	94.5	95.0
	83.0	84.0	85.0	86.0	87.0
	53.0	55.0	57.0	59.0	61.0
	46.0	46.0	46.0	46.0	46.0
18	96.0	96.0	96.0	96.0	96.0
	93.0	93.0	93.0	93.0	93.0
	Note: Lower frequencies were not well defined on the Fourier Analysis Graphs.				

The trailer has been significantly modified during this thesis, but the present trailer configuration has serious design deficiencies that could be rectified using the following procedures.

The most serious problem in the trailer design was not being able to mount the accelerometer directly onto the test tire axle. This problem could be corrected by constructing a stub axle which would not turn and would

allow for direct axle mounting of the accelerometer. Also, when the axle was being redesigned, a more convenient method for changing a test tire specimen should be considered. The present configuration calls for the entire axle assembly to be removed and separated; the new test tire installed, then reinstallation of the entire axle assembly as one unit. The axle assembly with the test tire mounted weighs approximately 35 pounds and is very awkward to position. This axle modification would greatly simplify test tire changing and allow for a more precise location for the accelerometer.

A significant trailer modification that should be incorporated is the replacement of the starter-generator, used as a D.C. motor, for a more versatile D.C. motor. The present motor is rated at 14 horsepower (no more than 5 horsepower is needed), drawing approximately 150 amperes and has a minimum speed of 2200 rpm (fixed by the internal windings). This low speed restriction hampers the overall speed range of the counter-rotating disks. Example, higher disks speeds could have been obtained by enlarging the D.C. motor drive pulley to the spur gears, but with the low speed restriction, the changing of this pulley would also increase the minimum low speed. Now the lowest obtainable speed could be well above the lowest tire resonant frequency. Therefore, in selecting a new D.C. motor, one should be acquired that has a wider speed range. Also

this new motor should be powered by 12 volts rather than the 24 volts which is now required. This would reduce the overall number of batteries required to operate the trailer.

A more feasible motor drive unit would be to employ an internal combustion engine which would be coupled to the disk drive mechanism through a flexible shaft. With this arrangement, this motor would have to be supported such that its own induced vibratory effects would not be transmitted to the test trailer. Use of the motor would eliminate the need to recharge batteries plus would delete the extra weight and storage presently found with the batteries.

Another change to be considered is the relocating of the ballast weight to obtain a lower center of gravity for the entire trailer. This could be accomplished by widening the test tire subframe and positioning the ballast weight on special platforms built within this widened subframe. Note that the 12 volt batteries used to power the trailer could be used as part of the ballast weight.

A less significant modification that would be helpful in moving the trailer around inside the Mechanical Engineering Laboratory would be to move the outside stabilization wheels (on the outside trailer subframe) forward and connect them directly to the trailer subframe found behind the present location of the batteries. This

change would reduce the overall length and width of the trailer assembly, but still provide sufficient stabilization.

These modifications, if accomplished, represent a significant amount of time and money, but the author feels that spending this amount of resources would greatly improve trailer operations plus make the trailer easier to operate for future tire tests. It should be reemphasized that the present trailer design will not permit counter-rotating disk speeds over 6600 rpm. Attempts to increase disk speeds could result in serious injury. If additional disk speeds are required for a test series, the trailer should be reanalyzed and modifications made to ensure an overall safety factor of at least 3.0.

LIST OF REFERENCES

1. Campbell, Gary D. "A Mechanical System For Determining The Resonant Frequencies Of Loaded Tires Rolling On Flat Surfaces". M.S. Thesis, Mechanical Engineering Department, Texas Tech University, December 1973.

2. Tavakoli, Nasser. "Improvements On The Design Of A Mechanical System For Determining The Resonant Frequencies Of Loaded Tires Rolling On A Flat Roadway", M.S. Report, Mechanical Engineering Department, Texas Tech University, May 1973.

3. Pirtle, Robert B. "Determination Of Resonant Frequencies Of A Loaded Tire Utilizing An Experimental Instrumentated Trailer", M.S. Report, Mechanical Engineering Department, Texas Tech University, December 1974.

4. Mathew, Rajan C. "An Investigation Of The Effects Of Pressure And Temperature On The Vibrational Characteristics Of Tires", M.S. Report, Mechanical Engineering Department, Texas Tech University, January 1976.

5. Thomson, William T. Theory Of Vibration With Application. New Jersey: Prentice-Hill, Inc. 1972.

6. Project THOR Technical Report No. 47. "The Resistance Of Various Metallic Materials To Performation By Steel Fragments; Empirical Relationships For Fragment Residual Velocity And Residual Weight", The Johns Hopkins University, April 1961.

7. Myklestad, N.O. Vibration Analysis. New York: McGraw-Hill Book Company, Inc. 1944.

8. Broch, Jens T. Mechanical Vibration And Shock Measurements. Denmark: K. Larsen and Son, 1971.

9. Timoshenko, S. Theory Of Elasticity. New York: McGraw-Hill Company, 1934.

10. Cernica, John N. Strength Of Materials. New York: Holt, Rinehart and Winston, Inc. 1966.

11. Smith, Gerald M. and Downey, Glenn L. Advanced Engineering Dynamics. Scranton, Pa., International Textbook Company, 1968.

12. Stamper, Eugene and Dublin, Stanley, Mechanical Engineering And Economics And Ethics For Professional Engineering Examinations. New Jersey: Hayden Book Company, Inc., 1971.

13. Prince, Wilson and Miller, Merlin, Elements Of Data Processing Mathematics. New York: Holt, Rinehart and Winston, Inc., 1967.

APPENDIX A

PRESENTATION OF RAW TEST DATA

This appendix will present in strip chart form typical raw data that was manually reduced in performing the overall analysis. These strip charts are made through the use of a Tanberg four channel analog recorder and a Hewlett-Packard Sanborn oscillographic recorder. Each test was performed a minimum of three times, to ensure consistency, and the results averaged to produce a single resonant frequency. If the frequency was within two hertz of the trailer resonant frequency, from Table III, it was not considered in the results.

Also included in this appendix are the Fourier analysis X-Y plots produced by the Firestone Tire and Rubber Co., Arkon, Ohio. Through arrangements made with their Research Division, they were able to read the analog taped data produced by the Tanberg recorder. Then they used an analog to digital converter that sampled the taped roadway data at a predetermined time interval. This sampling measured the intensity or amplitude of the incoming signal. Next a digital computer was employed to convert the amplitude signal into a Fast Fourier frequency analysis. As previously discussed, each roadway speed, tire pressure combination was run a minimum of three

times, but when Firestone analyzed the data, they grouped the three runs together and produced an "average" Fourier analysis for each combination. These data are presented in graphical form and are grouped by tire pressure, Figures A-5, A-6 and A-7. Also included are the Fourier analysis of the initial baseline laboratory tests which were used to establish baseline data, Figure A-4.

At this point, it should be noted that in reducing the Fourier analysis data, some of the lower frequencies could not be determined. The author feels that due to the averaging that Firestone's computer program performed, the lower frequencies, which were established from the Hewlett-Packard Sanborn oscillographic recorder, were "averaged out" of the data spectrum. Firestone's program combined the three similar roadway tests at a given tire pressure for a data point. Thus if only one of the tests showed a low frequency response, the "averaged" resonant frequency recorded would be plotted lower than if there were two or three data points present. Therefore, when comparing the two types of data reduction, the manual reading method (Hewlett-Packard Sanborn frequency strip charts) produced more discernible data values, but were subjective to human error. Whereas, the Fourier analysis data were produced by electronic methods and did generate more accurate values, except for the shortcomings due to the averaging process.

Upon reviewing Figures 6-4, 6-5, 6-7 and 6-8, it can be shown the two methods yielded similar and comparable results, except at the lower frequency ranges.

LIBRARY

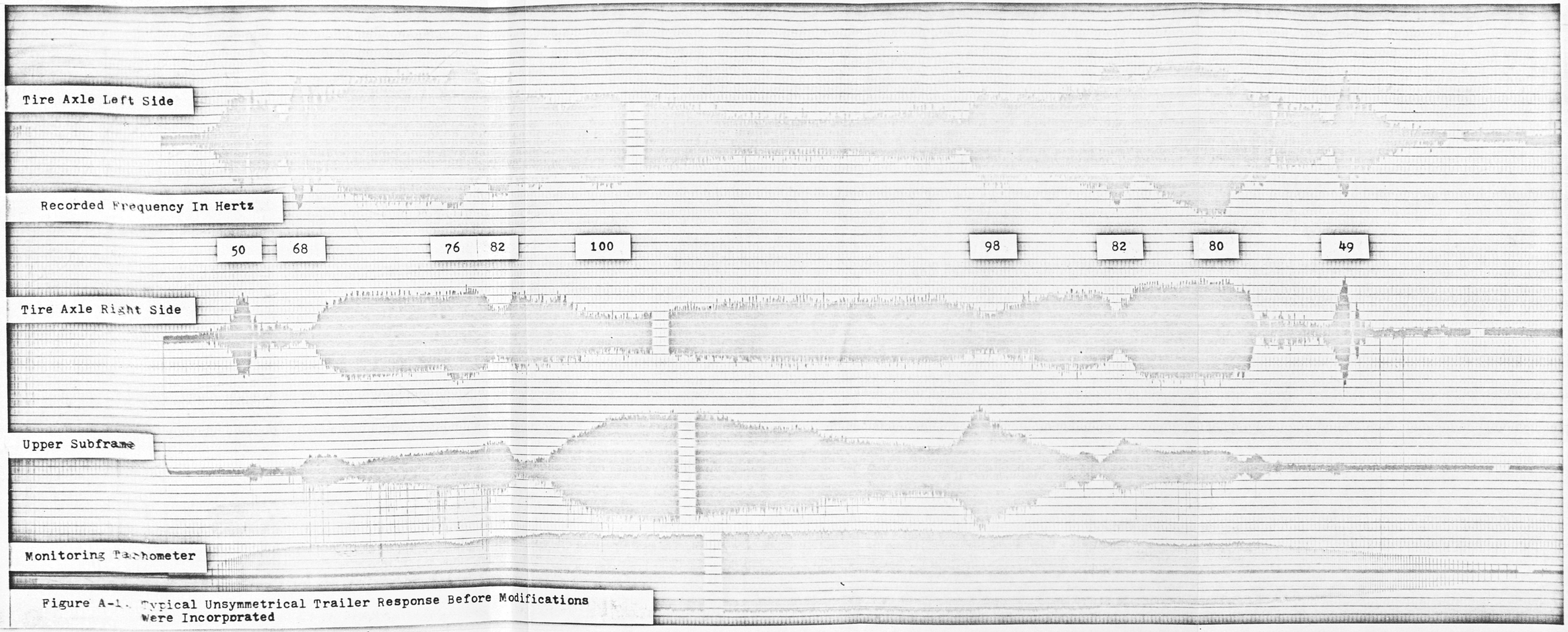

Figure A-1. Typical Unsymmetrical Trailer Response Before Modifications Were Incorporated

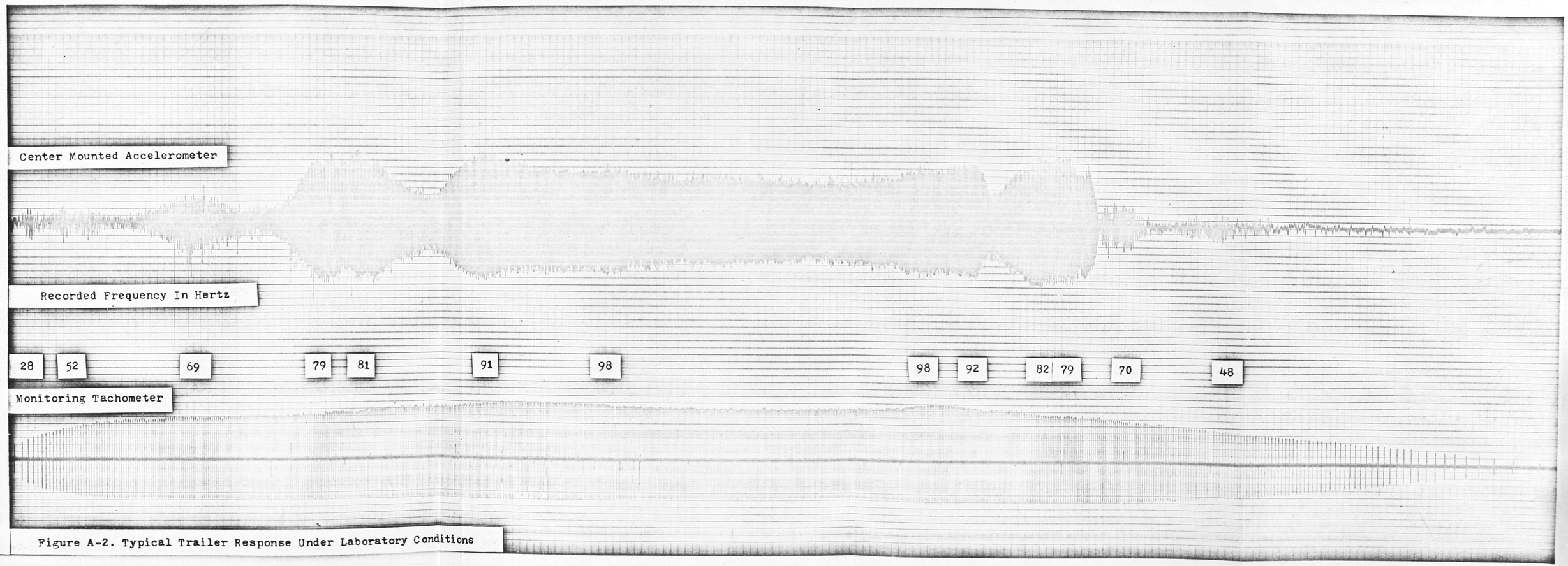

Figure A-2. Typical Trailer Response Under Laboratory Conditions

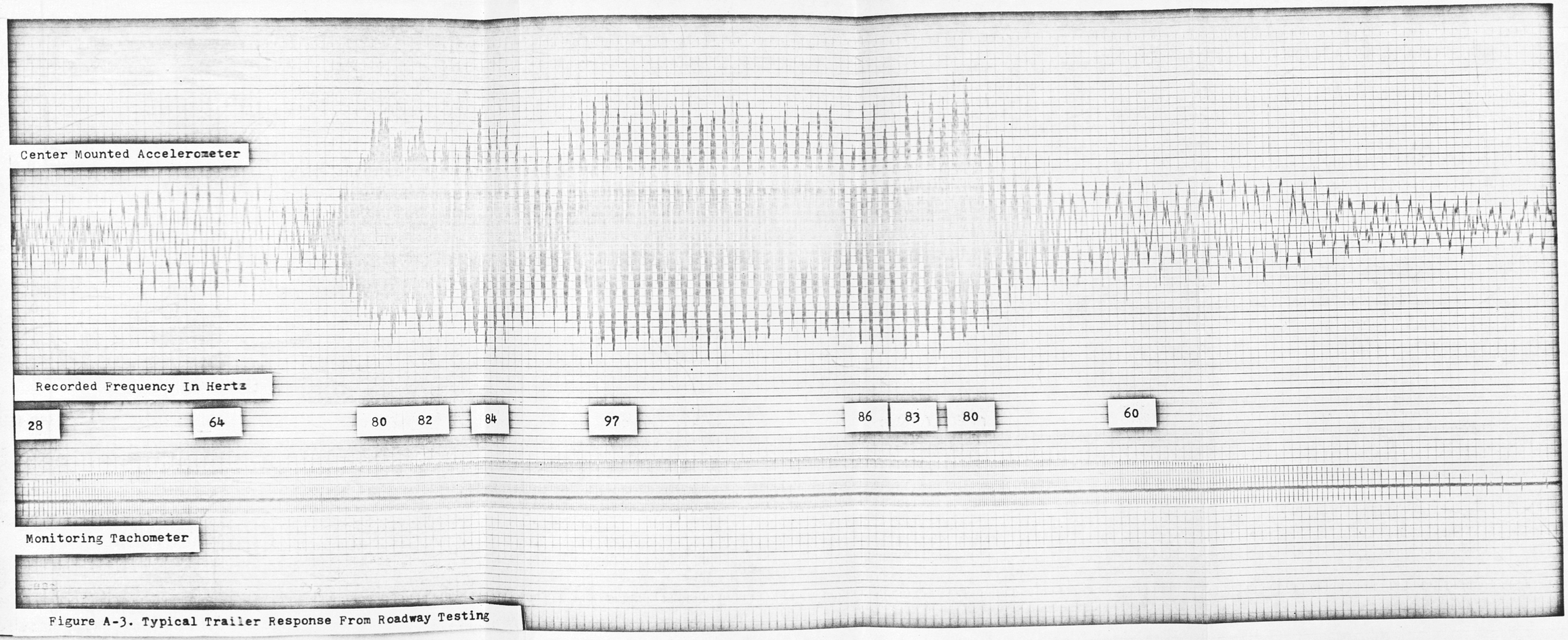

Figure A-3. Typical Trailer Response From Roadway Testing

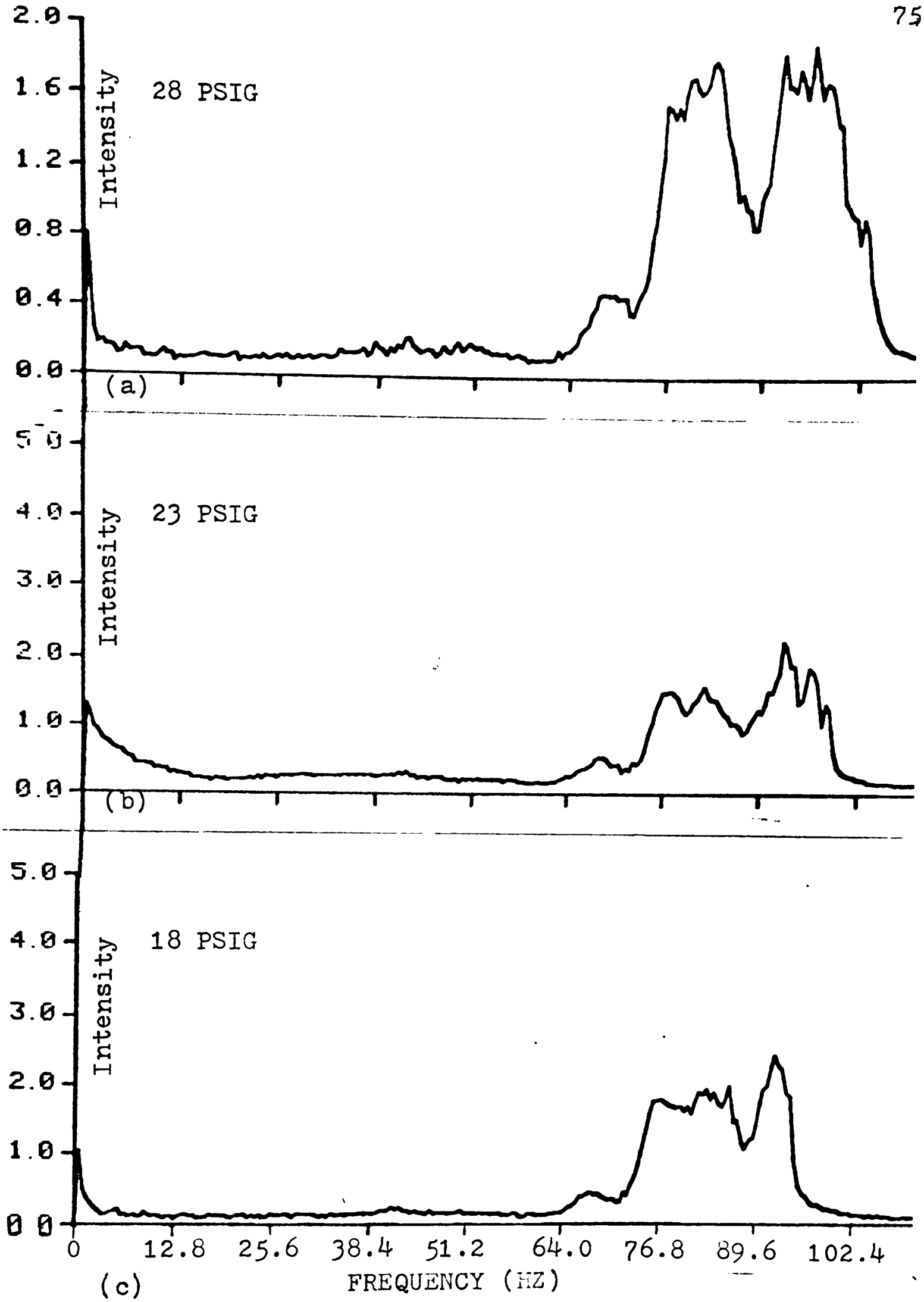

Figure A-4. Fourier Analysis - Static Laboratory Conditions

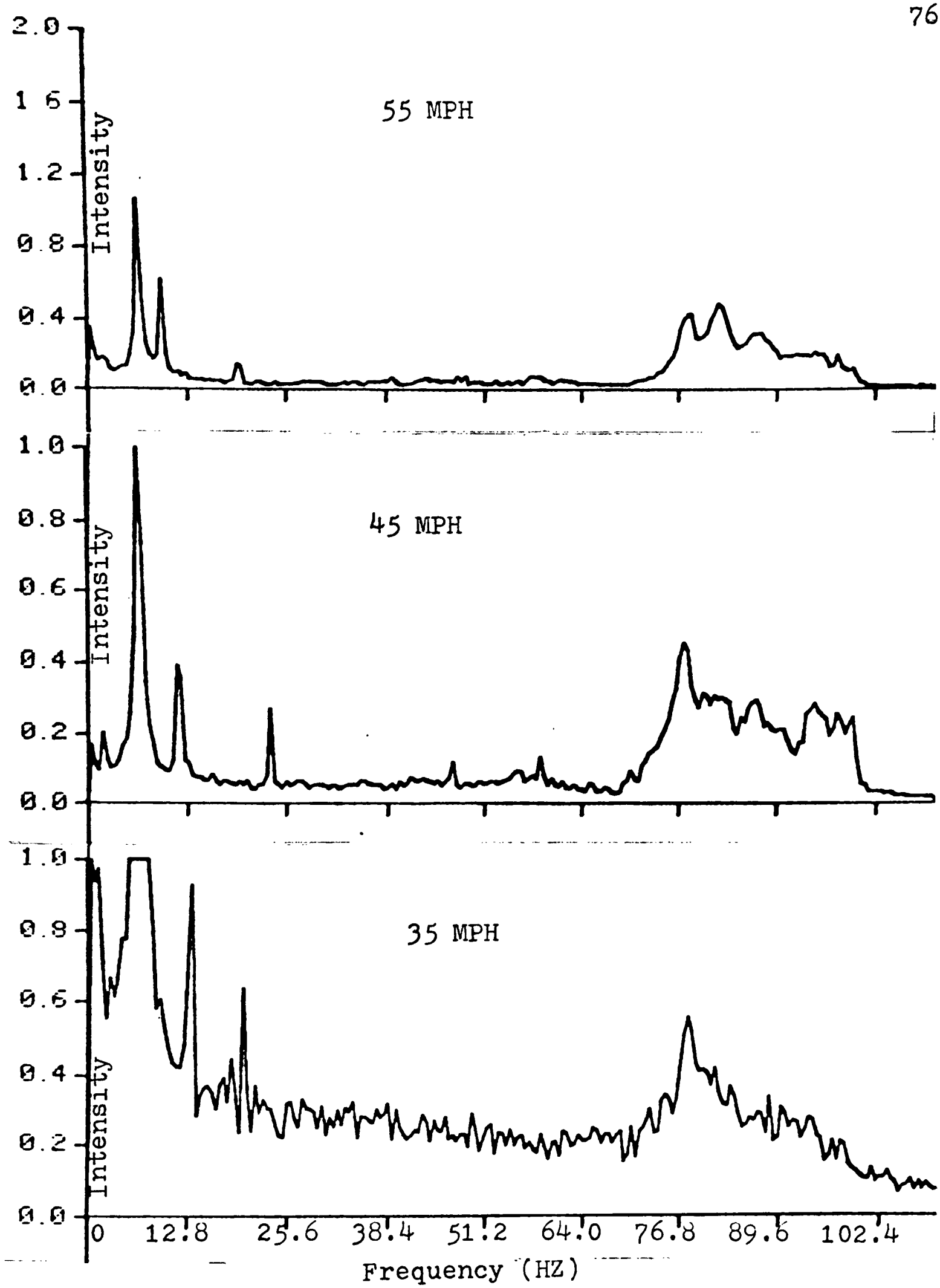

Figure A-5. Fourier Analysis - Roadway Speeds For 18 PSIG

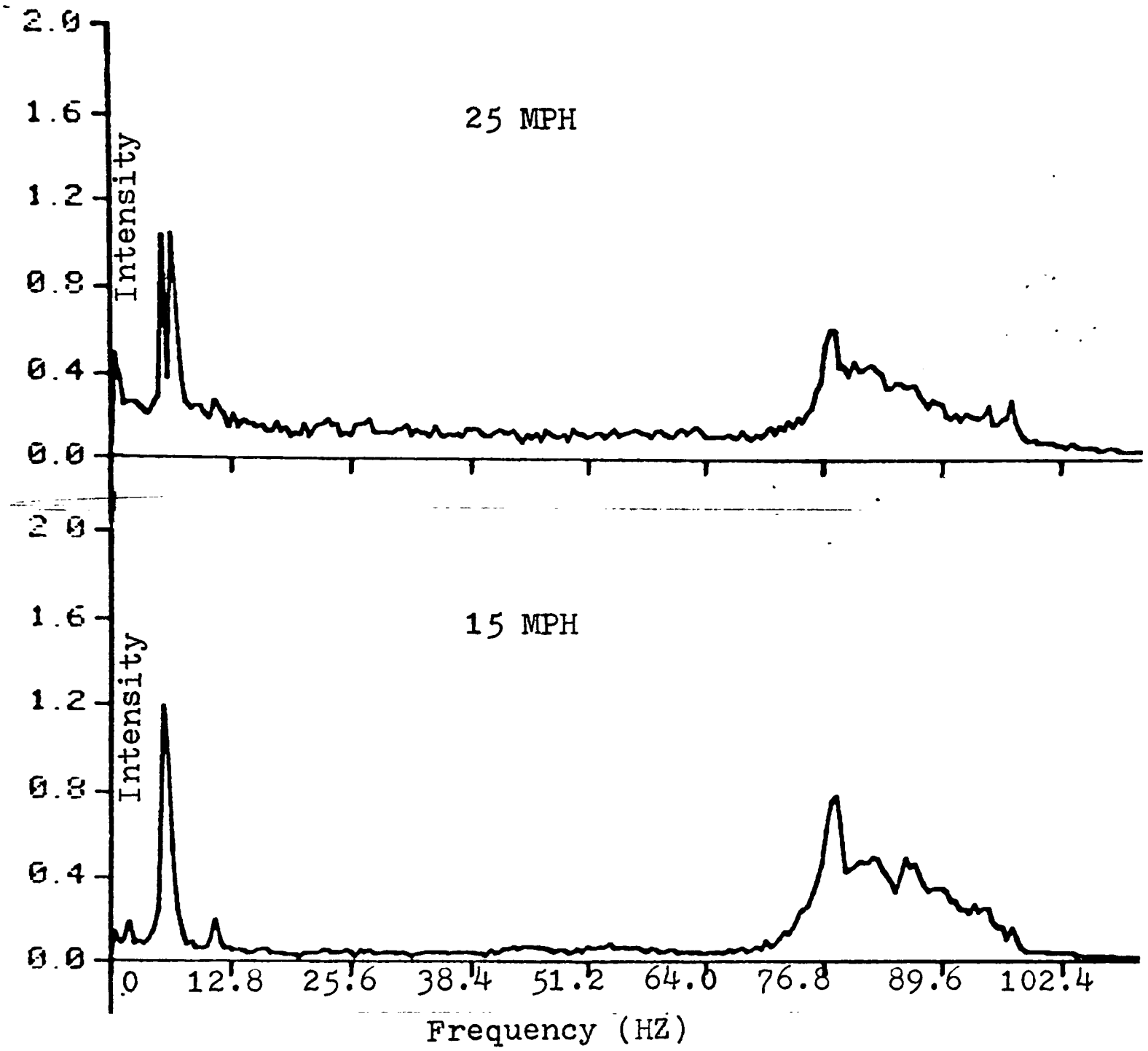

Figure A-5 Con't.

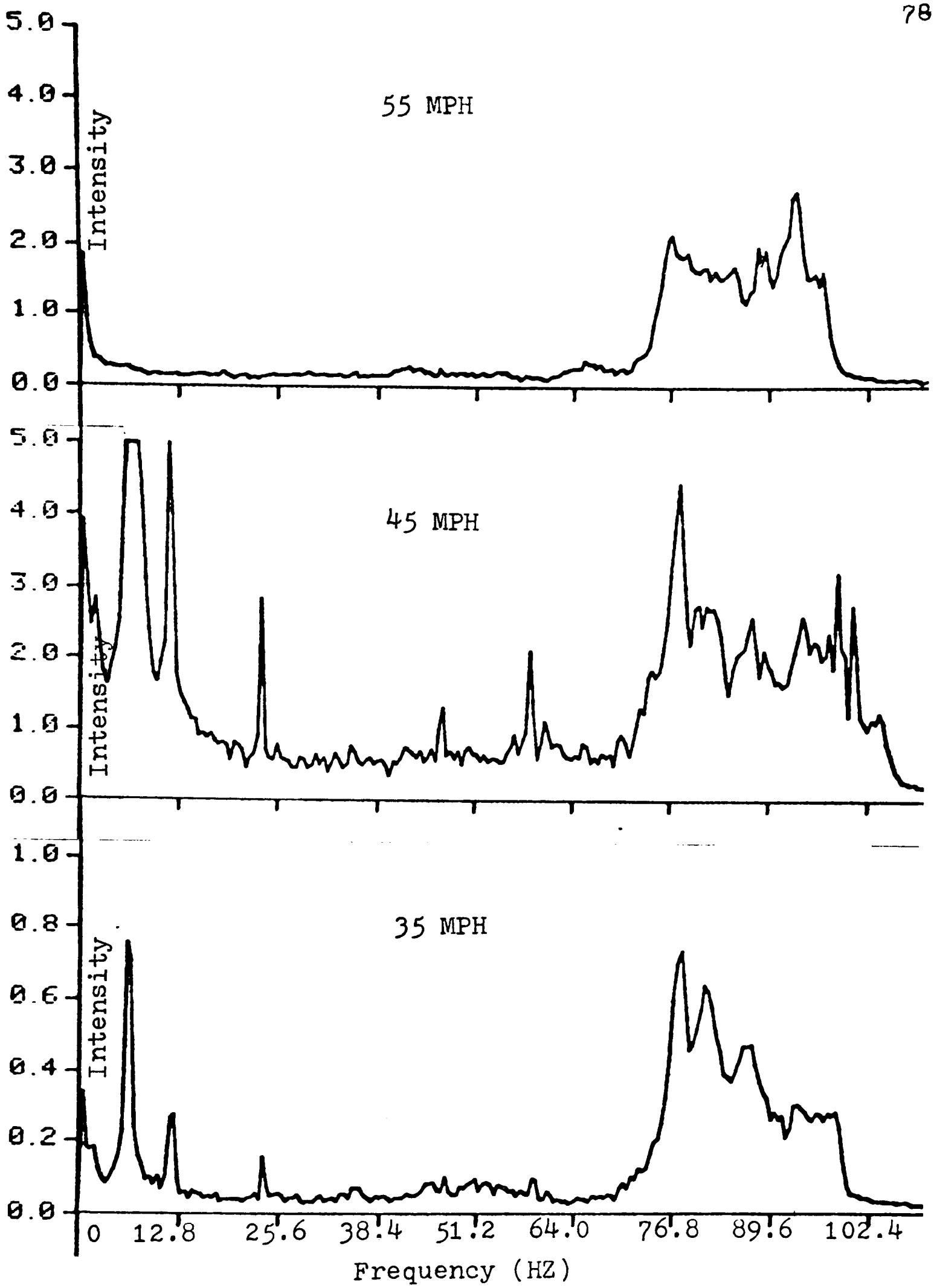

Figure A-6. Fourier Analysis - Roadway Speeds For 23 PSIG

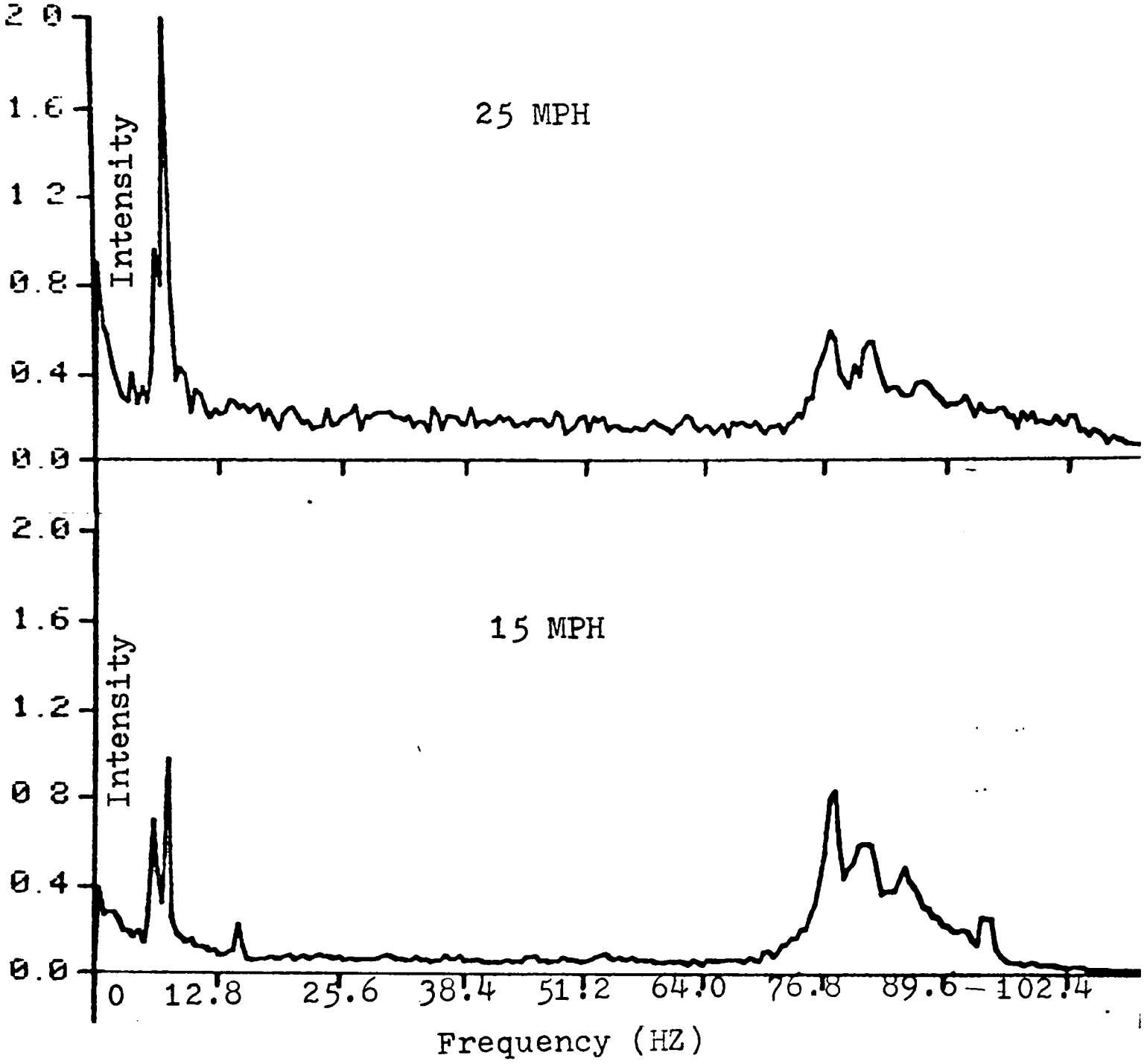

Figure A-6.Con't.

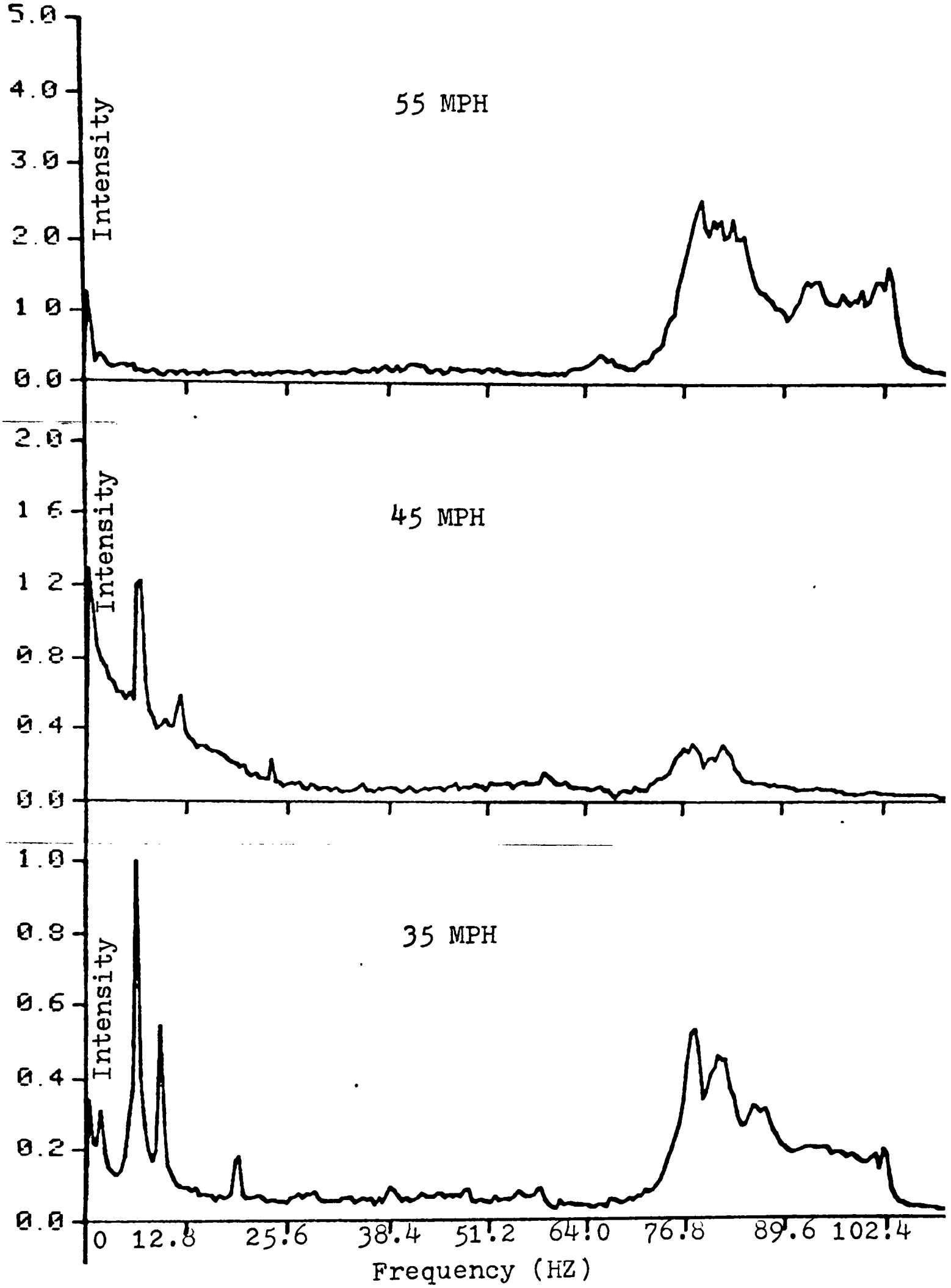

Figure A-7. Fourier Analysis - Roadway Speeds For 28 PSIG

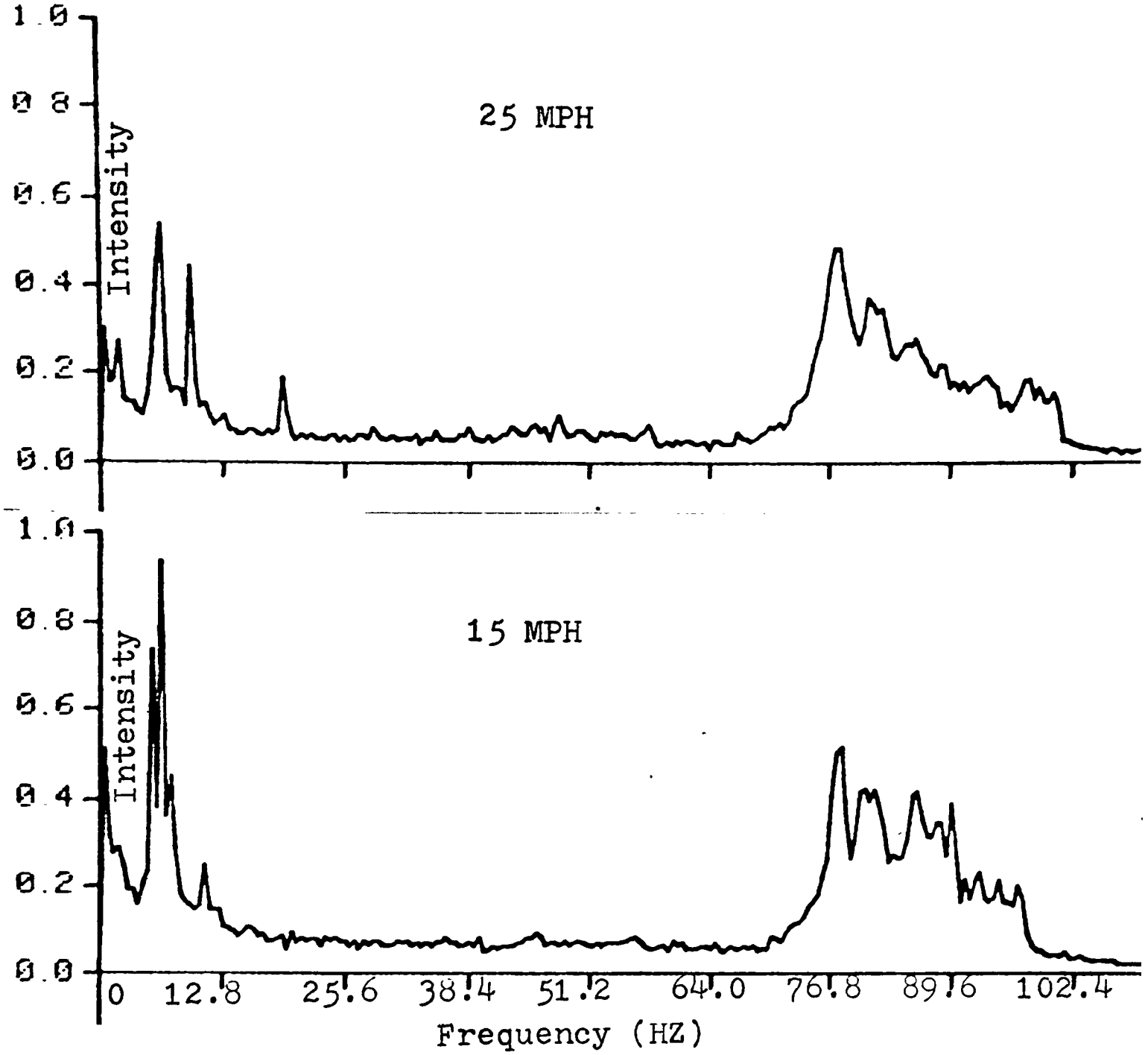

Figure A-7 Con't.

APPENDIX B

PROJECT THOR COMPUTER ANALYSIS

This appendix presents the complete computer program developed under Project THOR, that was used to analyze individual disk separation. The program is designed to read in individual fragment weights, an impact velocity and obliquity angle and print out and plot computed residual velocity and mass per fragment. The program will accept thirty impacting fragment masses and velocities plus eighteen different striking obliquity angles for a given computer run. Although the program can consider nine impacted plate materials, only four are presented; hard steel, mild steel, cast iron, and aluminum. Also included are typical output tables. Tables VI, VII, and VIII predict, respectively the residual velocities of a 1293, 900, and 650 grain mild steel fragment impacting a mild steel plate, i.e., a "broken" piece of the counter-rotating disk and the safety shields.

TABLE V. PENETRATION CONSTANTS FOR THOR COMPUTER PROGRAM

Material	C	α	β	γ	λ
Hard Steel	6.475	.889	- .945	1.262	.019
Mild Steel	6.399	.889	- .945	1.262	.019
Cast Iron	4.840	1.042	-1.051	1.028	.523
Aluminum	7.047	1.029	-1.072	1.251	-.139

The material constants presented in Table V were evaluated from firing mild steel fragments at the different material plates listed. After all tests had been completed, penetration curves were plotted as a function of impact velocity and plate thickness. Then using the general penetration equation in Chapter III, this equation was "fitted" to each individual material plate curve. As a result of the curve fitting, the individual material constants were determined. This method of determining fragment penetration is used extensively by the military services and has proved to be quite accurate for target modeling procedures.

```
      DIMENSION RMS(30),VS(30),ANGL(18),RMR(30,30,2),VR(30,30,2)
      DIMENSION AMAT(3)
      INTEGER O,X
    1 FORMAT (3I5)
    2 FORMAT(16F5.0)
    3 FORMAT(6F7.3,I2,I3)
    4 FORMAT(18F5.0)
    5 FORMAT(1HO,F4.0,4X,11(3X,F7.1))
    6 FORMAT(1HO,F4.0,4X,11(2X,F8.1)/)
    7 FORMAT(F8.4,7F8.5,F8.4)
    8 FORMAT(1H ,40X,
     130HRESIDUAL MASS AND VELOCITY FOR,F6.3,15H INCH MATERIAL ,3A4,//
     11H ,50X,20HSTRIKING OBLIQUITIES,I3,8H DEGREES///
     19H FRAGMENT,49X,35HFRAGMENT VELOCITY (FEET PER SECOND)
     11H ,5H MASS/)
    9 FORMAT(1H1)
   20 FORMAT(7F8.5,I2,I3)
   21 FORMAT(3F6.2,   3F6.1,F6.2,F6.3,F6.5,F6.1,I3)
   37 FORMAT(1X,8H(GRAINS),11F10.0)
  101 FORMAT(11F5.3,2I5,3A4)
  102 FORMAT(1X,11F6.3,2I5,3A4)
C*************************************************************************
C
C   N=NUMBER OF MASSES CONSIDERED   30 MAX
C   M=NUMBER OF VELOCITIES CONSIDERED  30 MAX
C   L=NUMBER OF OBLIQUITIES CONSIDERED   18 MAX
C
C   CC,AA,BB,DD,FF,C,A,B,D,F ARE CORRESPONDING THOR EQUATION RESISTANCE
C   CONSTANTS WITH MATERIAL CODES
C
```

```
C
C   EP=THICKNESS INCREMENTS IN THOUSANDS: EXAMPLE .025 THICK=25 ON CARD
C   JP=NUMBER OF TABLES DESIRED BY THICKNESS INCREMENTS
C   MAT=MATERIAL CODES
C
C
C   MATERIAL CODES
C       101  HARD STEEL
C       102  MILD STEEL
C       103  CAST IRON
C       104  2024 ALUMINUM
C       105  PLEXIGLAS
C       106  WATER
C       107  RUBBER
C       108  PERSONNEL
C       109  HARD WOOD
C       110  DUMMY RECORD FLAG
C
C   RMS=THE MASSES TO BE COMPUTED
C   VS= THE VELOCITIES TO BE COMPUTED
C   ANGL= THE OBLIQUITIES OF IMPACT ANGLES TO BE COMPUTED
C
C   AMAT IS THE NAME OF THE MATERIAL CODE
C
C**************************************************************************
      DO 27 NM=1,2
      READ(5,1)N,M,L
      WRITE(6,1) N,M,L
      READ(5,2) (RMS(I),I=1,N)
      WRITE(6,2)(RMS(I),I=1,N)
      READ(5,2)  (VS(J),J=1,M)
      WRITE(6,2) (VS(J),J=1,M)
      READ(5,4)  (ANGL(K),K=1,L)
      WRITE(6,4) (ANGL(K),K=1,L)
```

```
C*****************************************************************************
C      AM IS THE SHAPE FACTOR OF THE TYPE FRAGMENT USED
C
C      AM FOR STEEL SPHERES EQUALS .00753
C      AM FOR STEEL CUBES EQUALS .0095
C      AM FOR FORGED STEEL DEMO AND G.P. FRAGMENTATION EQUALS .01422
C
C*****************************************************************************
      AM=.0095
   25 READ(5,101)CC,AA,BB,DD,FF,C,A,B,D,F,EP,JP,MAT,(AMAT(LL),LL=1,3)
      WRITE(6,102) CC,AA,BB,DD,FF,C,A,B,D,F,EP,JP,MAT,(AMAT(LL),LL=1,3)
      IF(110-MAT) 27,27,28
   28 BB=BB+.66667*AA
      B=B+.66667*A
      CC=10.**CC*AM**AA
      C=10.**C*AM**A
      E=0.
      DO 26 JJ=1,JP
      E=E+EP
      E=E+.0005
      O=0
      DO 13 K=1,L
      DO 13 I=1,N
      DO 13 J=1,M
      O=O+1
  113 VR(J,I,K)=VS(J)-(CC*E**AA*RMS(I)**BB*(1./COS(ANGL(K)/57.296))
     1**DD*VS(J)**FF)
   13 RMR(J,I,K)=RMS(I)-(C*E**A*RMS(I)**B*(1./COS(ANGL(K)/57.296))**D*
     1VS(J)**F)
      DO 16 K=1,L
      O=1
      LK=11
      IF(LK.GE.M) LK=M
```

```
34 WRITE(6,9)
   WRITE(6,8) E,(AMAT(LL),LL=1,3),ANGL(K)
   WRITE(6,37)  (VS(J),J=0,LK)
   DO 17 I=1,N
   WRITE(6,5)RMS(I),(RMR(LL,I,K),LL=0,LK)
   WRITE(6,6)RMS(I),(VR(LL,I,K),LL=0,LK)
17 CONTINUE
   0=0+11
   LK=LK+11
   IF(0-M) 31,31,32
31 IF(LK-M) 34,34,33
33 LK=M
   GO TO 34
32 CONTINUE
16 CONTINUE
26 CONTINUE
   GO TO 25
27 CONTINUE
   CALL EXIT
    END
```

TABLE VI. COMPUTER OUTPUT FROM THOR PROGRAM FOR .125 INCH MILD STEEL PLATE

Residual Mass and Velocity With a Striking Obliquity of 0 Degrees

Fragment Mass (Grains)	Fragment Velocity (Feet Per Second)				
	200.	225.	250.	275.	300.
650.	621.9	619.3	616.7	614.2	611.8
650.	-512.1	-488.7	-465.1	-441.4	-417.6
900.	862.1	858.5	855.0	851.6	848.3
900.	-434.9	-411.4	-387.6	-363.8	-339.9
1293.	1293.9	1234.9	1230.1	1225.3	1220.7
1293.	-358.9	-335.1	-311.2	-287.2	-263.2

TABLE VII. COMPUTER OUTPUT FROM THOR PROGRAM FOR .250 INCH MILD STEEL PLATE

Residual Mass and Velocity With a Striking Obliquity of 0 Degrees

Fragment Mass (Grains)	Fragment Velocity (Feet Per Second)				
	200.	225.	250.	275.	300.
650.	619.1	616.2	613.4	610.6	608.0
650.	-1118.7	-1096.7	-1074.3	-1051.7	-1028.9
900.	858.2	854.3	850.5	846.8	843.1
900.	-975.9	-953.5	-930.9	-908.0	-884.9
1293.	1234.6	1229.1	1223.8	1218.5	1213.5
1293.	-834.9	-812.3	-789.3	-766.2	-742.9

TABLE VIII. COMPUTER OUTPUT FROM THOR PROGRAM FOR .375 INCH MILD STEEL PLATE

Residual Mass and Velocity With a Striking Obliquity of 0 Degrees

Fragment Mass (Grains)	Fragment Velocity (Feet Per Second)				
	200.	225.	250.	275.	300.
650.	617.3	614.3	611.3	608.4	605.5
650.	-1691.0	-1670.2	-1649.0	-1627.5	-1605.6
900.	855.8	851.7	847.7	843.7	839.9
900.	-1486.2	-1464.9	-1443.3	-1421.4	-1399.2
1293.	1231.2	1225.4	1219.8	1214.3	1208.9
1293.	-1284.1	-1262.4	-1240.4	-1218.1	-1195.6

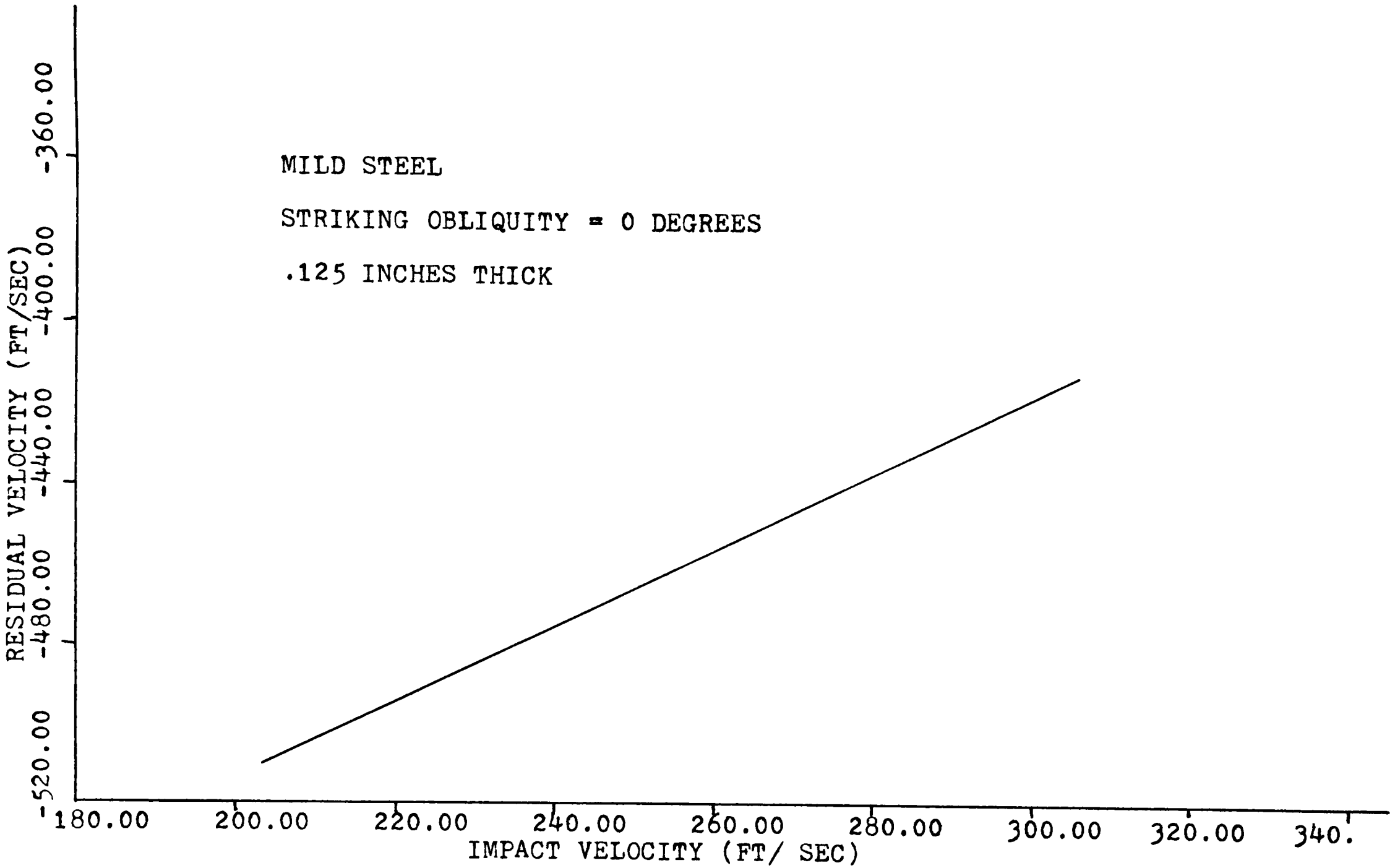

Figure B-1. Computer Plot of a 1293 Grain Mild Steel Fragment Penetrating .125 Inch Mild Steel Plate

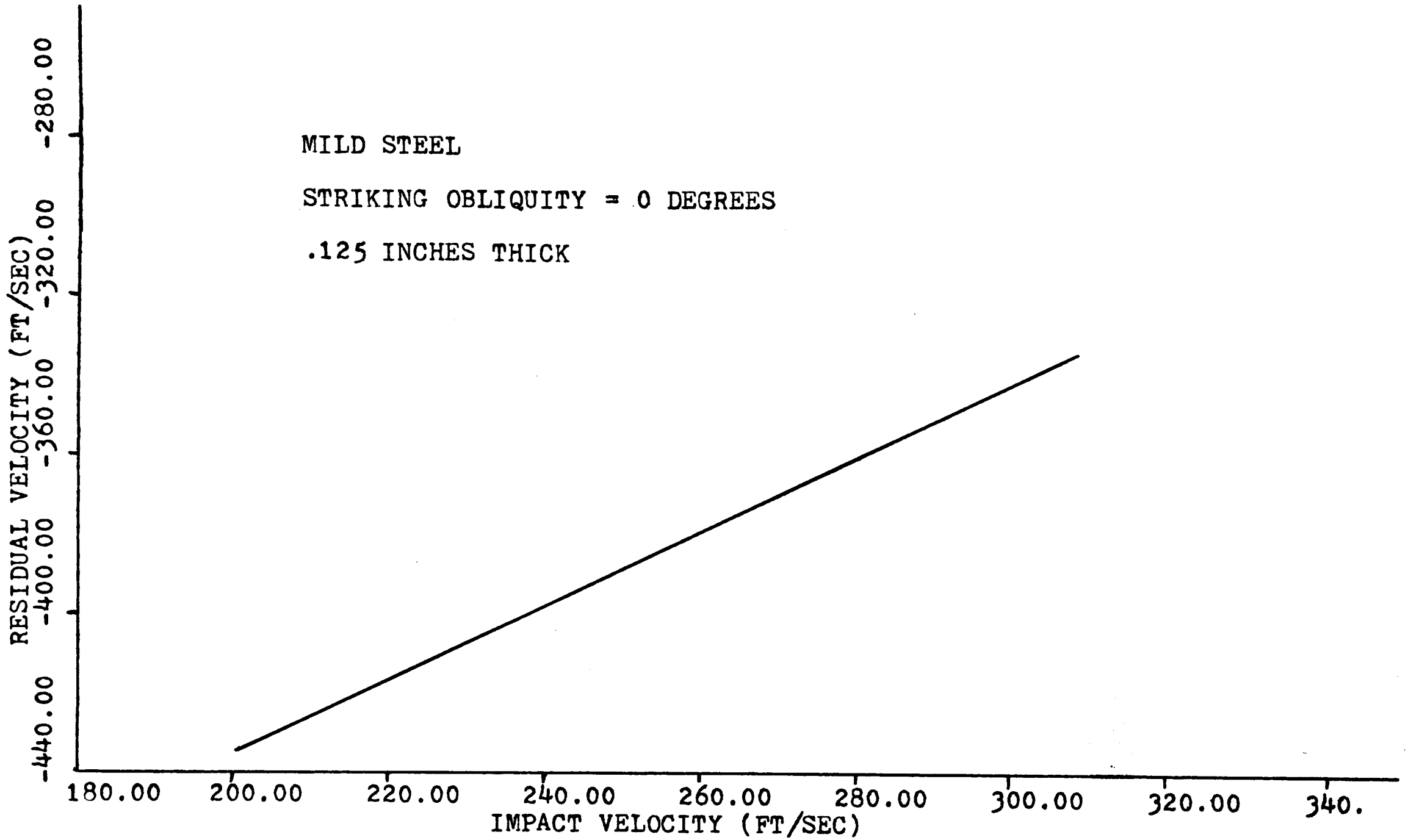

Figure B-2. Computer Plot of a 900 Grain Mild Steel Fragment Penetrating .125 Inch Mild Steel Plate

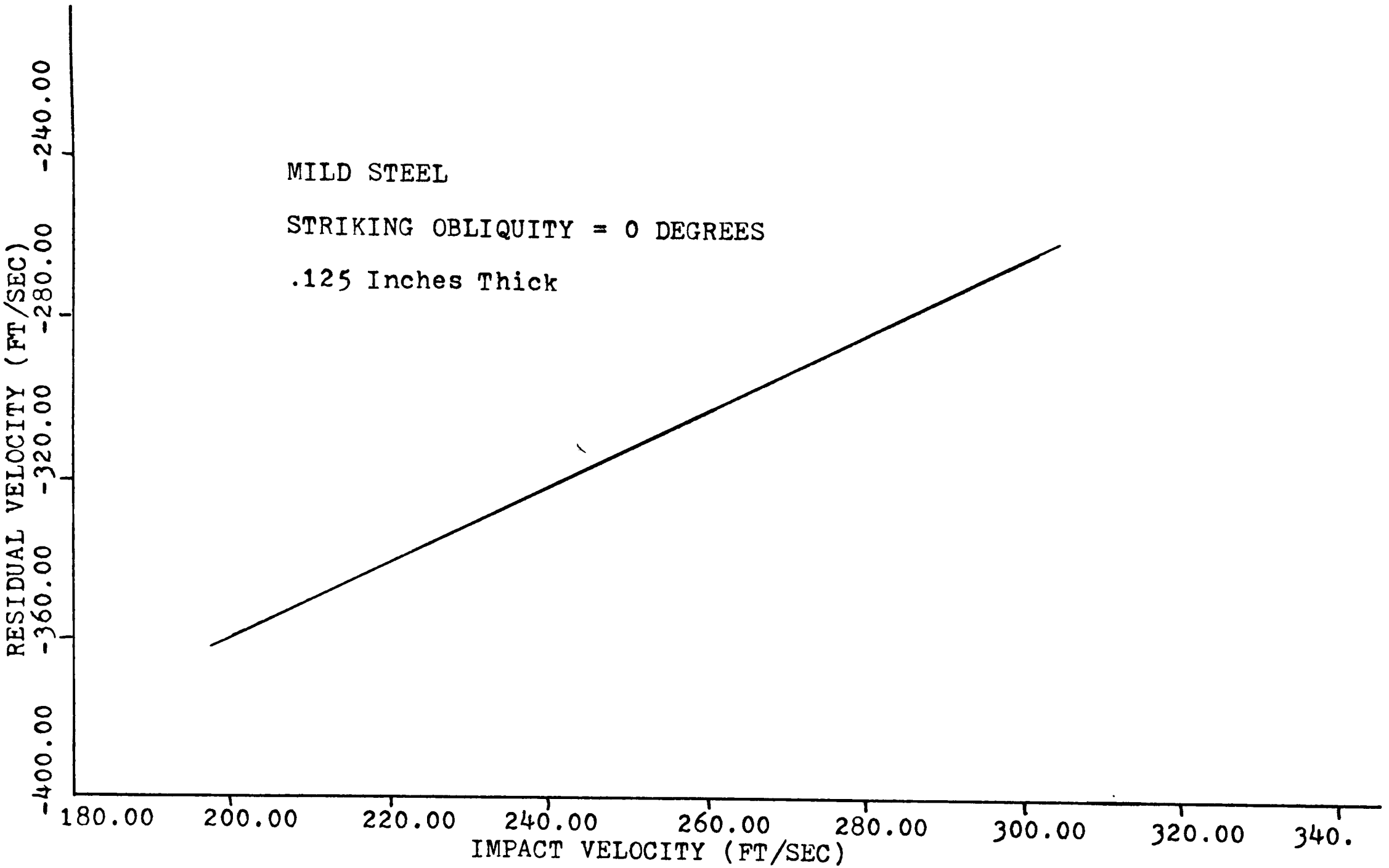

Figure B-3. Computer Plot of a 650 Grain Mild Steel Fragment Penetrating .125 Inch Mild Steel Plate

APPENDIX C

The method for analyzing the structural resonances of the lower subframe, containing the test tire, is described in Campbell (1). The basis of this analysis is similar to the Myklestad Method, fully explained in Myklestad (7). This method uses a lumped element model of the subframe. Campbell (1) also contains a computer program with some documentation describing program implementation. Although when the author tried to use the included computer program, which was written in FORTRAN IV, it did not produce correct results. Overall program results were compared with hand calculations and it was noted the matrix multiplication was in error. A modification was made plus an additional subprogram was written to plot specific beam responses, given a range of driving frequencies. The modified computer program, written in FORTRAN IV, along with an example plot of each of the nine types of beam response, Figures C-1 to C-9, are included. The computer plots were produced using Texas Tech's CalCom plotter. Note that this program will determine the lower frame response if it was the only beam in the system, but this is not the case. The overall trailer is comprised of three dependent trailers or subframes, each relying upon the response of the other. In order to predict overall trailer response, given a driving

frequency, a new computer model would have to be developed to describe the dependency of the three frames interactions. All required parameters would be known, i.e., beam material and weight, spring constants, frame dimensions, etc., except for the test tire response. At present, the test tire frequency response is a doctoral project being investigated by a graduate student. Thus until his work is completed, a complete computer program will not be available to analyze the entire trailer.

Beam Matrix Method Computer Program Listing

```
C     ******************************************************************
C     ******************************************************************
C     ***   MATRIX METHOD FOR DETERMINING THE RESONANT   ***************
C     ****                FREQUENCIES OF BEAMS                 **********
C     ******************************************************************
C     ******************************************************************
C     ******************************************************************
C     ******************************************************************
C              PROGRAMMER:  JACK WINGER                         *********
C     ******************************************************************
C                            TERM DEFINITIONS                          **
C                            ****************
C      NSTA            =NUMBER OF STATIONS
C       TMAT(I,4,4)    =TRANSFER MATRIX OF I-TH SECTION
C       MASS(I)        =MASS OF I-TH SECTION(LBM)
C       LENGTH(I)      =LENGTH OF I-TH SECTION (INCHES)
C       FI(I)          =STIFFNESS OF I-TH SECTION (LBF-IN**21)
C       P              =FREQUENCY IN HZ
C       PSTART         =STARTING FREQUENCY
C       PSTOP          =STOPPING FREQUENCY
C       PSTEP          =SIZE OF FREQUENCY INCREMENTS DESIRED
C       F              =FREQUENCY IN RADIANS/SECONDS
C       FSQ            =SQUARE OF F
C       BUFF(4,4)      =BUFFER ARRAY
C       U(4,4)         =OVERALL TRANSFER MATRIX OF BEAM
C       DET            =DETERMINANT OF MATRIX WHICH MUST GO TO ZERO AT
C                       THE NATURAL FREQUENCY
C       NDS            =NUMBER OF DATA SETS TO BE RUN
C       PAGE           =OUTPUT PAGE COUNTER
C       LINE           =LINE COUNTER
```

```
C       ENDCON          =PARAMETER INDICATIONG END CONDITIONS
C                        ACCORDING TO FOLLOWING CODE
C                         1      FIXED-FIXED
C                         2      FIXED-PINNED
C                         3      FIXED-FREE
C                         4      PINNED-PINNED
C                         5      PINNED-FIXED
C                         6      PINNED-FREE
C                         7      FREE-FREE
C                         8      FREE-FIXED
C                         9      FREE-PINNED
C       CMNT1,CMNT2,CMNT3 ARE ALPHAMERIC VARIABLES
C       CONTAINING COMMENTS ON EACH DATA SET SUCH AS
C       A DESCRIPTION OF THE BEAM,NUMBER OF SECTIONS,END
C       CONDITIONS, ETC. IF NOT USED, BLANK CARDS MUST
C       BE INSERTED IN THEIR PLACE AMONG THE DATA CARDS.
C      ****************************************************************
C
       REAL LENGTH(25),MASS(25)
       INTEGER ENDCON,BEAM,RANGE,PAGE
       DIMENSION CMNT1(20), P(43), DET(43)
       DIMENSION TMAT(25,4,4), EI(25), X(4,4), Y(4,4), Z(4,4), U(4,4)
       PI=3.141592
C      IDIAG = 0 NO DIAGNOSTICS
C      IDIAG=1 FULL DIAGNOSTICS
C      IPLT = 0 IF PLOT SUBROUTINE IS NOT TO BE CALLED
C      IPLT = 1 IF PLOT SUBROUTINE IS TO BE CALLED
       READ (5,320) NDS,IDIAG,NSTA,IPLT
       WRITE (6,330) NDS,IDIAG,NSTA,IPLT
       READ (5,360) (LENGTH(I),MASS(I),EI(I),I=1,NSTA)
       WRITE (6,420)
       WRITE (6,430) (I,MASS(I),LENGTH(I),EI(I),I=1,NSTA)
```

```
      DO 20 I=1,NSTA
20    MASS(I)=MASS(I)/386.4
      IJ=0
      PAGE=0
30    IJ=IJ+1
      IF (IJ.GT.NDS) GO TO 290
      READ (5,370) (CMNT1(I),I=1,20)
      WRITE (6,380) (CMNT1(I),I=1,20)
      READ (5,340) ENDCON,NSTO,PSTART,PSTOP,PSTEP
      WRITE (6,350) ENDCON,NSTO,PSTART,PSTOP,PSTEP
      PAGE=PAGE+1
      WRITE (6,410) PAGE
      WRITE (6,390) (CMNT1(I),I=1,20)
C     ************************************************************
C       CHANGE MASS TO PROPER UNITS BY DIVIDING BY
C       UNIVERSAL GRAVITATIONAL CONSTANT
C     ************************************************************
      ITER=(PSTOP-PSTART)/PSTEP+1.5
      DO 40 I=1,43
40    P(I)=-5.0
      DO 280 LR=1,ITER
      P(LR)=P(LR)+LR*PSTEP
      IF (IDIAG.EQ.1) GO TO 50
      GO TO 60
50    WRITE (6,440) LR,P(LR)
60    CONTINUE
      F=P(LR)*2.0*PI
      FSQ=F**2
C     ************************************************************
C               LOAD ALL MATRICES
C     ************************************************************
```

```
      DO 70 I=1,NSTA
      TMAT(I,1,1)=1.0
      TMAT(I,1,2)=LENGTH(I)
      TMAT(I,1,3)=(LENGTH(I)**2)/(2.0*EI(I))
      TMAT(I,1,4)=TMAT(I,1,3)*LENGTH(I)/3.0
      TMAT(I,2,1)=0.0
      TMAT(I,2,2)=1.0
      TMAT(I,2,3)=LENGTH(I)/EI(I)
      TMAT(I,2,4)=TMAT(I,2,3)*LENGTH(I)/2.0
      TMAT(I,3,1)=0.0
      TMAT(I,3,2)=0.0
      TMAT(I,3,3)=1.0
      TMAT(I,3,4)=LENGTH(I)
      TMAT(I,4,1)=MASS(I)*FSQ
      TMAT(I,4,2)=TMAT(I,4,1)*LENGTH(I)
      TMAT(I,4,3)=TMAT(I,4,1)*LENGTH(I)/2.0/EI(I)
70    TMAT(I,4,4)=1.0+TMAT(I,4,3)*LENGTH(I)/3.0
      IF (IDIAG.EQ.1) GO TO 80
      GO TO 90
80    IF (LR.EQ.1) WRITE (6,450) (((TMAT(I,J,K),K=1,4),J=1,4),I=1,NSTA)
90    CONTINUE
C     ***************************************************************
C               CARRY OUT MATRIX MULTIPLICATION
C     ***************************************************************
      DO 100 I=1,4
      DO 100 J=1,4
100   Z(I,J)=0.0
      DO 110 J=1,4
      DO 110 K=1,4
110   Y(J,K)=TMAT(19,J,K)
      IF (IDIAG.EQ.1) GO TO 120
      GO TO 130
```

```
120     WRITE (6,460) ((Y(I,J),J=1,4),I=1,4)
130     CONTINUE
        DO 160 I=1,18
        NN=NSTA-I
        DO 140 J=1,4
        DO 140 K=1,4
140     X(J,K)=TMAT(NN,J,K)
        CALL XY (X,Y,Z)
        DO 150 J=1,4
        DO 150 K=1,4
150     Y(J,K)=Z(J,K)
160     CONTINUE
        DO 170 I=1,4
        DO 170 J=1,4
170     U(I,J)=Y(I,J)
C       ************************************************************************
C          EVALUATE DETERMINANT FOR PROPER END CONDITIONS
C       ************************************************************************
        GO TO (180,190,200,210,220,230,240,250,260), ENDCON
180     DET(LR)=U(1,3)*U(2,4)-U(1,4)*U(2,3)
        GO TO 270
190     DET(LR)=U(1,3)*U(3,4)-U(1,4)*U(3,3)
        GO TO 270
200     DET(LR)=U(3,3)*U(4,4)-U(3,4)*U(4,3)
        GO TO 270
210     DET(LR)=U(1,2)*U(3,4)-U(1,4)*U(3,2)
        GO TO 270
220     DET(LR)=U(1,2)*U(2,4)-U(1,4)*U(2,2)
        GO TO 270
230     DET(LR)=U(3,2)*U(4,4)-U(3,4)*U(4,2)
        GO TO 270
240     DET(LR)=U(3,1)*U(4,2)-U(3,2)*U(4,1)
        GO TO 270
250     DET(LR)=U(1,1)*U(2,2)-U(2,1)*U(1,2)
```

```
      GO TO 270
260   DET(LR)=U(1,1)*U(3,2)-U(1,2)*U(3,1)
270   CONTINUE
280   CONTINUE
      WRITE (6,400) (P(K),DET(K),K=1,41)
      GO TO 30
290   CONTINUE
      IF (IPLT) 300,310,300
300   CALL IPLOT (P,DET)
310   CONTINUE
      CALL EXIT
C
320   FORMAT (4I5)
330   FORMAT (1X,4I5)
340   FORMAT (2I5,3F10.0)
350   FORMAT (1X,2I5,3F10.0)
360   FORMAT (F11.0,2E20.6)
370   FORMAT (20A4)
380   FORMAT (1X,20A4)
390   FORMAT (1X,20A4,//,10X,8HFREQ(HZ),10X,11HDETERMINANT)
400   FORMAT (10X,F7.2,9X,E15.8)
410   FORMAT (1H1,10X,4HPAGE,I3)
420   FORMAT (1X,7HSTATION,8X,8HMASS(LB),8X,14HLENGTH(INCHES),7X,18HSTIF
     1FNESS(LBF-IN2)//)
430   FORMAT (5X,I2,5X,3G20.6)
440   FORMAT (1X,I10,F10.2,8HLR AND P)
450   FORMAT (1X,4E20.4)
460   FORMAT (1X,4F20.4,5HFIRST)
      END
```

```
      SUBROUTINE XY (A,B,C)
      DIMENSION A(4,4), B(4,4), C(4,4)
      DO 10 I=1,4
      DO 10 J=1,4
      C(I,J)=0.0
      DO 10 K=1,4
10    C(I,J)=C(I,J)+A(I,K)*B(K,J)
      RETURN
      END
      SUBROUTINE IPLOT (P,DET)
      DIMENSION P(43), DET(43), PP(25), DDET(25)
      DO 10 J=1,25
      PP(J)=P(J)
10    DDET(J)=DET(J)
      CALL PLOTS (0,0,9)
      CALL PLOT (0.0,0.5,-3)
      CALL SCALE (PP,30.0,25,1)
      CALL SCALE (DDET,30.0,25,1)
      CALL AXIS (0.0,0.0,18HFREQUENCY IN HERTZ,-18,30.0,0.0,P(42),P(43))
      CALL AXIS (0.0,0.0,27HMATRIX RESPONSE DETERMINANT,27,30.0,90.0,DET
     1(42),DET(43))
      CALL LINE (PP,DDET,25,1,1,2)
      CALL SYMBOL (0.5,12.0,.21,20HTEST CASE NUMBER SIX,0.0,20)
      CALL PLOT (12.0,0.0,999)
      RETURN
      END
```

TABLE IX. COMPUTER OUTPUT FROM BEAM MATRIX METHOD FOR FIXED-FIXED BEAM RESPONSE

Test Case Number One

Freq (Hz)	Determinant*
0.00	0.21912716E-09
5.00	0.21223201E-09
10.00	0.19184609E-09
15.00	0.15881541E-09
20.00	0.11453638E-09
25.00	0.60912830E-10
30.00	0.31596947E-12
35.00	-0.64485306E-10
40.00	-0.13035617E-09
45.00	-0.19393909E-09
50.00	-0.25169911E-09
55.00	-0.30003022E-09
60.00	-0.33534064E-09
65.00	-0.35414160E-09
70.00	-0.35333016E-09
75.00	-0.32997605E-09
80.00	-0.28171598E-09
85.00	-0.20656898E-09
90.00	-0.10339818E-09
95.00	0.27682745E-10
100.00	0.18764013E-09

*When the determinant values are plotted as a function of frequency, the zero values represent the beam vibrating at a resonant frequency.

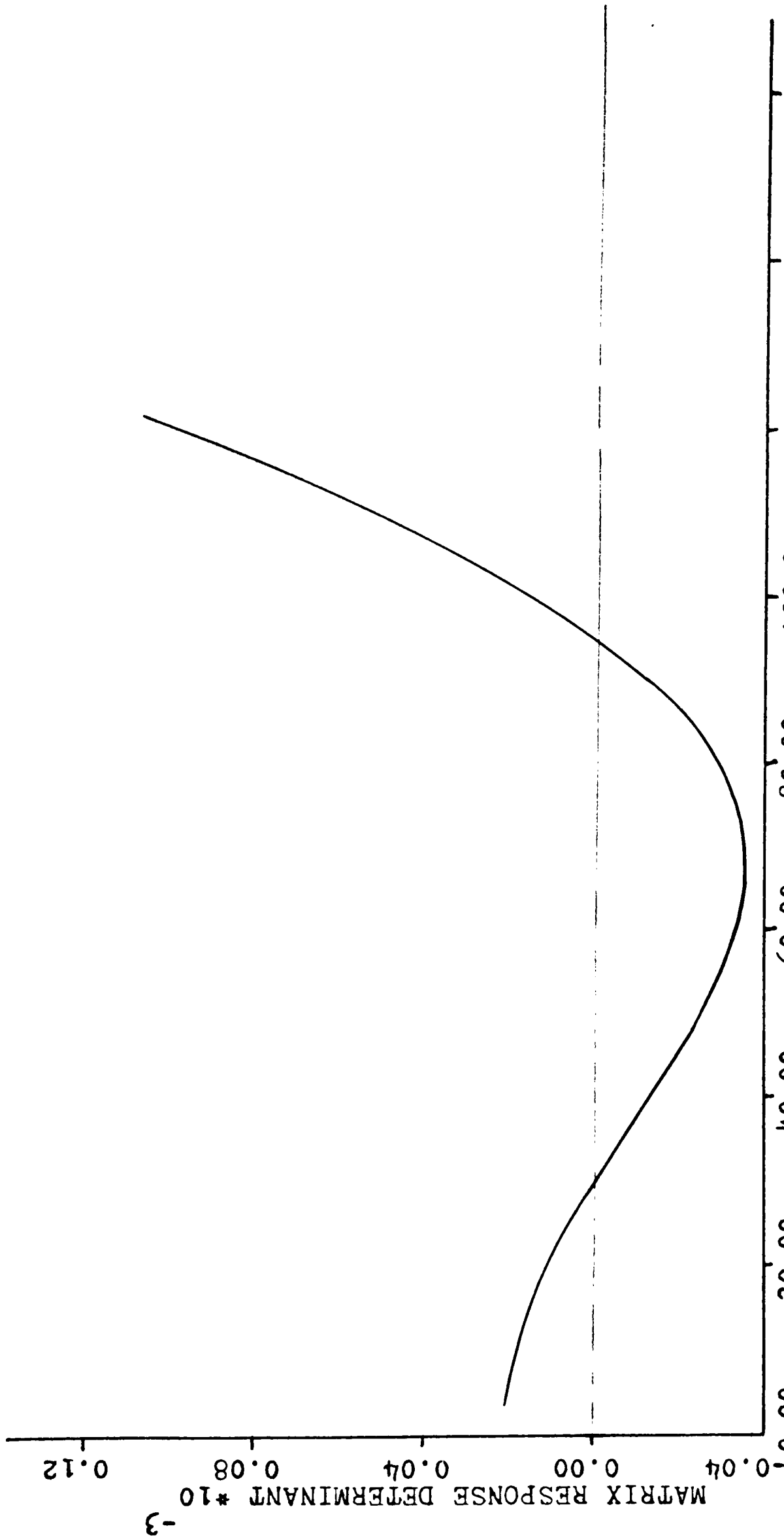

Figure C-1. Computer Plot of a Fixed-Fixed Beam Response

TABLE X. COMPUTER OUTPUT FROM BEAM MATRIX METHOD FOR FIXED-PINNED BEAM RESPONSE

Test Case Number Two

Freq (Hz)	Determinant
0.00	0.12306948E-02
5.00	0.11658357E-02
10.00	0.97466446E-03
15.00	0.66707470E-03
20.00	0.25929511E-03
25.00	-0.22661686E-03
30.00	-0.76340884E-03
35.00	-0.13193488E-02
40.00	-0.18592700E-02
45.00	-0.23455285E-02
50.00	-0.27393103E-02
55.00	-0.30019283E-02
60.00	-0.30950249E-02
65.00	-0.29860735E-02
70.00	-0.26425123E-02
75.00	-0.20390153E-02
80.00	-0.11576414E-02
85.00	0.14543533E-04
90.00	0.14781952E-02
95.00	0.32215118E-02
100.00	0.52347183E-02

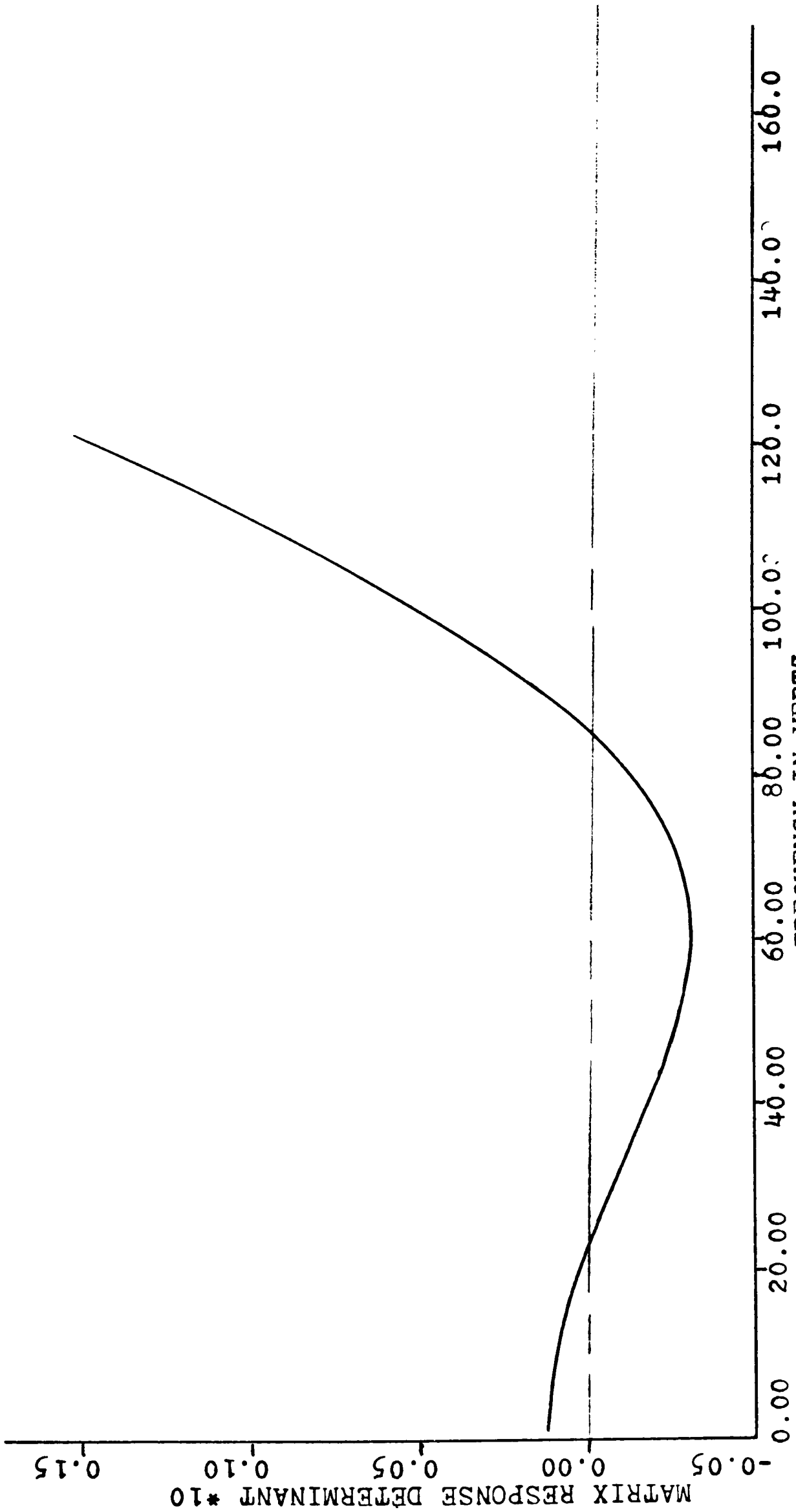

Figure C-2. Computer Plot of a Fixed-Pinned Beam Response

TABLE XI. COMPUTER OUTPUT FROM BEAM MATRIX METHOD FOR FIXED-FREE BEAM RESPONSE

Test Case Number Three

Freq (Hz)	Determinant
0.00	0.10000000E+01
5.00	0.70429265E+00
10.00	-0.13460827E+00
15.00	-0.13760471E+01
20.00	-0.27981110E+01
25.00	-0.41156464E+01
30.00	-0.50045013E+01
35.00	-0.51311493E+01
40.00	-0.41853027E+01
45.00	-0.19162598E+01
50.00	0.18305664E+01
55.00	0.70798340E+01
60.00	0.13697021E+02
65.00	0.21361084E+02
70.00	0.29531250E+02
75.00	0.37476563E+02
80.00	0.44207031E+02
85.00	0.48562500E+02
90.00	0.49195313E+02
95.00	0.44578125E+02
100.00	0.33164063E+02

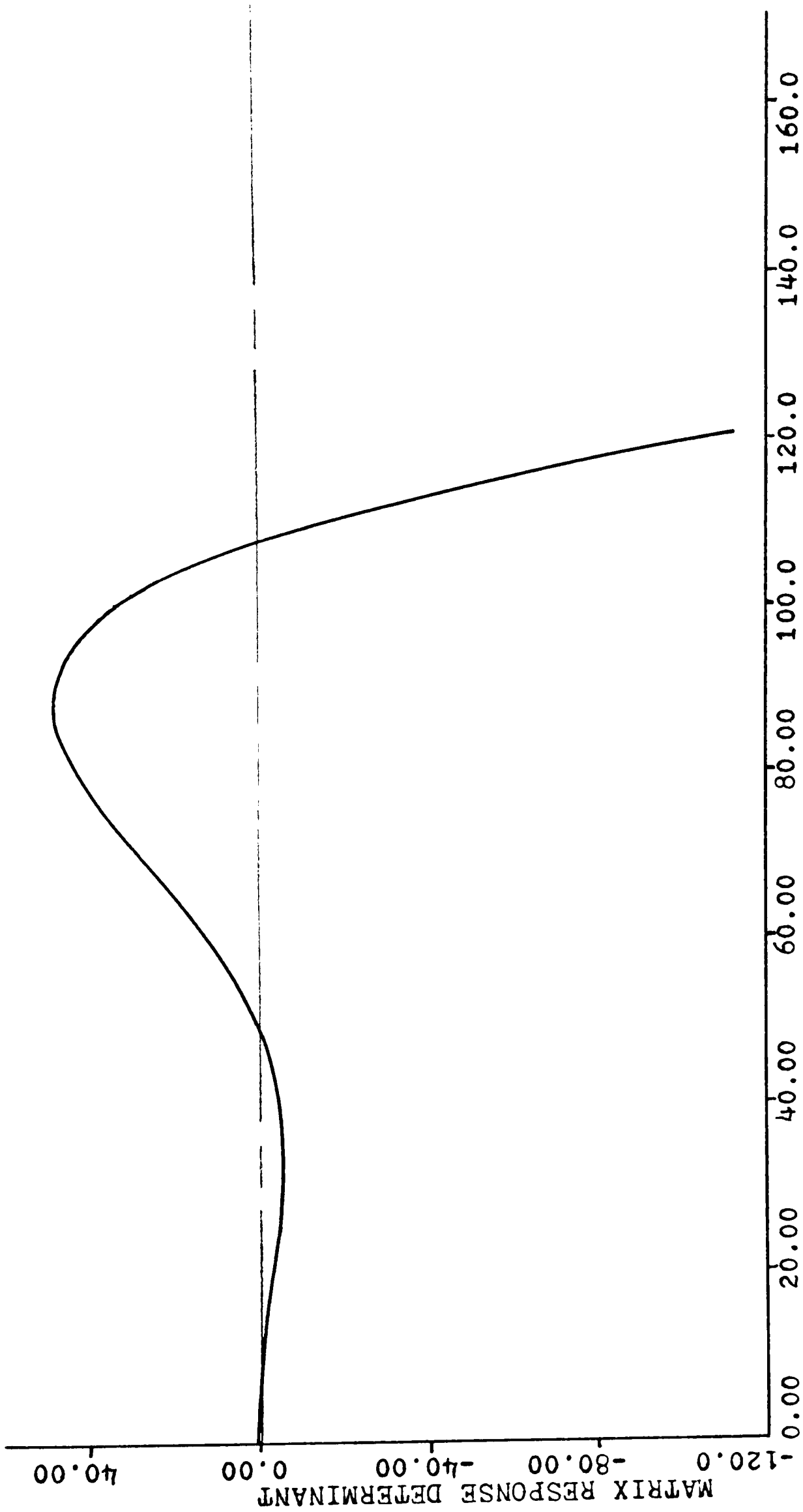

Figure C-3. Computer Plot of a Fixed-Free Beam Response

TABLE XII. COMPUTER OUTPUT FROM BEAM MATRIX METHOD FOR PINNED-PINNED BEAM RESPONSE

Test Case Number Four

Freq (Hz)	Determinant
0.00	0.51840000E+04
5.00	0.44630117E+04
10.00	0.23629297E+04
15.00	-0.93127344E+03
20.00	-0.51193125E+04
25.00	-0.97982500E+04
30.00	-0.14479125E+05
35.00	-0.18606313E+05
40.00	-0.21584375E+05
45.00	-0.22802313E+05
50.00	-0.21666438E+05
55.00	-0.17628000E+05
60.00	-0.10217000E+05
65.00	0.92900000E+03
70.00	0.16029000E+05
75.00	0.35131000E+05
80.00	0.58096000E+05
85.00	0.84595000E+05
90.00	0.11401000E+06
95.00	0.14552000E+06
100.00	0.17811200E+06

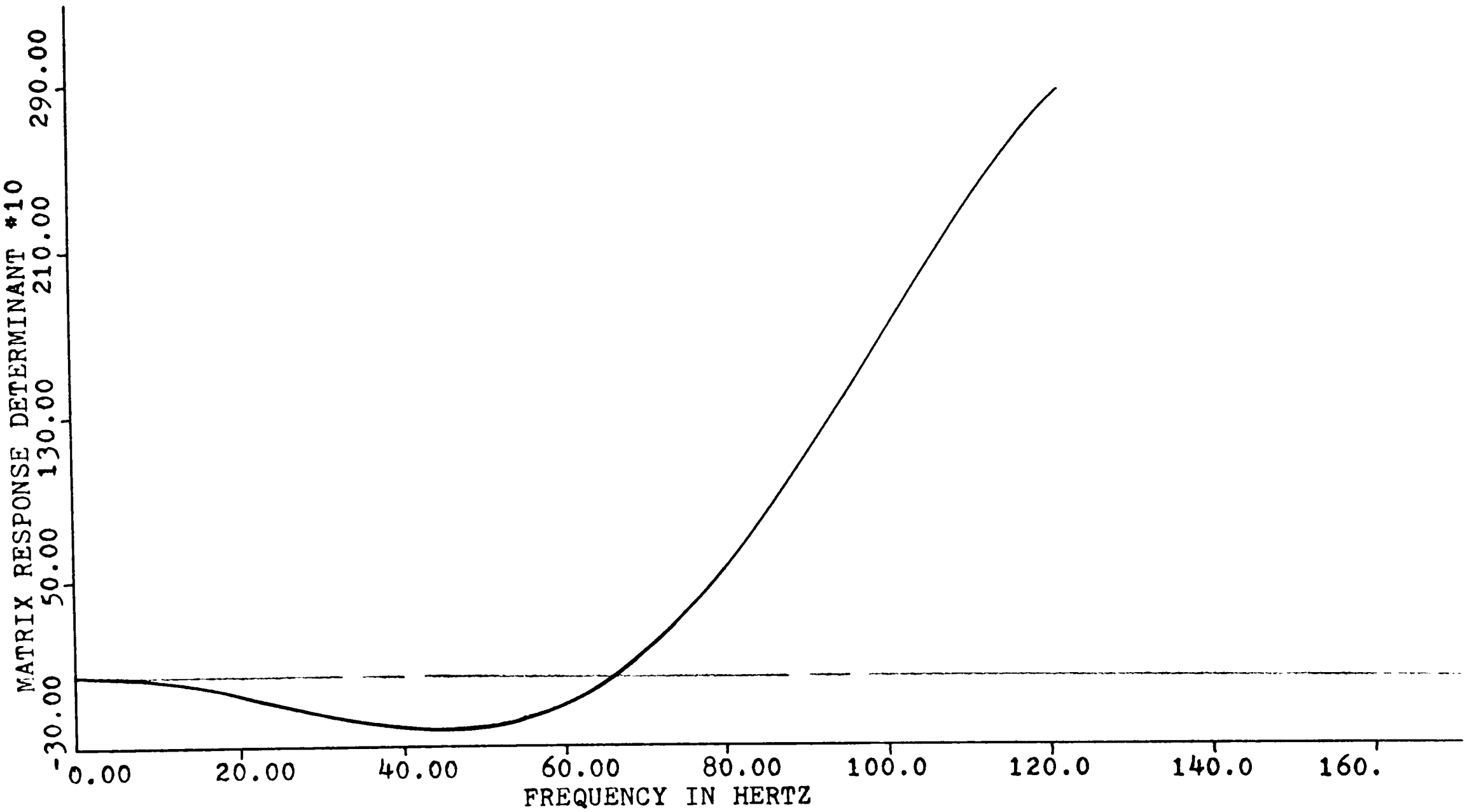

Figure C-4. Computer Plot of a Pinned-Pinned Beam Response

TABLE XIII. COMPUTER OUTPUT FROM BEAM MATRIX METHOD FOR PINNED-FIXED BEAM RESPONSE

Test Case Number Five

Freq (Hz)	Determinant
0.00	0.12306948E-02
5.00	0.11471391E-02
10.00	0.90215122E-03
15.00	0.51235780E-03
20.00	0.48801303E-05
25.00	-0.58365241E-03
30.00	-0.12083836E-02
35.00	-0.18177070E-02
40.00	-0.23554005E-02
45.00	-0.27624965E-02
50.00	-0.29798150E-02
55.00	-0.29506087E-02
60.00	-0.26224256E-02
65.00	-0.19506812E-02
70.00	-0.90026855E-03
75.00	0.55134296E-03
80.00	0.24089813E-02
85.00	0.46663284E-02
90.00	0.72927475E-02
95.00	0.10241508E-01
100.00	0.13446808E-01

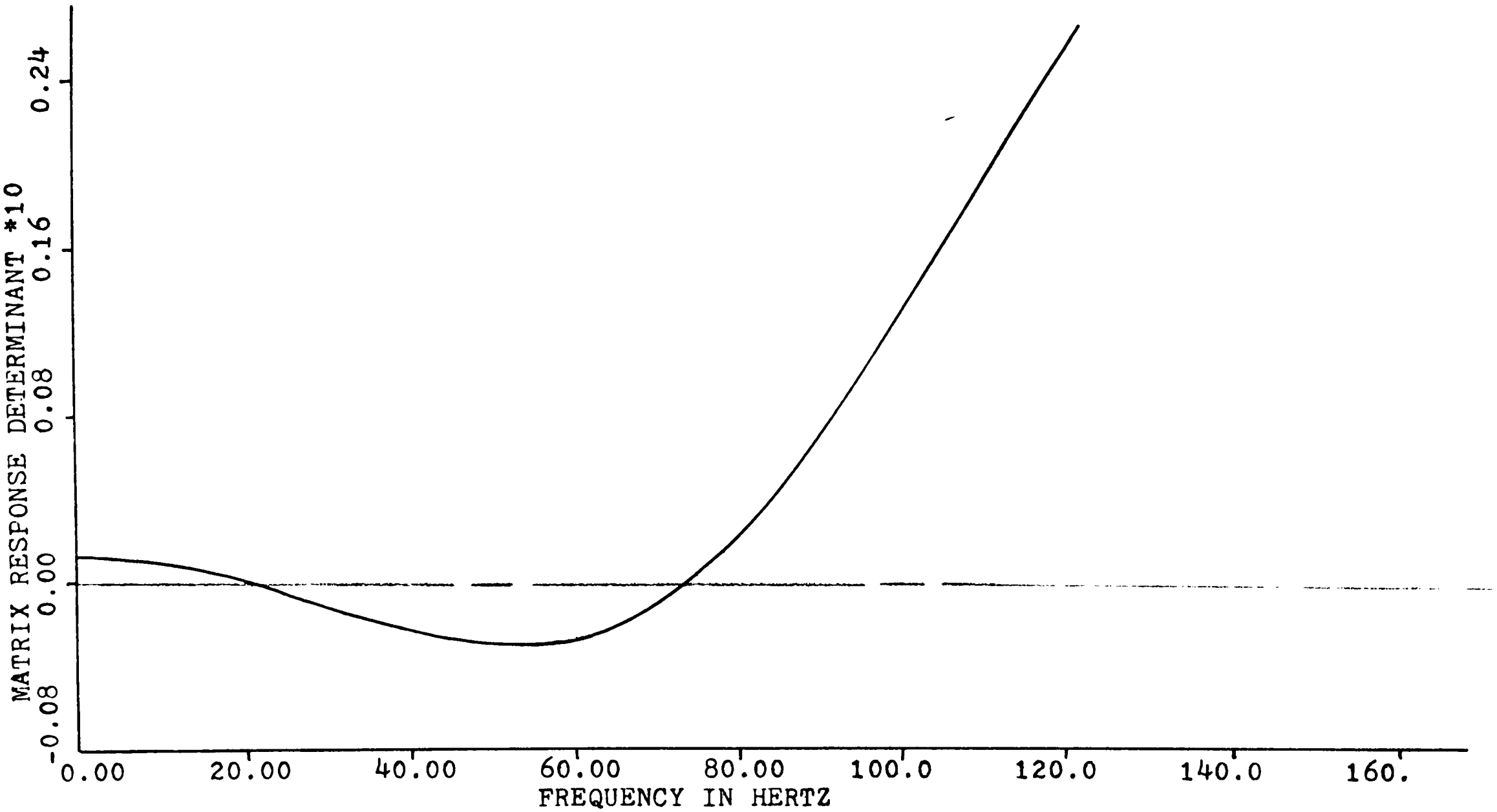

Figure C-5. Computer Plot of a Pined-Fixed Beam Response

TABLE XIV. COMPUTER OUTPUT FROM BEAM MATRIX METHOD FOR PINNED-FREE BEAM RESPONSE

Test Case Number Six

Freq (Hz)	Determinant
0.00	0.0
5.00	-0.23031930E+07
10.00	-0.85397120E+07
15.00	-0.16767728E+08
20.00	-0.24003744E+08
25.00	-0.26590720E+08
30.00	-0.20675840E+08
35.00	-0.27788800E+07
40.00	0.29588224E+08
45.00	0.77287424E+08
50.00	0.13896499E+09
55.00	0.21058765E+09
60.00	0.28494234E+09
65.00	0.35162931E+09
70.00	0.39674266E+09
75.00	0.40376730E+09
80.00	0.35330458E+09
85.00	0.22472294E+09
90.00	-0.28835840E+07
95.00	-0.34963456E+09
100.00	-0.83243827E+09

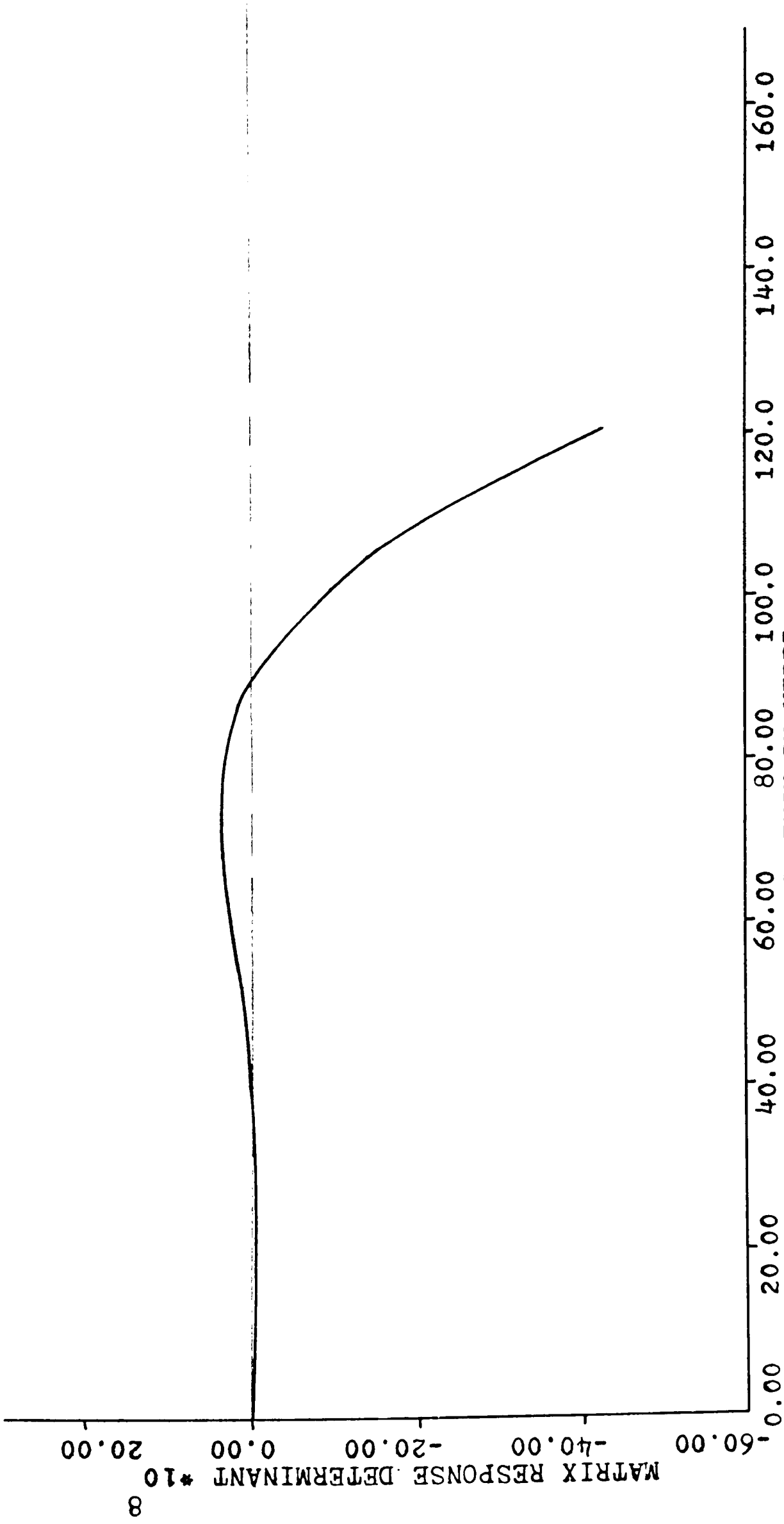

Figure C-6. Computer Plot of a Pinned-Free Beam Response

TABLE XV. COMPUTER OUTPUT FROM BEAM MATRIX METHOD FOR FREE-FREE BEAM RESPONSE

Test Case Number Seven

Freq (Hz)	Determinant
0.00	0.00
5.00	0.15175229E+10
10.00	0.23405003E+11
15.00	0.11123268E+12
20.00	0.32033473E+12
25.00	0.68785747E+12
30.00	0.11990341E+13
35.00	0.17533533E+13
40.00	0.21360584E+13
45.00	0.20024278E+13
50.00	0.88207891E+12
55.00	-0.17977122E+13
60.00	-0.66427038E+13
65.00	-0.14213657E+14
70.00	-0.24872156E+14
75.00	-0.38654706E+14
80.00	-0.55027121E+14
85.00	-0.72709501E+14
90.00	-0.89429809E+14
95.00	-0.10170912E+15
100.00	-0.10438489E+15

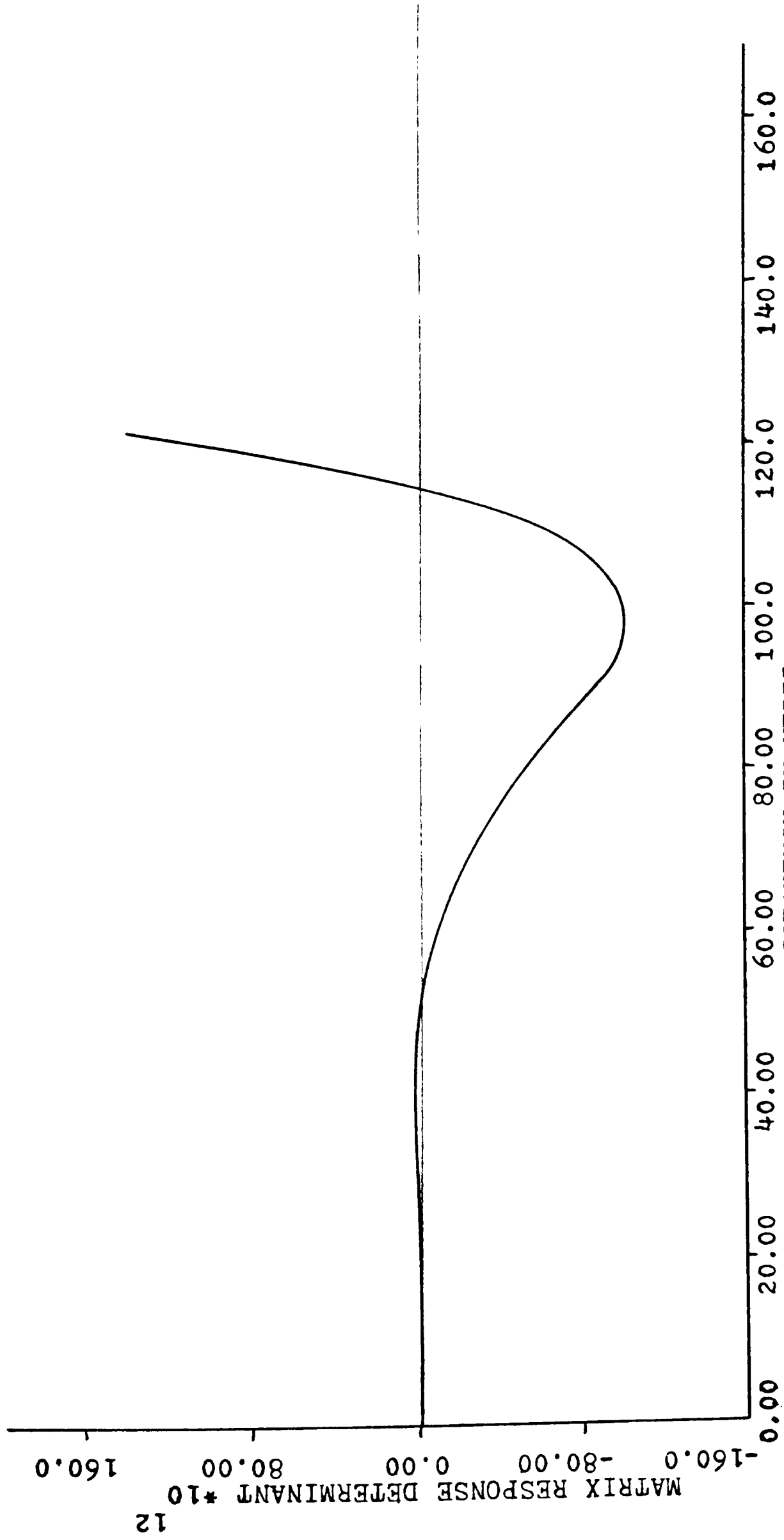

Figure C-7. Computer Plot of a Free-Free Beam Response

TABLE XVI. COMPUTER OUTPUT FROM BEAM MATRIX METHOD FOR FREE-FIXED BEAM RESPONSE

Test Case Number Eight

Freq (Hz)	Determinant
0.00	0.10000000E+01
5.00	-0.13142586E+00
10.00	-0.31401529E+01
15.00	-0.69047546E+01
20.00	-0.96704407E+01
25.00	-0.92160645E+01
30.00	-0.30756836E+01
35.00	0.11178223E+02
40.00	0.35641602E+02
45.00	0.71738281E+02
50.00	0.11985938E+03
55.00	0.17905859E+03
60.00	0.24671484E+03
65.00	0.31829297E+03
70.00	0.38712500E+03
75.00	0.44400000E+03
80.00	0.47818750E+03
85.00	0.47562500E+03
90.00	0.42087500E+03
95.00	0.29693750E+03
100.00	0.84687500E+02

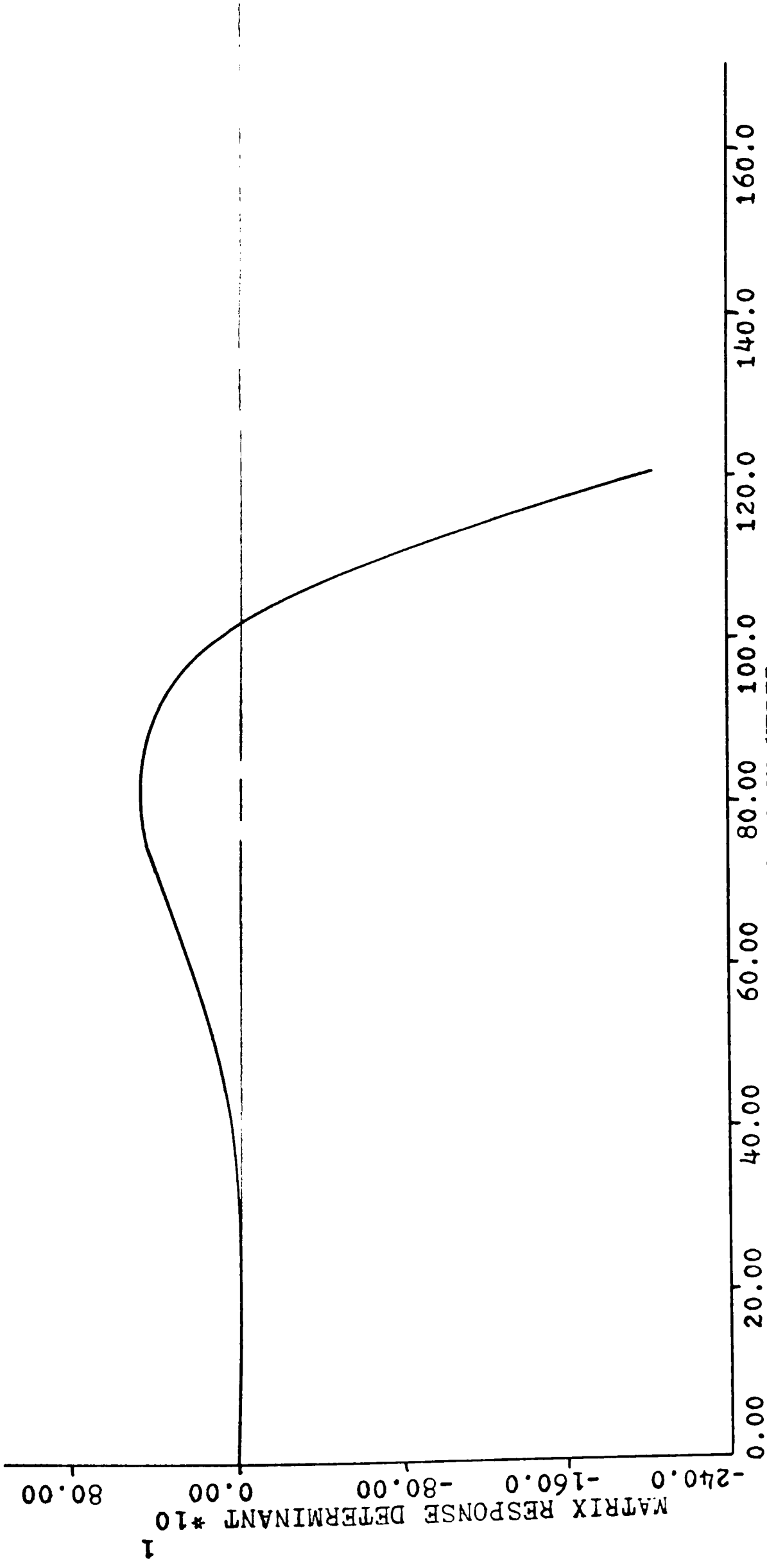

Figure C-8. Computer Plot of a Free-Fixed Beam Response

TABLE XVII. COMPUTER OUTPUT FROM BEAM MATRIX METHOD FOR FREE-PINNED BEAM RESPONSE

Test Case Number Nine

Freq (Hz)	Determinant
0.00	0.00
5.00	-0.62287490E+07
10.00	-0.21225424E+08
15.00	-0.34333184E+08
20.00	-0.29143808E+08
25.00	0.14540288E+08
30.00	0.11808845E+09
35.00	0.30085530E+09
40.00	0.57671270E+09
45.00	0.95029248E+09
50.00	0.14131855E+10
55.00	0.19406520E+10
60.00	0.24881398E+10
65.00	0.29896868E+10
70.00	0.33555087E+10
75.00	0.34716385E+10
80.00	0.32045138E+10
85.00	0.23928504E+10
90.00	0.86822093E+09
95.00	-0.15518925E+10
100.00	-0.50625249E+10

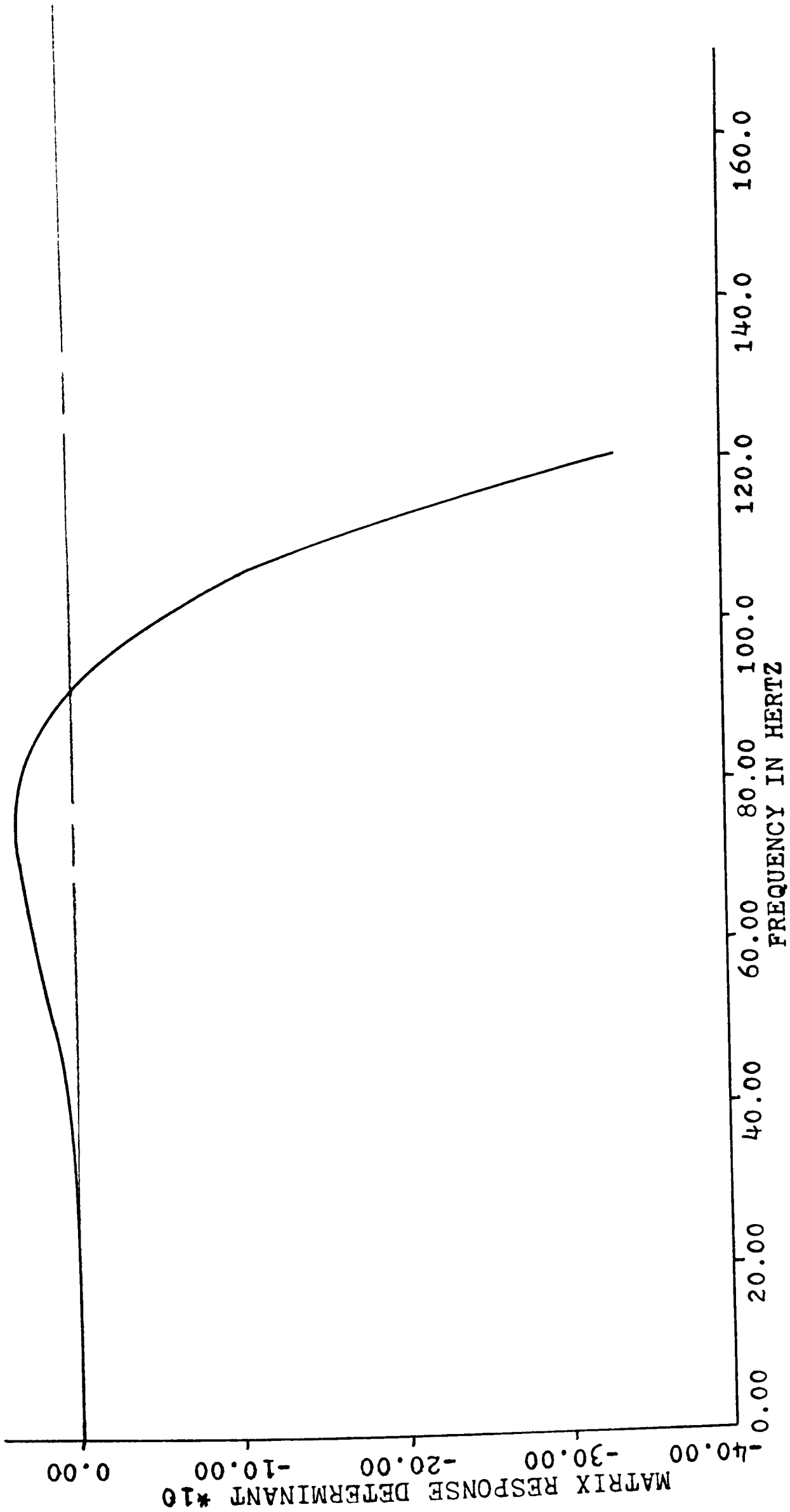

Figure C-9. Computer Plot of a Free-Pinned Beam Response

RESONANT FREQUENCIES OF THE LOWER SUBFRAME

Again using Campbell (1) as a guide, the author reanalyzed the lower subframe into different lumped elements. This was done to more accurately describe the overall computer model. Table XVIII presents the revised beam description.

TABLE XVIII. SECTION PARAMETERS OF LUMPED ELEMENT MODEL

Station	Mass (lb)	Length (Inches)	Stiffness (lbf-in^2)
1	4.7332	0.00	0.101094E+09
2	4.7332	4.00	0.101094E+09
3	4.7332	4.00	0.101094E+09
4	4.7332	4.00	0.101094E+09
5	4.7332	4.00	0.101094E+09
6	4.7332	4.00	0.101094E+09
7	4.7332	4.00	0.101094E+09
8	4.7332	4.00	0.101094E+09
9	3.5499	3.00	0.101094E+09
10	23.4055	1.00	0.101094E+09
11	93.6222	4.00	0.101094E+09
12	93.6222	4.00	0.101094E+09
13	93.6222	4.00	0.101094E+09
14	93.6222	4.00	0.101094E+09
15	93.6222	4.00	0.101094E+09
16	93.6222	4.00	0.101094E+09
17	93.6222	4.00	0.101094E+09
18	93.6222	4.00	0.101094E+09

19	93.6222	4.00	0.101094E+09
20	93.6222	4.00	0.101094E+09
21	93.6222	4.00	0.101094E+09

APPENDIX D

This appendix is designed to present a summary relating the previously used equipment to the replacement equipment that was installed during the progress of this thesis. Also presented is the additional equipment installed either to improve trailer operational safety or to enhance overall trailer functional capability.

	Old Equipment		Replacement Equipment
1.	1.5 ft x 2.5 ft x 3/4 inch plywood control board	1.	7 inch x 9 inch x 4 inch aluminum control box
2.	500 milliohm shunt and ampere meter	2.	--
3.	a) 12 volt battery b) 60 ampere-2 position, field control knife switch c. 0-5 ohm variable resistor d. 1 ohm resistor	3.	a) 25 ohm - 10 watt variable resistor b) 25 ohm resistor (5 ea. 125 ohm, parallel connected)
4.	60 ampere-2 position D.C. motor control switch	4.	a) 3 ampere-125 volt toggle switch b) 28 volt-300 ampere Reverse Current Relay

	c) 3 ampere-125 volt toggle switch
	d) 2 ea.-28 volt-200 ampere solenoid switches
5. Non-shielded wire	5. Shielded wire
6. Tachometer mounted in a separate wooden box	6. Tachometer incorporated into aluminum control box
7. ± 50 g Genisco accelerometers	7. ± 5 g Conrac accelerometers
8. No excess ballast	8. 700 pounds of ballast mounted on the upper frame
9. No stablization control mechanisms	9. a) Rear stablization torsion rod b) Rear horizontal control plate
10. 3/8 inch rod diameter lightweight coil springs	10. 1/2 inch rod diameter medium weight Chevy Vega front coil springs
11. No tension pulleys on drive belts for counter-rotating disks	11. One idler pulley/tension mechanism per individual drive belt